

Electronic supplementary information for:

BODIPY Based Realtime, Reversible and Targeted Fluorescent Probes for Biothiols Imaging in Living Cells

Rongkun He,^{a, b} Yichuan Zhang,^a Suresh Madhu,^a Quan Gao,^a Qianjin Lian,^a Sriram Srinivasa Raghavan^c and Jin Geng^{a, *}

^aInstitute of Biomedicine and Biotechnology, Shenzhen Institutes of Advanced Technology, Chinese Academy of Sciences, Shenzhen, China.

^bCollege of Chemistry and Chemical Engineering, Xiamen University, Xiamen, China.

^cMolecular Biophysics Unit, Indian Institute of Science, Bangalore, India.

Methods

Materials. All the materials were obtained from commercial suppliers and used without further purification.

Instruments. ^1H NMR and ^{13}C NMR spectra were recorded on a 500 MHz Bruker Advance 500 III spectrometer or Bruker ARX 400 MHz spectrometer at 25 °C. All chemical shifts (δ) reported in ppm are relative to internal standard tetramethylsilane ($\delta = 0.00$ ppm), or relative to the signals of residual solvent CDCl_3 (7.26 ppm for ^1H , 77.16 ppm for ^{13}C) or $\text{DMSO-}d_6$ (2.50 ppm for ^1H , 39.52 ppm for ^{13}C), and coupling constant are given in Hz. Mass spectra were collected on Bruker FT-MS or on a GCT Premier CAB 048 mass spectrometer operating in MALDI-TOF mode. The microwave assisted synthesis reaction were completed on CEM Discovery[®]SP microwave instrument. The photo synthesis reaction was completed by using 150 W xenon lamp (CHF-XM-150W, Beijing Trusttech).

Kinetic measurements of BOD-JQ with GSH. The kinetic measurement of the reactions was carried out on an Applied Photophysics SX.20 stopped-flow spectrometer in a single-mixing mode of the instrument with a 1:1 (v/v) ratio at 25 °C, by mixing the two reactants. The SX.20 uses a novel cell cartridge system that has a dead time of around 1 ms with very high sensitivity. The 20 μL cell with 1 mm path length light guide with a dead-time around 500 μs was applied in the experiments. The time dependence of the response of BOD-JQ to GSH was determined in PBS and DMSO mixture (pH = 7.4) under pseudo-first-order reaction conditions (5 μM BOD-JQ and 1 mM GSH). The spectra changes of the reaction ($\lambda_{\text{max}} = 570$ nm) were monitored at time interval of 1.25 ms and the kinetic traces were analyzed by Pro-K Global analysis/simulation software.

Reversible reaction of BOD-JQ and GSH. GSH (1 mM in distilled water) was added into the solution of BOD-JQ (5 μM in DMSO / PBS) and followed by the addition of NEM (1 mM in DMSO). The addition of GSH and NEM was repeated alternately for 3 cycles. The experiments were recorded as Supplementary Movie 1.

Electron density distributions in the HOMO and LUMO. Molecular descriptors of the BODIPY dyes were calculated using DFT calculations. Initial geometries of the dyes were optimized using Berny's algorithm until potential energy converged to the least minima. Molecular geometry optimization was executed with Becker's hybrid three-parameter, and nonlocal exchange-correlation function of Lee, Yang, Parr (B3LYP) theory with 6-311 g++ (d) standard basis set with Diffuse functions on heavy atoms and

hydrogen. The reactive parameter of the BODIPY derivative was calculated based on hard/soft and acid-base theory (HASB). Chemical reactivity indicators such as ionization potential, electron affinity, chemical potential, hardness, softness, electrophilicity, electronegativity chemical reactivity, and site interaction specificity were calculated using natural bond orbital (NBO). Avogadro molecular editor was utilized for orbital visualization and rendering.

Preparation of cells. B16F10 and HEK-A cells were cultured in Dulbecco's modified Eagle's medium (DMEM) supplemented with 10 % FBS (fetal bovine serum) and 1 % penicillin-streptomycin. A375 cells were cultured in RPMI 1640 supplemented with 10 % FBS and 1 % penicillin-streptomycin. All cells were cultured at 37 °C in a CO₂ / air (5 % / 95 %) incubator. HBSS, DMEM or RPMI 1640 was used for imaging medium.

Cell imaging. The Probe solution was made by diluting 1 mM of probe in DMSO with suitable imaging buffer for a final probe concentration of 2 μM. DMEM and RPMI 1640 were used as the imaging buffer in this contribution if not otherwise specified. Confocal fluorescence and bright-field imaging were undertaken with Olympus FV1200.

Co-staining of cells with BODIPY probes and Mito Tracker / ER Tracker. B16F10 and HEK-A cells seeded on 8-well μ-slides were incubated in DMEM containing BOD-PPh₃ or BOD-Cl (2 μM, 0.2 % DMSO), MitoLite™ Blue FX490 or ER-Tracker™ Blue-White DPX at 37 °C for 30 min. The medium was removed and replaced with DMEM. For A375 cells RPMI 1640 was used. Sequential imaging was performed under the following conditions.

Seq.1 for Mito Tracker and ER Tracker; laser: 405 nm, detection: 430 – 470 nm (Ch1)

Seq.2 for BOD-PPh₃ or BOD-Cl; laser: 488 nm, detection 500 – 550 nm (Ch2); laser 561 nm, detection 570 – 620 nm (Ch3).

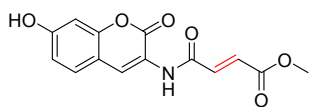
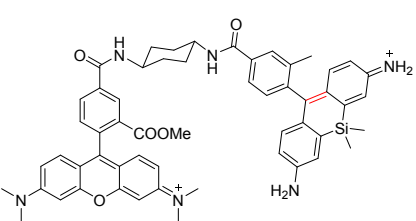
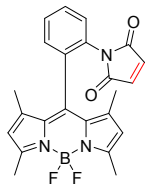
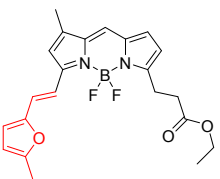
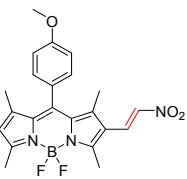
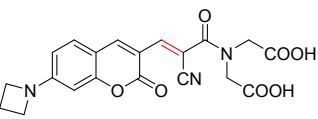
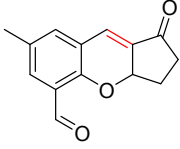
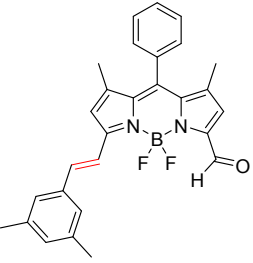
Evaluation of cytotoxicity of probes. Cells was seeded on a 96-well plate (ca. 1 × 10⁴ cells per well) and cultured overnight. Then probes (0, 1, 2, 5, 8, 10, 15, 20 μM in DMEM or RPMI 1640) was loaded and cultured for 24 h in an incubator. Then the cells were washed three times and cultured in DMEM or RPMI 1640. Cell viability was measured using Cell Counting Kit-8. Briefly, the medium was replaced with 100 μL of medium containing 10 % Cell Counting Kit-8 solution. After incubation for 30 minutes, the absorbance at 450 nm was measured using a plate reader.

Quantify GSH concentration in cells. A set of GSH solutions (0, 1, 2, 5, 8, 10, 15, 20 mM in mixture

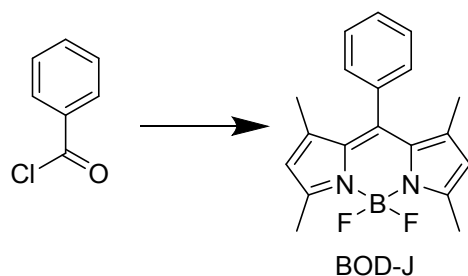
solution) in the presence of BOD-JQ (2 μM) was prepared in 8-well μ -slides, ibiTreat. Fluorescence images were acquired using a confocal microscope with the same settings used for quantification imaging. Then a calibration curve was obtained. Cells were cultured in 8-well μ -slides, ibiTreat, and BOD-JQ was applied according to the above protocol. Conversion of ratio values to GSH concentration was performed by using the obtained fitting equations / curves. The scale of ratio values was converted to that of GSH concentration by using ImageJ software, followed by fitting to the equations.

Real time live cells imaging of GSH and GSH dynamics in the presence of NEM. Fluorescence and bright-field imaging were undertaken with a Lionheart FX Automated Microscope (BioTek Instruments). Images were taken at $20\times$ with an Olympus phase objective every 30 s for 16 minutes in phase-contrast, RFP and YFP channels. The RFP and YFP image sequences were then overlapped into one, and the complete sequences was converted into an .avi file (Supplementary Movie 2). BOD-JQ treated cells (2 μM) were seeded, containing 300 μL of HBSS (without phenol red) and imaged for 16 minutes. At 5 minutes, the medium was changed to HBSS (300 μL) containing NEM (500 μM) and imaging was continued for a further 5 minutes. At 10.5 minutes, cells were washed twice and placed in HBSS (300 μL) containing GSH(Et) (5 mM). Fluorescence images were obtained every 30 seconds.

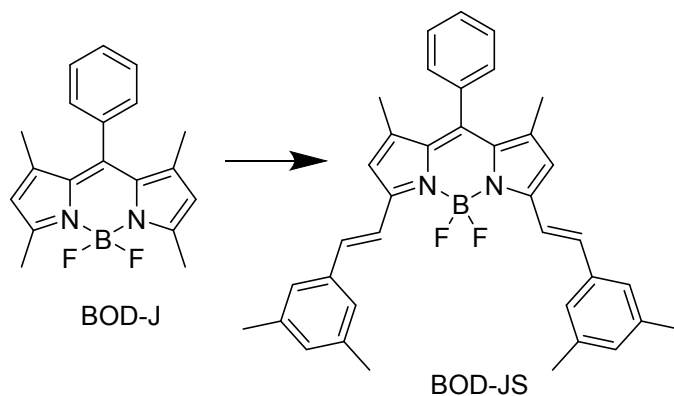
Table 1 Example probes for biothiols detection based on Michael reaction.

Probe	Representative probe The reaction sites are marked in red	Response type	$t_{1/2}$	Drawback	References
1		OFF/ON	3 ms	Turn on mechanism, emission wavelength was too short	[1]
2		FRET based ratiometric	620 ms	Complicated synthesis route, small emission shift (≤ 39 nm)	[2]
3		OFF/ON	> 1 min	Slow reaction kinetics	[3]
4		Reaction based ratiometric	> 1 min	Slow reaction kinetics	[4]
5		Reaction based ratiometric	> 1 min	Slow reaction kinetics	[5]
6		Reaction based ratiometric	Within 1 min	Slow reaction kinetics	[6]
7		OFF/ON	> 1 min	Slow reaction kinetics	[7]
8		Reaction based ratiometric	16 ms	-	This research

1. Synthesis

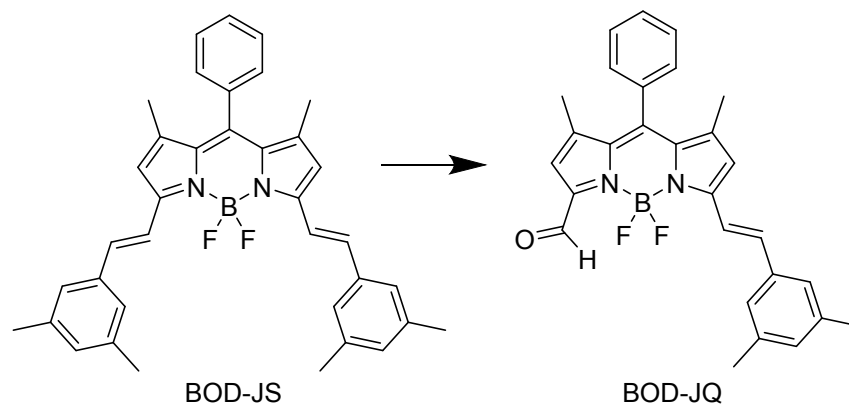


BOD-J⁸. Benzoylchloride (3.64 g, 25.00 mmol) and 2,4-dimethylpyrrole (5 mL, 3.7 g, 50.00 mmol) were added to 150 mL anhydrous CH₂Cl₂ via syringe under nitrogen atmosphere. Then the mixture was stirred at room temperature overnight under dark condition. Then Et₃N (30 mL) and BF₃•Et₂O (30 mL) were added under ice-cold condition, and reaction mixture was stirred for additional 2h. After the reaction, the mixture was poured into 300 mL water, the organic layer was collected and washed with water several times, dried over anhydrous MgSO₄. Then the CH₂Cl₂ was evaporated under reduced pressure. The product was further purified by silica gel column chromatography (petroleum ether / CH₂Cl₂ = 1 / 1) to give 1a (3.39g, yield: 43%). ¹H NMR (500 MHz, CDCl₃) δ: 7.50 – 7.46 (m, 3H), 7.28 (dd, J = 7.4, 2.0 Hz, 2H), 5.98 (s, 2H), 2.56 (s, 6H), 1.37 (s, 6H).

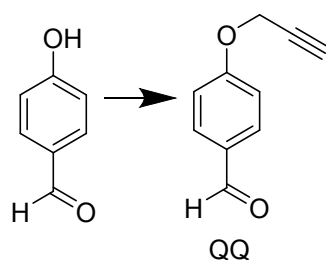


BOD-JS⁹⁻¹¹. BOD-J (64.8 mg, 0.2 mmol) was dissolved in anhydrous DMF (5 mL). 3,5-dimethylbenzaldehyde (107.3 mg, 0.8 mmol) was added, followed by acetic acid (100 μL) and piperidine (100 μL). The mixture was nitrogen saturated before it was subjected to microwave irradiation (50 min, 150 °C). The mixture was poured into 100 mL water, and extracted with CH₂Cl₂. The organic layer was washed with water, brine and dried over anhydrous MgSO₄. After removal of CH₂Cl₂ under reduced pressure, the residue was purified by silica gel column chromatography (petroleum ether / CH₂Cl₂ = 7 / 3) to give BOD-JS as brown solid (105.7 mg, yield: 95%). ¹H NMR (500 MHz, CDCl₃) δ: 7.72 (d, J =

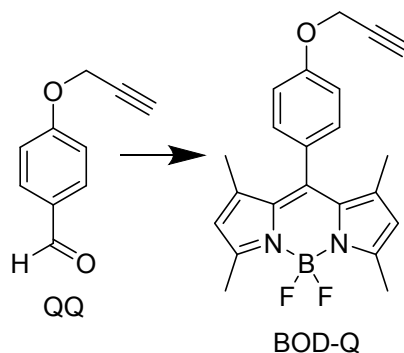
16.3 Hz, 2H), 7.50 (dd, $J = 4.8, 2.3$ Hz, 3H), 7.32 (dd, $J = 7.2, 2.1$ Hz, 2H), 7.26 (s, 4H), 7.21 (d, $J = 16.3$ Hz, 2H), 6.97 (s, 2H), 6.63 (s, 2H), 2.37 (s, 12H), 1.44 (s, 6H). ^{13}C NMR (125 MHz, CDCl_3) δ : 152.83 (s), 142.10 (s), 138.82 (s), 138.27 (s), 136.80 (s), 136.43 (s), 135.19 (s), 133.34 (s), 130.94 (s), 129.06 (d, $J = 14.9$ Hz), 128.46 (s), 125.52 (s), 118.76 (s), 117.86 (s), 21.30 (s), 14.65 (s).



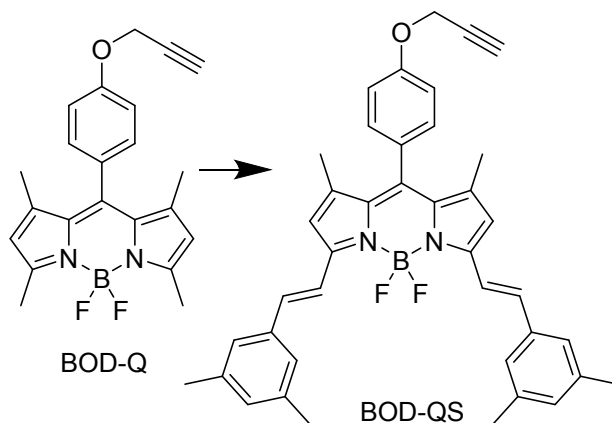
BOD-JQ. BOD-JS (55.6 mg, 0.1 mmol) was dissolved in 10 mL CH_2Cl_2 , then 2 g silica gel was added. After removal of CH_2Cl_2 under reduced pressure, the mixture was put into culture vessel as a thin layer. Then the mixture was suffered continuous irradiation under 100 W Xenon lamp with a distance of 10 cm. 4 h later, the color of the mixture was changed from dark green to dark violet. After the temperature of the mixture was cooled down to room temperature, the mixture was extracted with CH_2Cl_2 several times. Then combined the organic layer, and removal of CH_2Cl_2 under reduced pressure, the residue was purified by silica gel column chromatography (petroleum ether / $\text{CH}_2\text{Cl}_2 = 10 / 1$ to $2 / 1$) to give 1c as yellow solid (31.3 mg, yield: 69 %). ^1H NMR (500 MHz, CDCl_3) δ : 10.36 (s, 1H), 7.73 (d, $J = 16.3$ Hz, 1H), 7.57 – 7.52 (m, 3H), 7.43 (d, $J = 16.2$ Hz, 1H), 7.35 – 7.32 (m, 2H), 7.28 (s, 2H), 7.06 (s, 1H), 6.81 (d, $J = 8.8$ Hz, 2H), 2.37 (s, 6H), 1.52 (s, 3H), 1.41 (s, 3H). ^{13}C NMR (126 MHz, CDCl_3) δ : 184.46 (s), 161.08 (s), 148.14 (s), 143.48 (s), 143.22 (s), 141.58 (s), 138.69 (s), 137.00 (s), 135.30 (s), 134.22 (s), 133.39 (s), 132.76 (s), 129.53 (d, $J = 15.3$ Hz), 127.92 (s), 126.35 (s), 121.01 (s), 120.12 (s), 117.88 (s), 21.23 (s), 15.27 (s), 14.14 (s). FT-MS for $\text{C}_{28}\text{H}_{25}\text{BF}_2\text{N}_2\text{O}$ ($\text{M} + \text{Na}^+$) calculated 477.19202, found 477.19222.



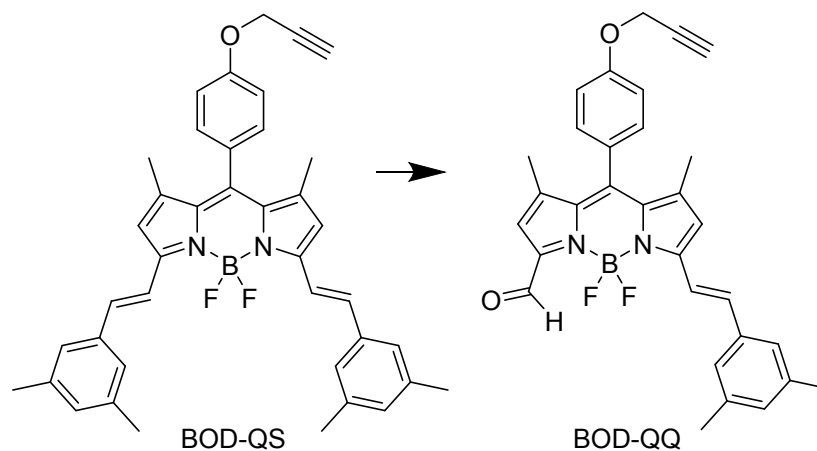
QQ¹². 4-hydroxybenzaldehyde (6.12g, 50.00 mmol) and propargyl bromide (11.90g, 100.00 mmol) were dissolved in 250 mL acetone. K₂CO₃ (9.67 g, 70.00 mmol) was added. Then the mixture was refluxed for 2 h. After cooling down to room temperature, the solvent was evaporated in vacuum, extracted with water and CHCl₃. Organic layer was dried with Na₂SO₄ and evaporated under reduced pressure. The crude product was purified by silica gel column chromatography (petroleum ether / CHCl₃ = 1 / 1) to give compound 1 (7.84 g, yield: 98%). ¹H NMR (500 MHz, CDCl₃) δ: 9.91 (s, 1H), 7.88 – 7.84 (m, 2H), 7.12 – 7.08 (m, 2H), 4.79 (d, J = 2.4 Hz, 2H), 2.57 (t, J = 2.4 Hz, 1H).



BOD-Q¹². 500 mL CH₂Cl₂ was purged with nitrogen for 30 min. Compound 1 (2.98 g, 18.60 mmol) and 2,4-dimethylpyrrole (3.80 g, 40.00 mmol) were added. The color of the solution turned into red after the addition of 3 drops of trifluoroacetic acid. Then the mixture was stirred at room temperature overnight under dark condition. Then 2,3-dichloro-5,6-dicyano-1,4-benzoquinone (DDQ) (4.22 g, 18.60 mmol) was added and the reaction mixture was stirred at room temperature for 1 h. Then 30 ml Et₃N and 30 mL BF₃•Et₂O were added under ice-cold condition, the reaction mixture was stirred for additional 2 h. Then it was extracted with water. Organic layer was dried with Na₂SO₄ and evaporated under reduced pressure. The crude product was purified by silica gel column chromatography (petroleum ether / CH₂Cl₂ = 1 / 1) to give BOD-Q (1.26 g, 18 %). ¹H NMR (500 MHz, CDCl₃) δ: 7.21 – 7.18 (m, 2H), 7.11 – 7.07 (m, 2H), 5.97 (s, 2H), 4.76 (d, J = 2.4 Hz, 2H), 2.55 (s, 7H), 1.42 (s, 6H).

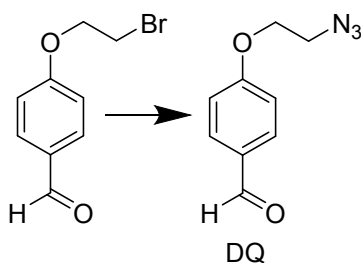


BOD-QS⁹⁻¹¹. BOD-Q (75.6 mg, 0.2 mmol) was dissolved in anhydrous DMF (5 mL). 3,5-dimethylbenzaldehyde (107.3 mg, 0.8 mmol) was added, followed by acetic acid (100 μ L) and piperidine (100 μ L). The mixture was nitrogen saturated before it was subjected to microwave irradiation (45 min, 150 $^{\circ}$ C). The mixture was poured into 100 mL water, and extracted with CH_2Cl_2 . The organic layer was washed with water, brine and dried over anhydrous MgSO_4 . After removal of CH_2Cl_2 under reduced pressure, the residue was purified by silica gel column chromatography (petroleum ether / $\text{CH}_2\text{Cl}_2 = 7 / 3$) to give BOD-QS as brown solid (114.7 mg, yield: 94%). ^1H NMR (500 MHz, CDCl_3) δ : 7.71 (d, $J = 16.3$ Hz, 2H), 7.25 (s, 3H), 7.23 (t, $J = 3.0$ Hz, 2H), 7.19 (s, 1H), 7.13 – 7.07 (m, 2H), 6.96 (s, 2H), 6.63 (s, 2H), 4.78 (d, $J = 2.4$ Hz, 2H), 2.57 (s, 1H), 2.37 (s, 12H), 1.49 (s, 6H). ^{13}C NMR (125 MHz, CDCl_3) δ : 158.15 (s), 152.77 (s), 142.08 (s), 138.56 (s), 138.26 (s), 136.75 (s), 136.42 (s), 133.67 (s), 130.92 (s), 129.72 (s), 128.20 (s), 125.51 (s), 118.76 (s), 117.82 (s), 115.59 (s), 78.10 (s), 75.93 (s), 56.07 (s), 21.29 (s), 14.85 (s).



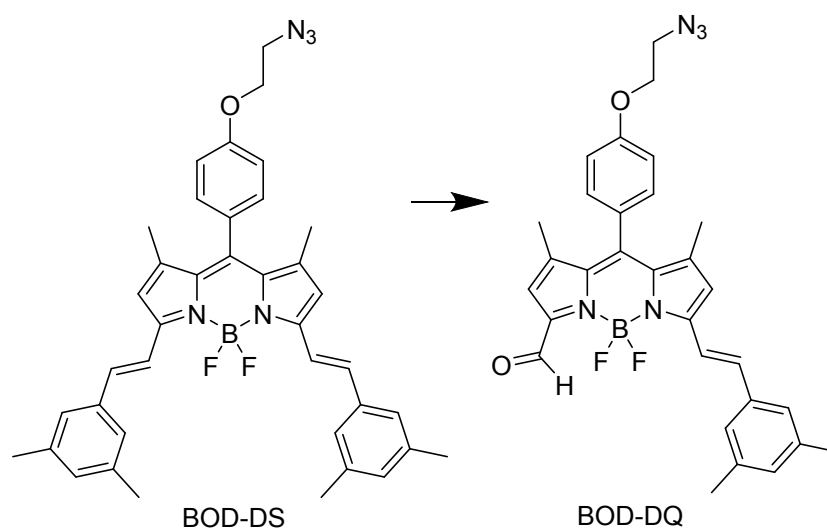
BOD-QQ. BOD-QS (61 mg, 0.1 mmol) was dissolved in 10 mL CH_2Cl_2 , then 2 g silica gel was added. After removal of CH_2Cl_2 under reduced pressure, the mixture was put into culture vessel as a thin layer.

Then the mixture was suffered continuous irradiation under 100 W Xenon lamp with a distance of 10 cm. 4 h later, the color of the mixture was changed from dark green to dark violet. After the temperature of the mixture was cooled down to room temperature, the mixture was extracted with CH₂Cl₂ several times. Then combined the organic layer, and removal of CH₂Cl₂ under reduced pressure, the residue was purified by silica gel column chromatography (petroleum ether / CH₂Cl₂ = 10 / 1 to 2 / 1) to give BOD-QQ as yellow solid (37 mg, yield: 72 %). ¹H NMR (500 MHz, CDCl₃) δ 10.35 (s, 1H), 7.73 (d, *J* = 16.1 Hz, 1H), 7.44 (d, *J* = 16.2 Hz, 1H), 7.28 (s, 2H), 7.24 (s, 2H), 7.15 (d, *J* = 8.4 Hz, 2H), 7.06 (s, 1H), 6.81 (d, *J* = 9.1 Hz, 2H), 4.79 (d, *J* = 2.0 Hz, 2H), 2.58 (s, 1H), 2.37 (s, 6H), 1.58 (s, 3H), 1.47 (s, 3H). ¹³C NMR (126 MHz, CDCl₃) δ 184.47 (s), 160.98 (s), 158.53 (s), 148.12 (s), 143.41 (s), 143.19 (s), 141.42 (s), 138.69 (s), 136.96 (s), 135.30 (s), 132.74 (s), 129.28 (s), 127.14 (s), 126.34 (s), 120.95 (s), 120.11 (s), 117.89 (s), 115.94 (s), 77.87 (s), 76.08 (s), 56.08 (s), 31.93 (s), 29.67 (s), 29.37 (s), 22.70 (s), 21.23 (s), 15.49 (s), 14.36 (s), 14.13 (s). FT-MS for C₂₈H₂₅BF₂N₂O(M + Na⁺) calculated 531.20259, found 531.20344.



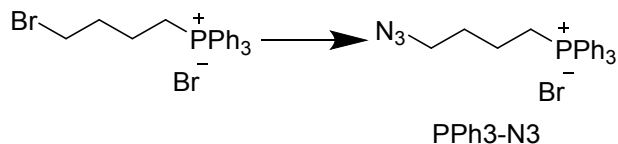
DQ¹⁴. A solution of 4-(2-Bromoethoxy)benzaldehyde (1.50 g, 6.50 mmol) and NaN₃ (0.51 g, 8.00 mmol) in dimethyl sulfoxide (5.0 mL) was heated at 50 °C for 24 h. The solution was cold to room temperature and 20 mL CH₂Cl₂ was added. The mixture was washed with water for several times and the organic layer was dried over anhydrous Na₂SO₄ and the solvent was distilled off under reduced pressure. The residue was purified by silica gel column chromatography (petroleum ether / AcOEt = 4 / 1) to give compound 2 (0.94 g, yield: 75%) as a white solid. ¹H NMR (500 MHz, CDCl₃) δ: 9.90 (s, 1H), 7.87 – 7.83 (m, 2H), 7.05 – 7.02 (m, 2H), 4.25 – 4.22 (m, 2H), 3.67 – 3.63 (m, 2H).

(100 μL). The mixture was nitrogen saturated before it was subjected to microwave irradiation (30 min, 150 $^{\circ}\text{C}$). The mixture was poured into 100 mL water, and extracted with CH_2Cl_2 . The organic layer was washed with water, brine and dried over anhydrous MgSO_4 . After removal of CH_2Cl_2 under reduced pressure, the residue was purified by silica gel column chromatography (petroleum ether / $\text{CH}_2\text{Cl}_2 = 7 / 3$) to give BOD-DS as brown solid (119.2 mg, yield: 93%). ^1H NMR (500 MHz, CDCl_3) δ : 7.71 (d, $J = 16.3$ Hz, 2H), 7.26 – 7.25 (m, 2H), 7.24 (s, 1H), 7.23 (s, 2H), 7.20 (s, 1H), 7.05 (d, $J = 8.7$ Hz, 2H), 6.97 (s, 2H), 6.63 (s, 2H), 4.24 – 4.20 (m, 2H), 3.69 – 3.64 (m, 2H), 2.37 (s, 12H), 1.50 (s, 6H). ^{13}C NMR (125 MHz, CDCl_3) δ : 158.82 (s), 152.75 (s), 142.11 (s), 138.63 (s), 138.29 (s), 136.75 (s), 136.41 (s), 133.69 (s), 130.95 (s), 129.80 (s), 127.91 (s), 125.51 (s), 118.76 (s), 117.82 (s), 115.12 (s), 66.98 (s), 50.25 (s), 21.29 (s).

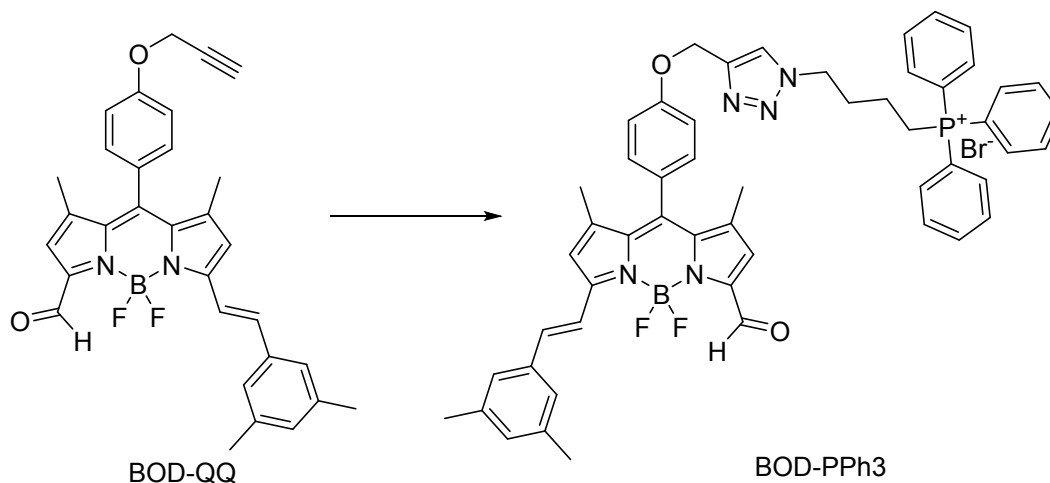


BOD-DQ. BOD-DS (64 mg, 0.1 mmol) was dissolved in 10 mL CH_2Cl_2 , then 2 g silica gel was added. After removal of CH_2Cl_2 under reduced pressure, the mixture was put into culture vessel as a thin layer. Then the mixture was suffered continuous irradiation under 100 W Xenon lamp with a distance of 10 cm. 4 h later, the color of the mixture was changed from dark green to dark violet. After the temperature of the mixture was cooled down to room temperature, the mixture was extracted with CH_2Cl_2 several times. Then combined the organic layer, and removal of CH_2Cl_2 under reduced pressure, the residue was purified by silica gel column chromatography (petroleum ether / $\text{CH}_2\text{Cl}_2 = 10 / 1$ to $2 / 1$) to give BOD-DQ as yellow solid (38 mg, yield: 70 %). ^1H NMR (500 MHz, CDCl_3) δ 10.35 (s, 1H), 7.73 (d, $J = 16.3$ Hz, 1H), 7.43 (d, $J = 16.2$ Hz, 1H), 7.28 (s, 2H), 7.24 (s, 2H), 7.11 – 7.07 (m, 2H), 7.06 (s, 1H), 6.81 (d, $J = 9.2$ Hz, 2H), 4.26 – 4.19 (m, 2H), 3.71 – 3.64 (m, 2H), 2.37 (s, 6H), 1.58 (s, 3H), 1.48 (s, 3H). ^{13}C NMR (126

MHz, CDCl₃) δ 184.47 (s), 161.00 (s), 159.24 (s), 148.11 (s), 143.43 (s), 143.18 (s), 141.43 (s), 138.69 (s), 137.42 (s), 136.93 (s), 135.30 (s), 133.73 (s), 132.75 (s), 129.41 (s), 126.93 (s), 126.34 (s), 120.97 (s), 120.09 (s), 117.88 (s), 115.43 (s), 67.05 (s), 50.22 (s), 31.94 (s), 29.67 (s), 22.71 (s), 21.23 (s), 15.55 (s), 14.42 (s), 14.14 (s). FT-MS for C₂₈H₂₅BF₂N₂O(M + Na⁺) calculated 562.21963, found 562.22073.



PPh₃-N₃. (4-bromobutyl) triphenylphosphonium bromide (0.478 g, 1 mmol), NaN₃ (0.195 g, 3 mmol) was dissolved in 10 mL DMF under Ar atmosphere. The mixture was stirred at 90 °C, overnight, and the color of the solution was from colorless to light yellow to red. After the reaction, the flask was cooled to room temperature and 50 mL of DCM was added until a large amount of precipitate was produced. The precipitate was filtered through a buchner funnel, and the organic phase was collected and dried in vacuum to afford light yellow solid product. The light-yellow solid was recrystallized from DCM and EAC. The precipitate was filtered through a buchner funnel and dried in vacuum to afford white crystal product (0.398 g, yield: 87 %). ¹H NMR (400 MHz, Chloroform-d) δ 7.87 (d, J = 12.6 Hz, 6H), 7.81 (d, J = 2.0 Hz, 3H), 7.71 (d, J = 3.4 Hz, 6H), 3.96 (d, J = 3.5 Hz, 2H), 3.45 (s, 2H), 2.04 (d, J = 1.8 Hz, 2H), 1.74 (d, J = 8.0 Hz, 2H).



BOD-PPh₃. BOD-QQ (50.8 mg, 0.1 mmol) and (4-azidobutyl)triphenylphosphonium bromide (43.9 mg, 0.1 mmol) were dissolved in the mixture of solvents (14 mL, CHCl₃ : EtOH : H₂O = 12:1:1, v/v), then CuSO₄•5H₂O (25 mg, 0.1 mmol) and sodium ascorbate (19.8 mg, 0.1 mmol) were added. The mixture was nitrogen saturated stirred at room temperature for 24 h under dark condition. After the reaction, the

BOD-Cl. BOD-QQ (50.8 mg, 0.1 mmol) and 1-azido-3-chloropropane (11.9 mg, 0.1 mmol) were dissolved in the mixture of solvents (10 mL, DMSO : CH₂Cl₂ = 1:1, v/v), then CuSO₄•5H₂O (25 mg, 0.1 mmol) and sodium ascorbate (19.8 mg, 0.1 mmol) were added. The mixture was nitrogen saturated stirred at room temperature for 24 h under dark condition. After the reaction, the mixture was poured into 200 mL water, the mixture was extracted with CH₂Cl₂ several times, the organic layer was collected and washed with water several times, dried over anhydrous Na₂SO₄. Then the CH₂Cl₂ was evaporated under reduced pressure. The product was further purified by silica gel column chromatography (CH₂Cl₂ / MeOH = 20/ 1 to 10 / 1) to give BOD-Cl (28.2 mg, yield: 45%).¹H NMR (400 MHz, CDCl₃) δ 10.35 (s, 1H), 7.78 – 7.67 (m, 2H), 7.43 (d, J = 16.2 Hz, 1H), 7.27 (s, 2H), 7.25 – 7.21 (m, 2H), 7.16 (d, J = 8.4 Hz, 2H), 7.06 (s, 1H), 6.81 (d, J = 6.7 Hz, 2H), 5.28 (s, 2H), 4.61 (t, J = 6.6 Hz, 2H), 3.55 (t, J = 6.0 Hz, 2H), 2.44 (p, J = 6.2 Hz, 2H), 2.37 (s, 6H), 1.57 (s, 3H), 1.46 (s, 3H).¹³C NMR (101 MHz, CDCl₃) δ 184.45, 161.00, 159.23, 148.13, 143.46, 143.09, 141.42, 138.67, 137.41, 136.84, 135.28, 133.74, 132.74, 129.35, 126.81, 126.33, 123.60, 120.98, 120.09, 117.83, 116.52, 115.68, 62.00, 47.18, 41.09, 32.46, 29.71, 29.35, 21.23, 15.51, 14.38. FT-MS for C₃₄H₃₃BF₂N₅O₂NaCl(M + Na⁺) calculated 650.2276, found 650.2287.

2. NMR and Mass Spectrum

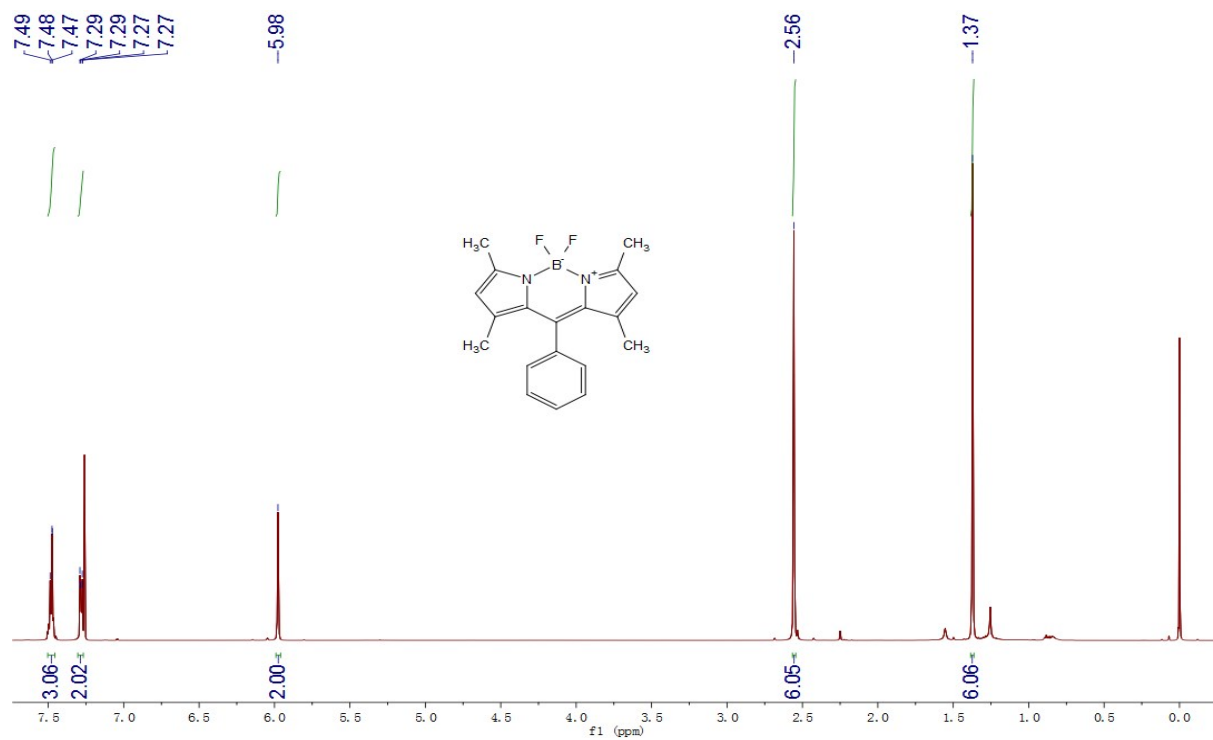


Fig. S1 ^1H NMR spectrum of BOD-J (in CDCl_3).

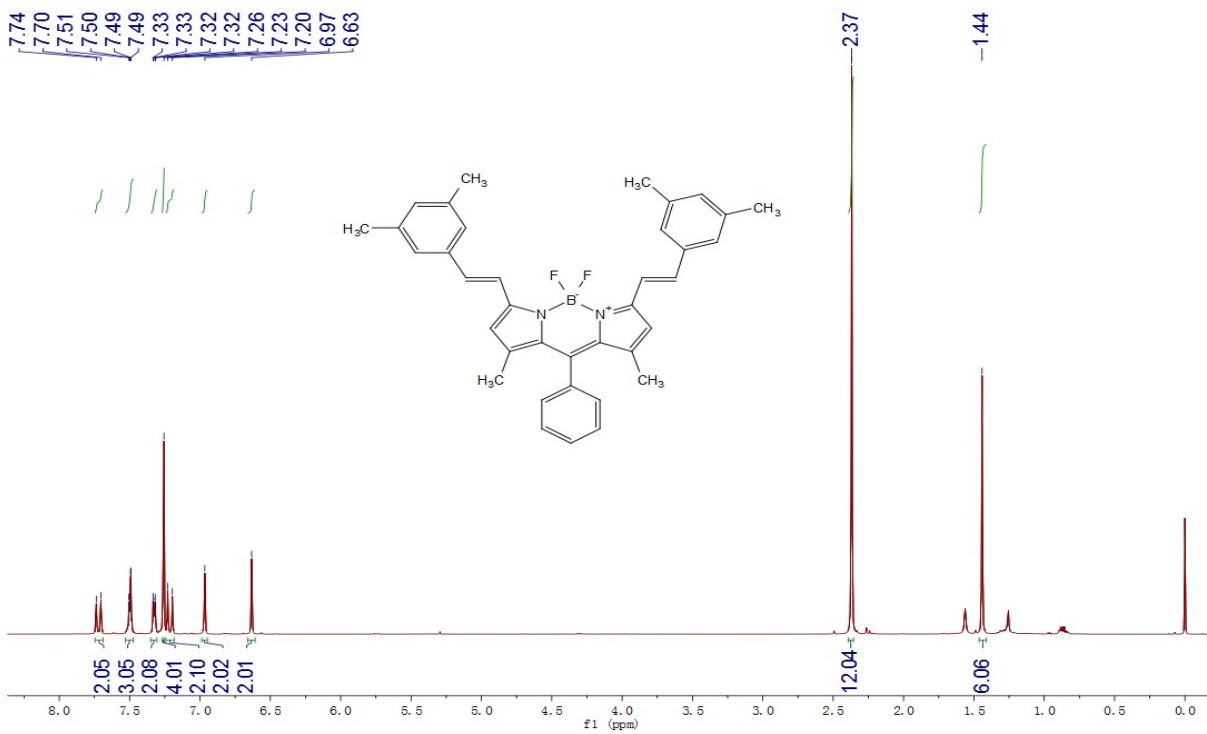


Fig. S2 ¹H NMR spectrum of BOD-JS (in CDCl₃)

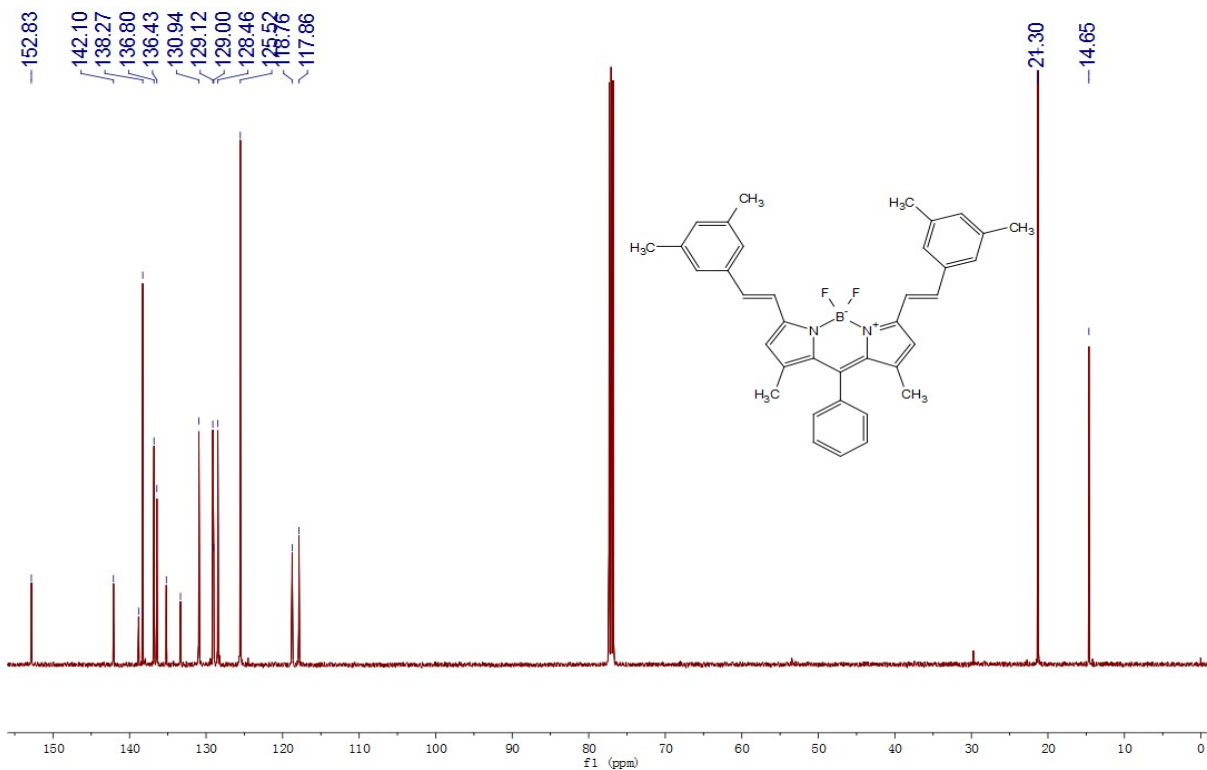


Fig. S3 ^{13}C NMR spectrum of BOD-JS (in CDCl_3).

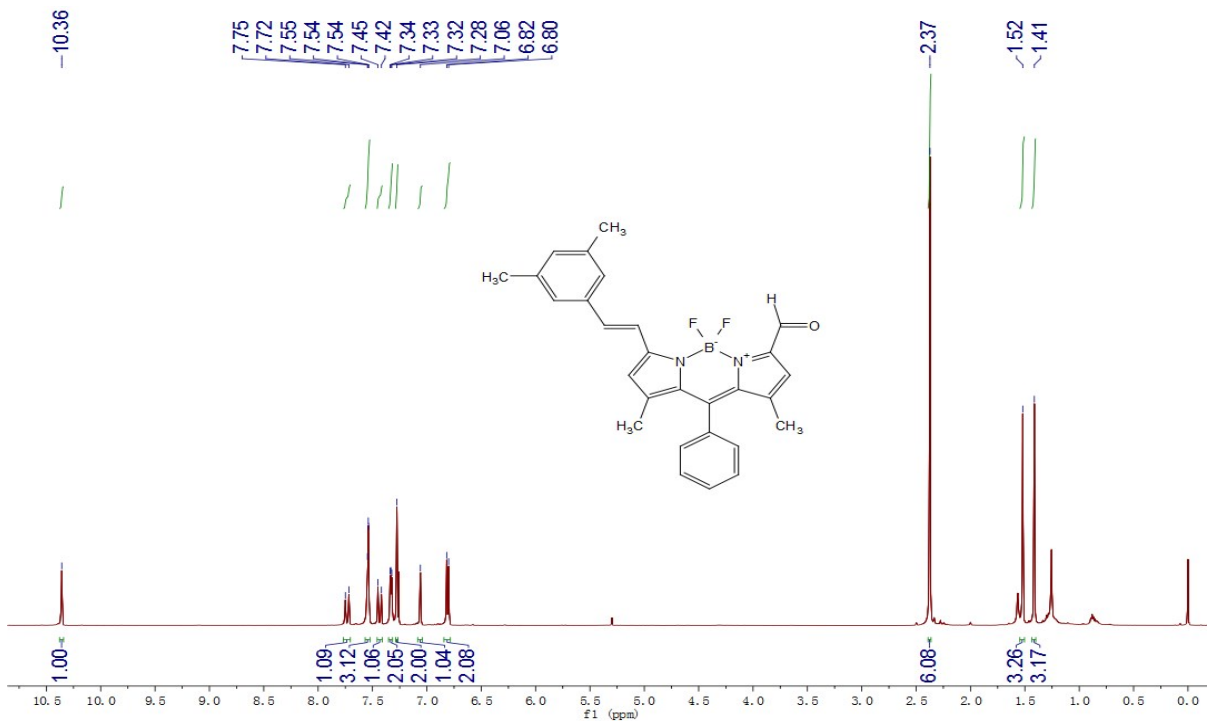


Fig. S4 ^1H NMR spectrum of BOD-JQ (in CDCl_3).

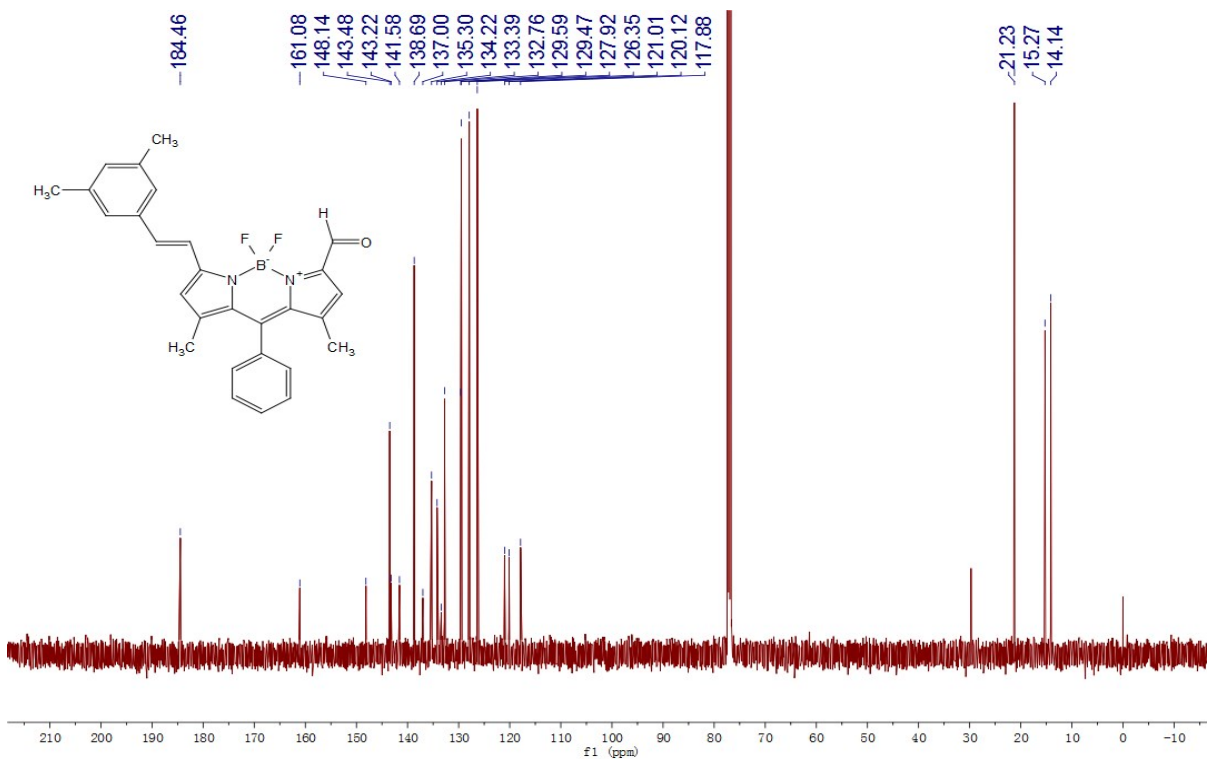


Fig. S5 ^{13}C NMR spectrum of BOD-JQ (in CDCl_3).

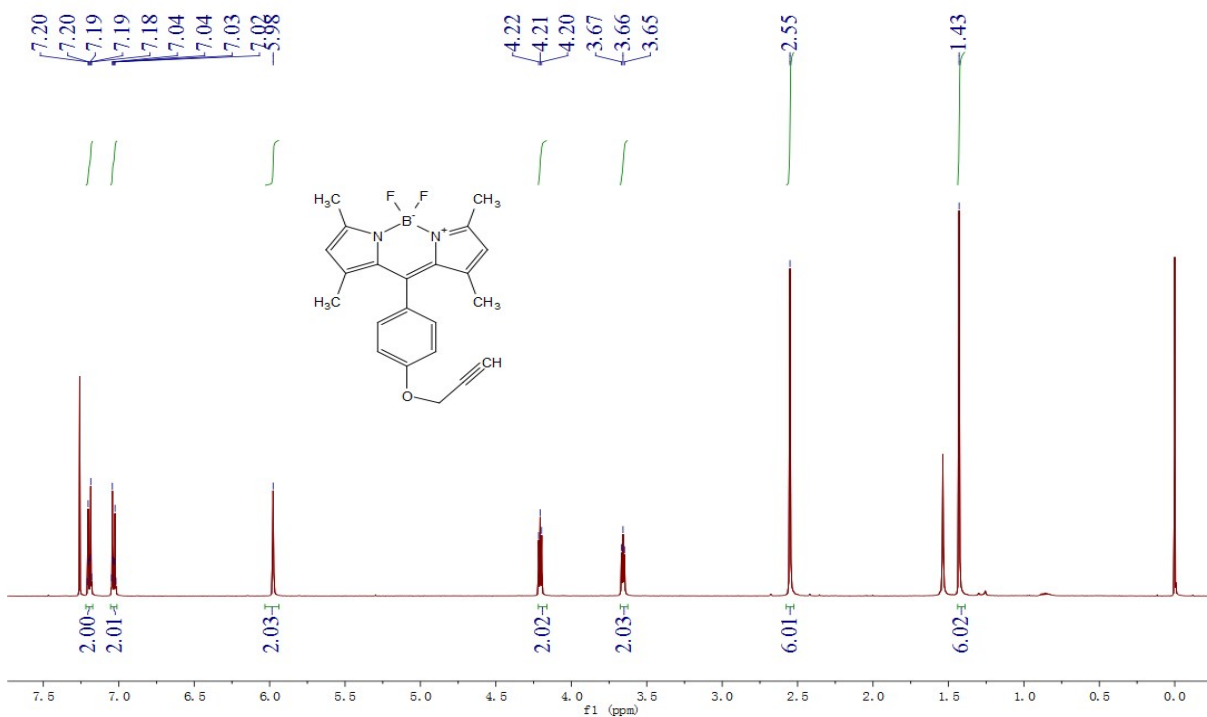


Fig. S6 ¹H NMR spectrum of BOD-Q (in CDCl₃).

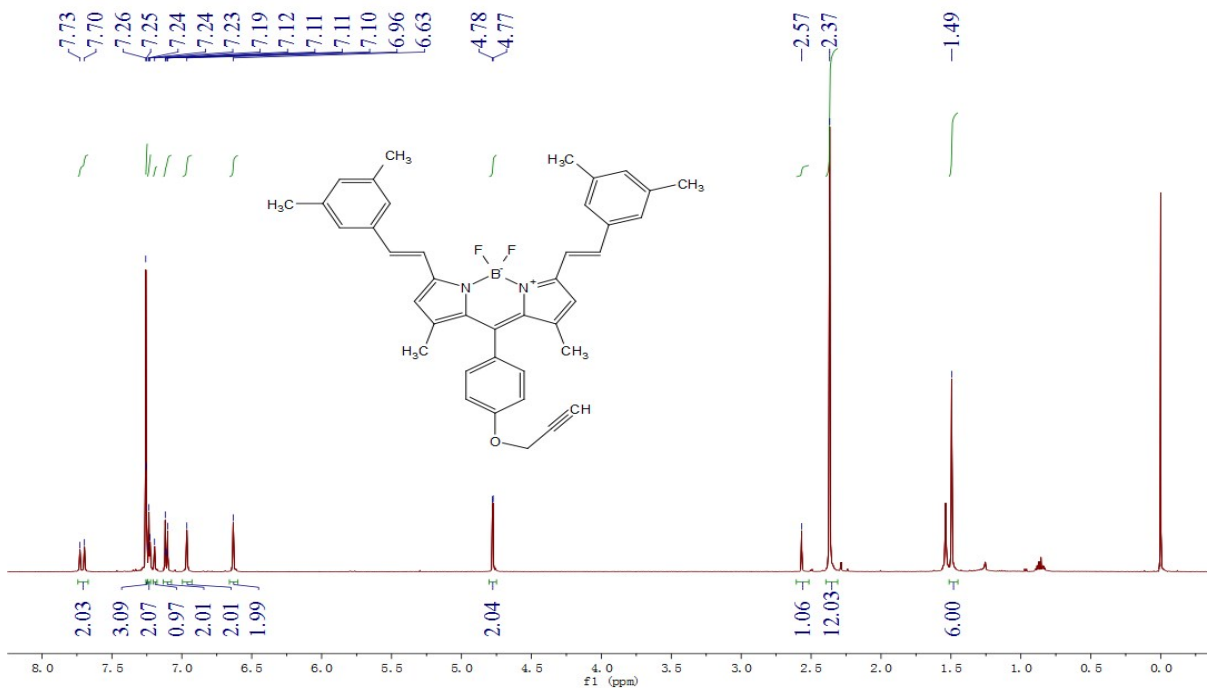


Fig. S7 ¹H NMR spectrum of BOD-QS (in CDCl₃).

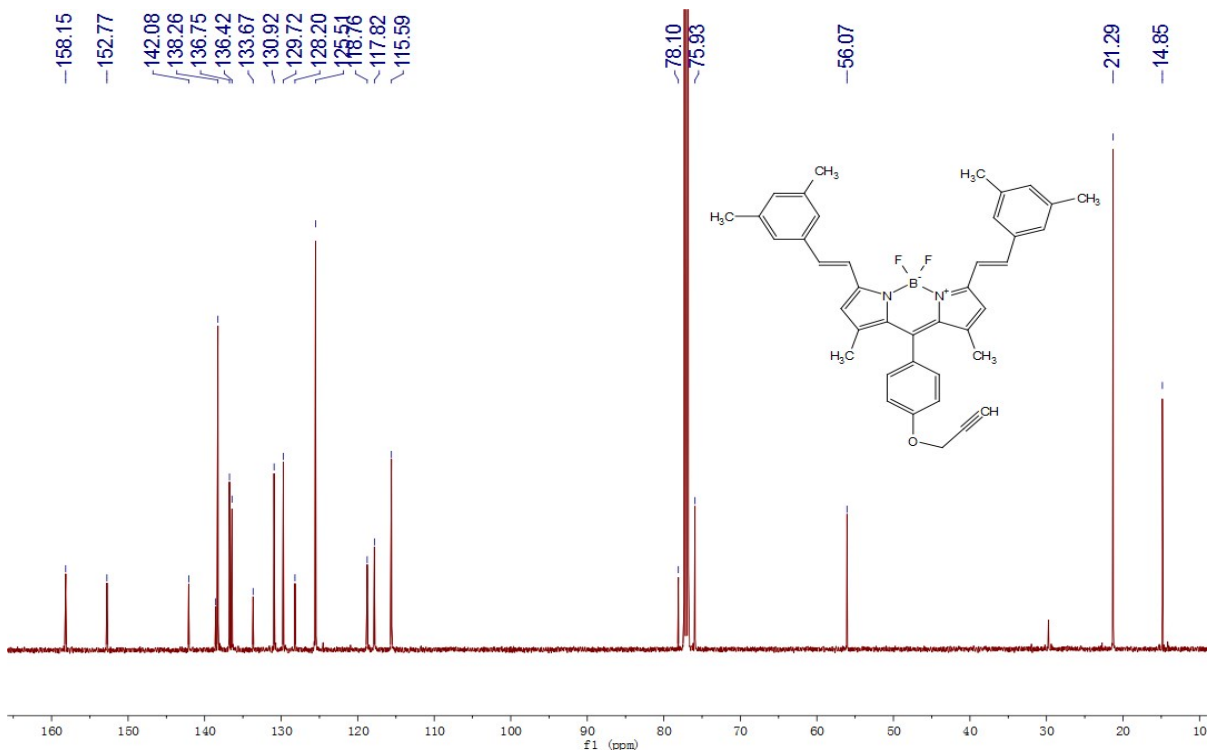


Fig. S8 ¹³C NMR spectrum of BOD-QS (in CDCl₃)

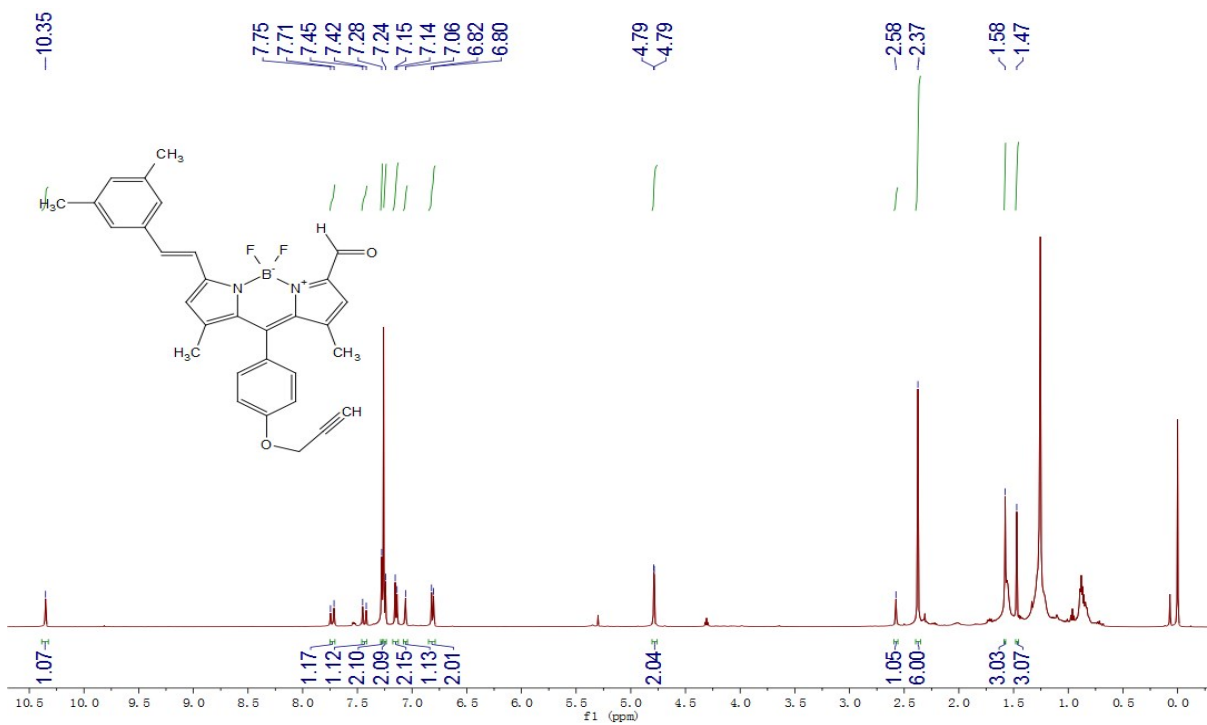


Fig. S9 ¹H NMR spectrum of BOD-QQ (in CDCl₃).

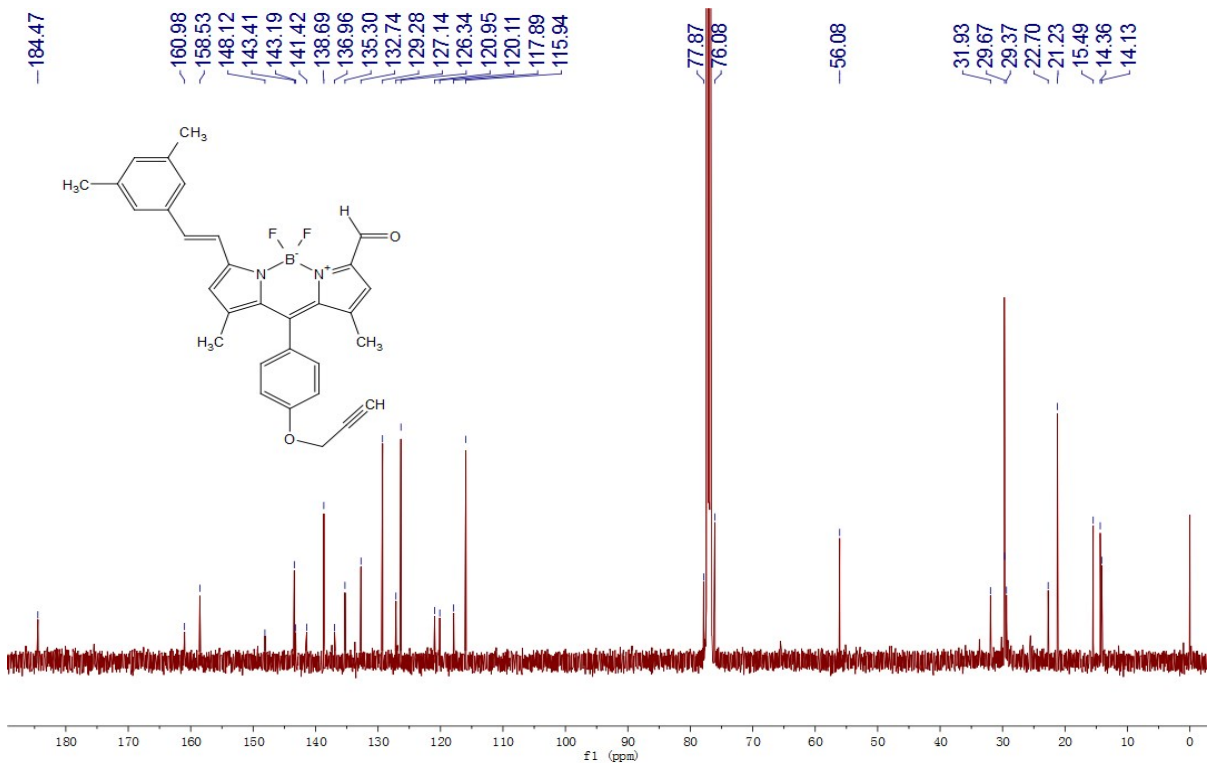


Fig. S10 ^{13}C NMR spectrum of BOD-QQ (in CDCl_3).

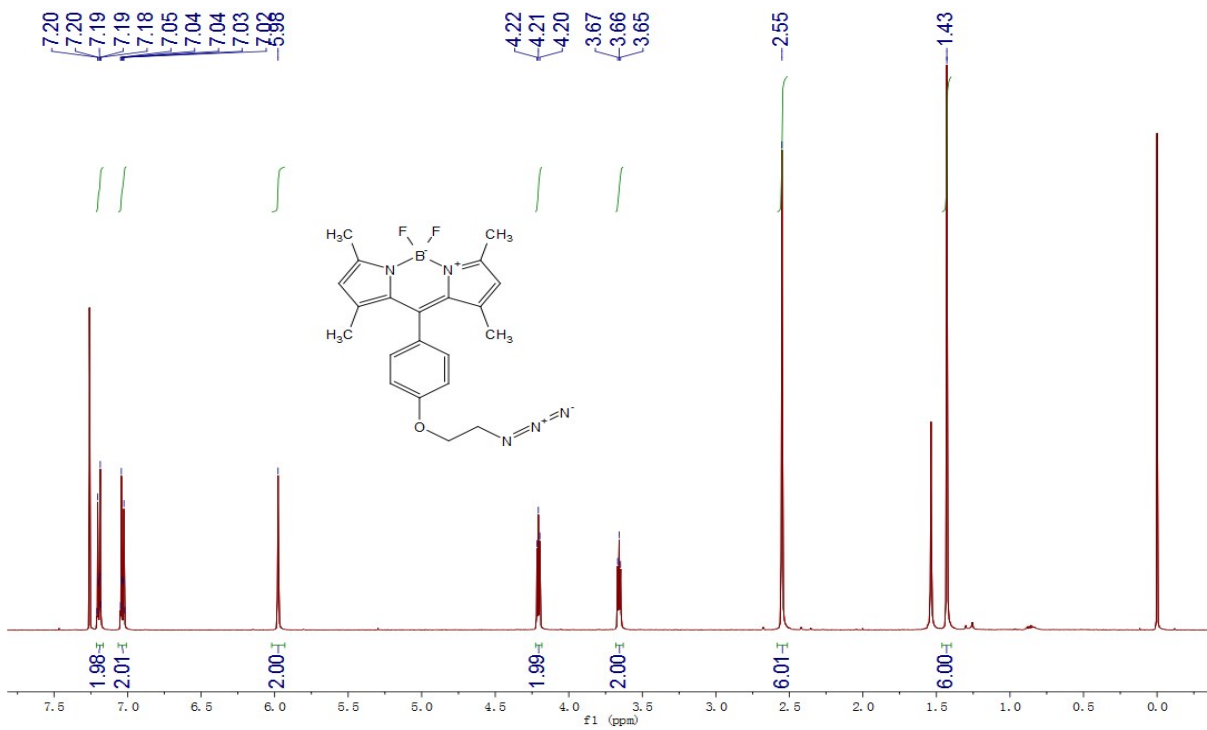


Fig. S11 ¹H NMR spectrum of BOD-D (in CDCl₃).

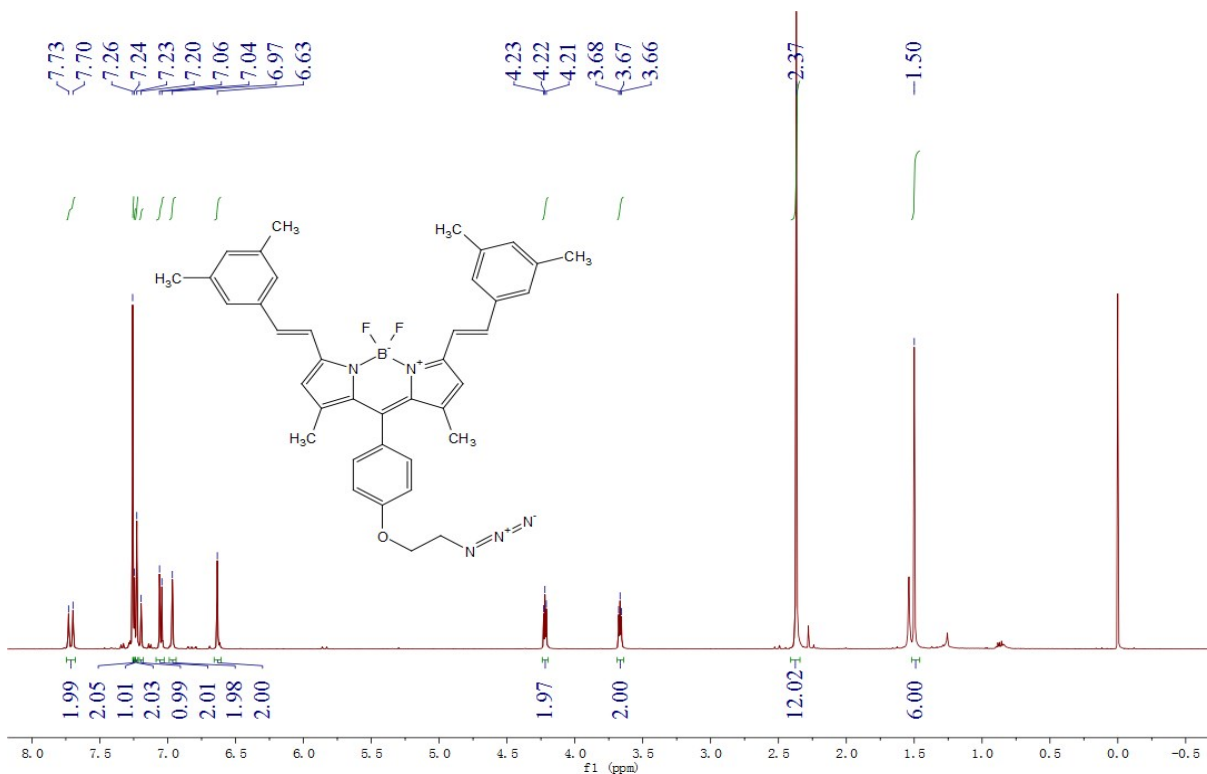


Fig. S12 ^1H NMR spectrum of BOD-DS (in CDCl_3).

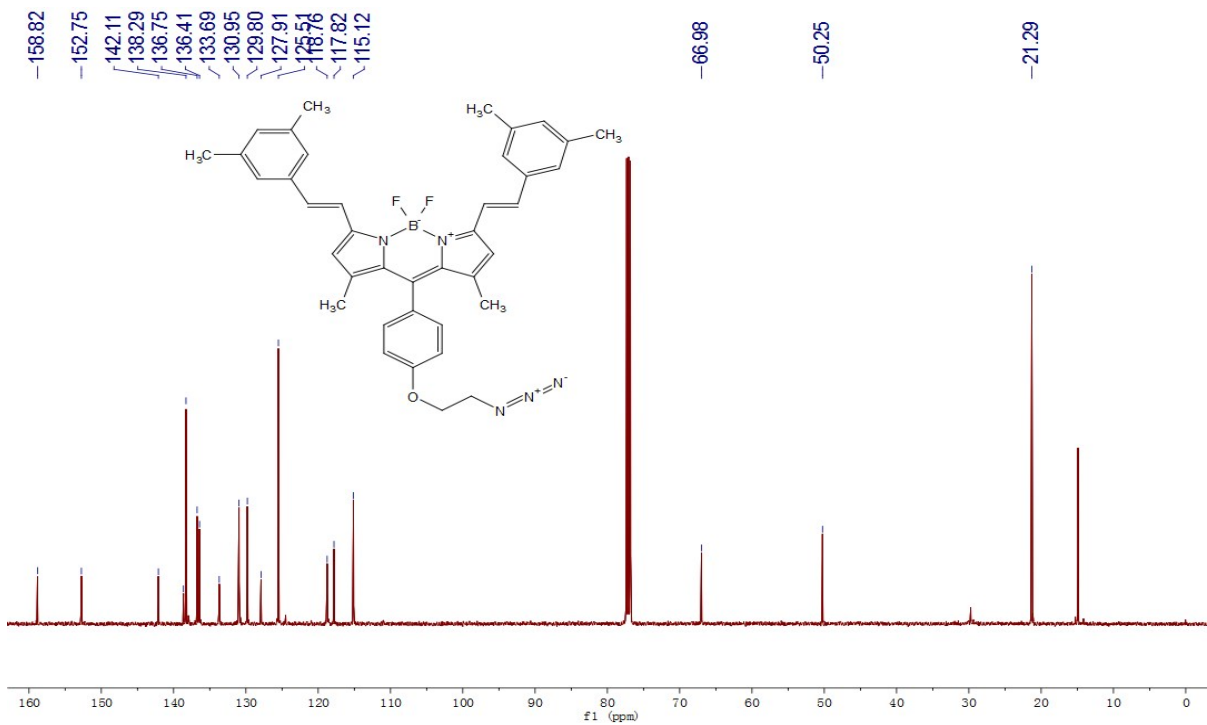


Fig. S13 ¹³C NMR spectrum of BOD-DS (in CDCl₃).

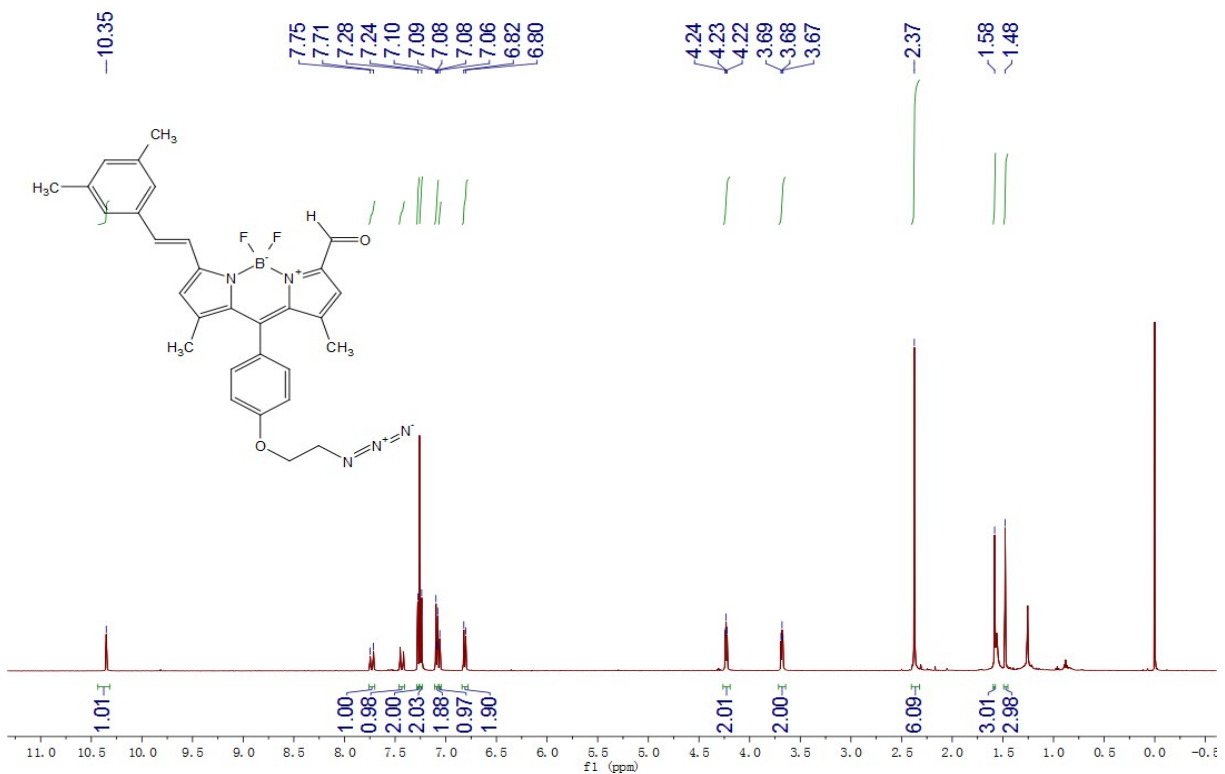


Fig. S14 ^1H NMR spectrum of BOD-DQ (in CDCl_3).

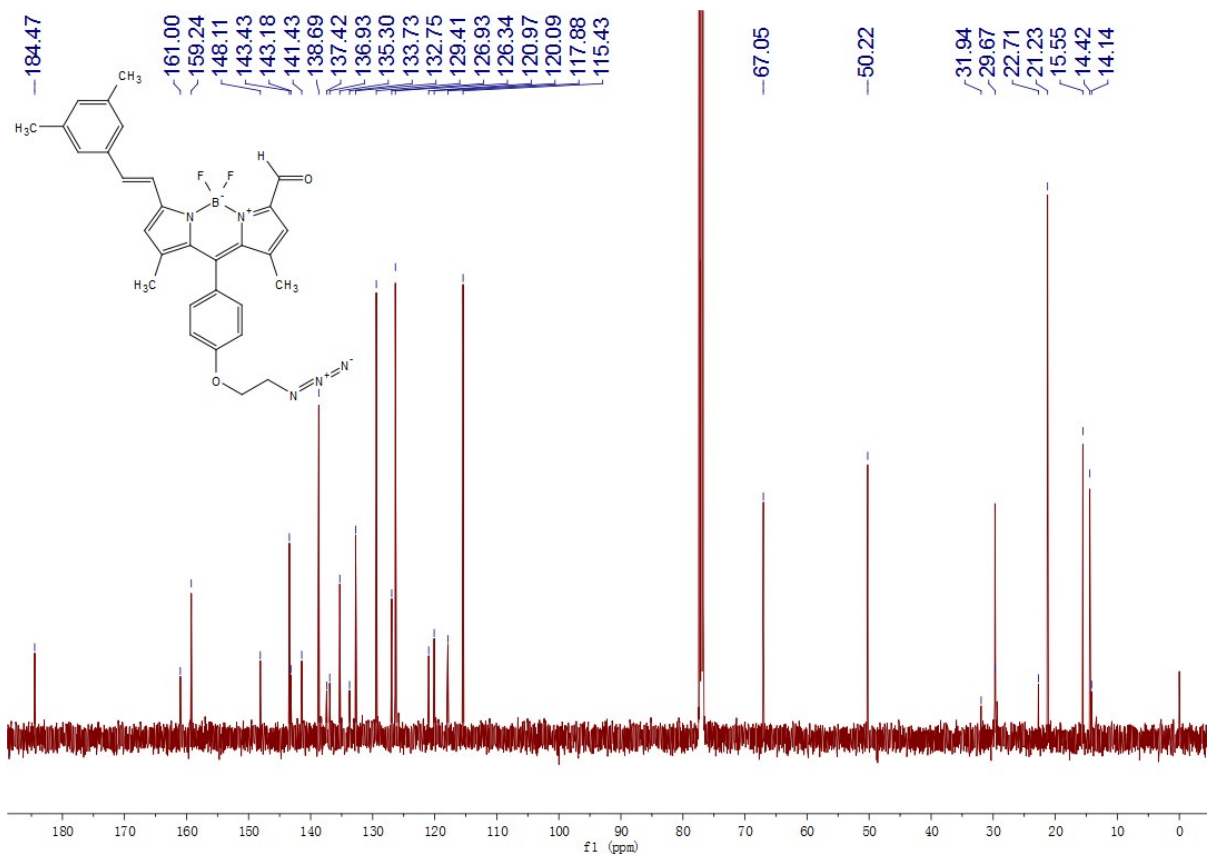


Fig. S15 ^{13}C NMR spectrum of BOD-DQ (in CDCl_3).

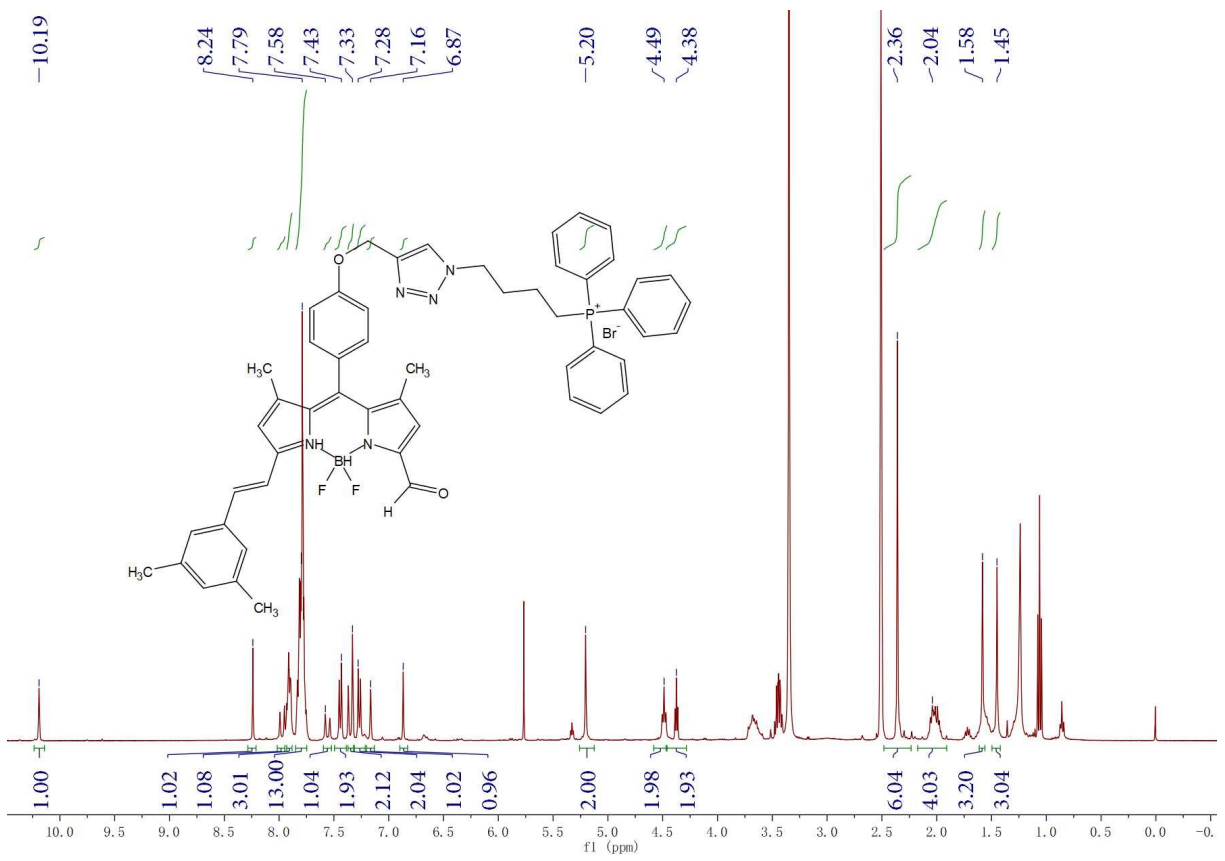


Fig. S16 ¹H NMR spectrum of BOD-PPh₃ (in d₆-DMSO).

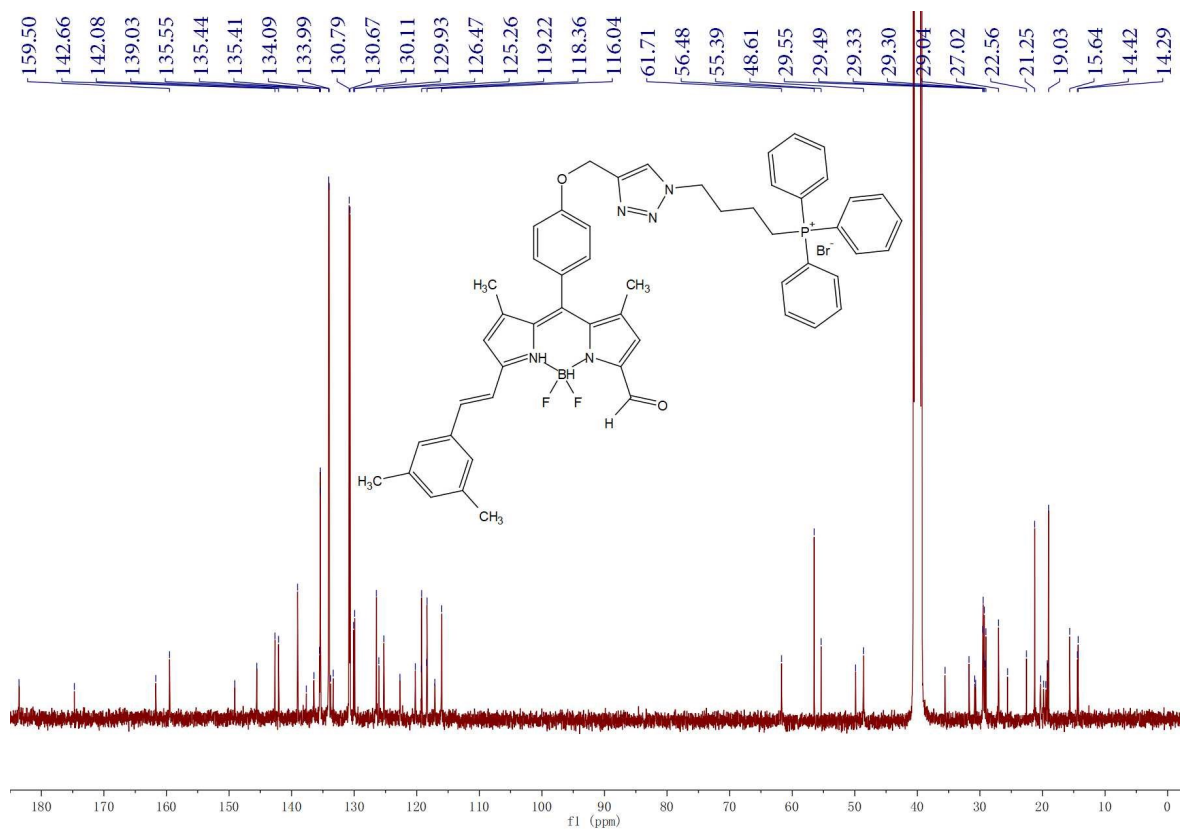


Fig. S17 ^{13}C NMR spectrum of BOD-PPh₃ (in d_6 -DMSO).

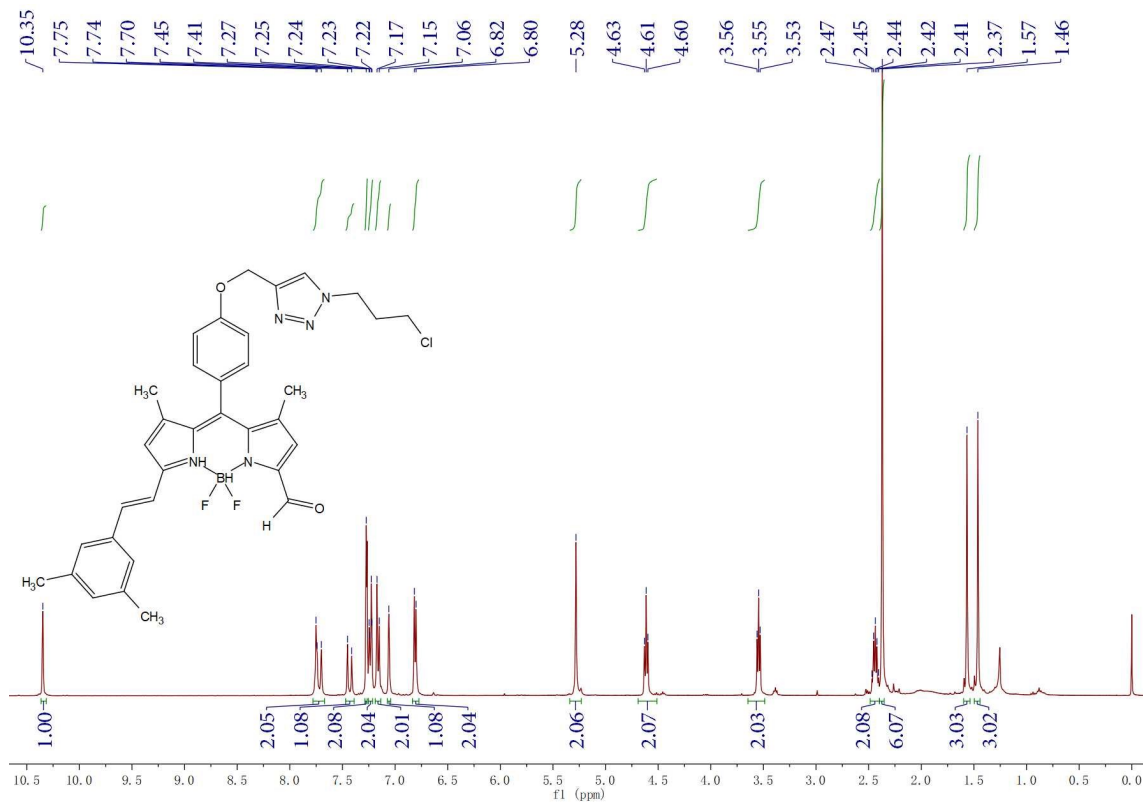


Fig. S18 ¹H NMR spectrum of BOD-Cl (in CDCl₃).

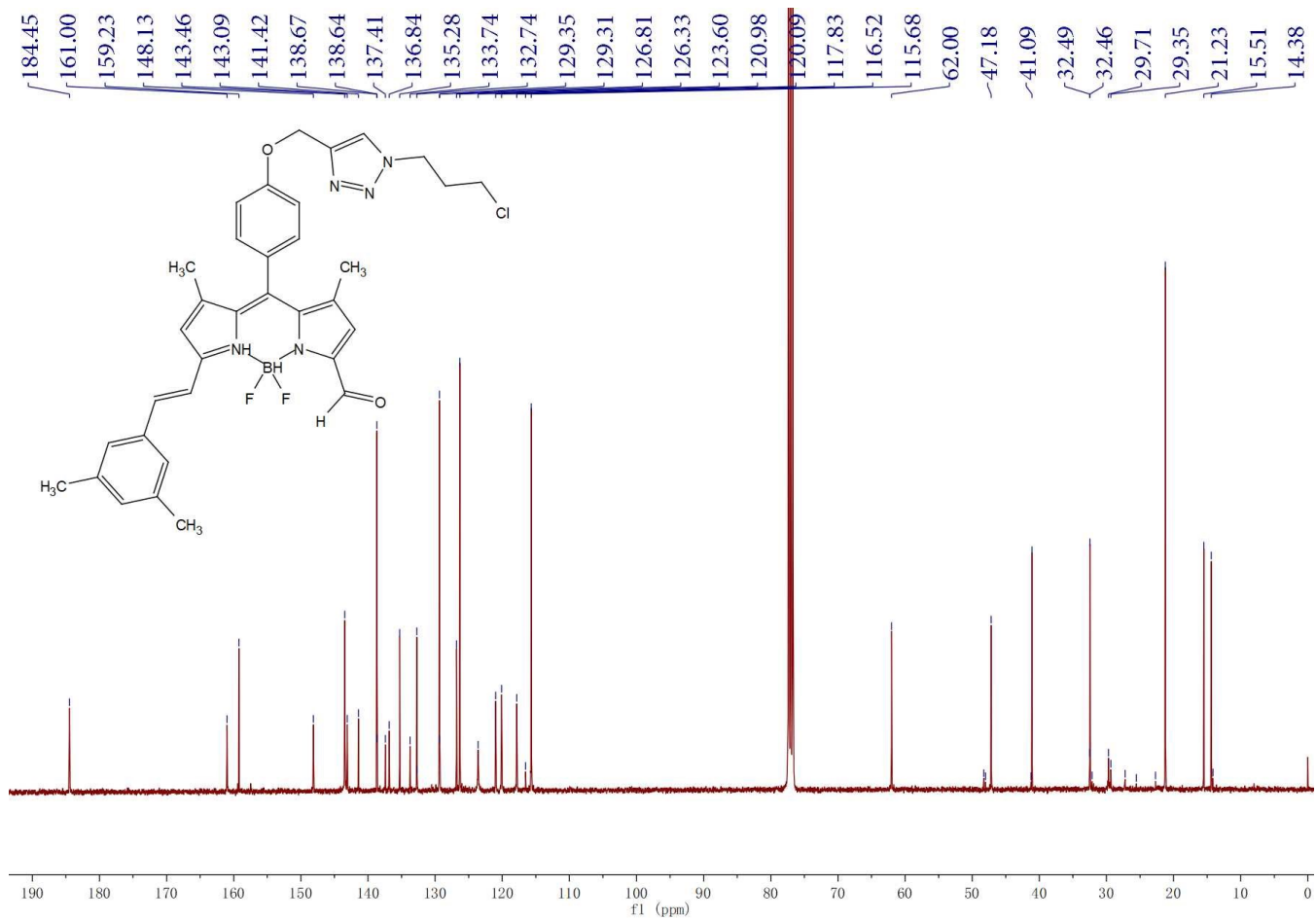


Fig. S19 ^{13}C NMR spectrum of BOD-Cl (in CDCl_3).

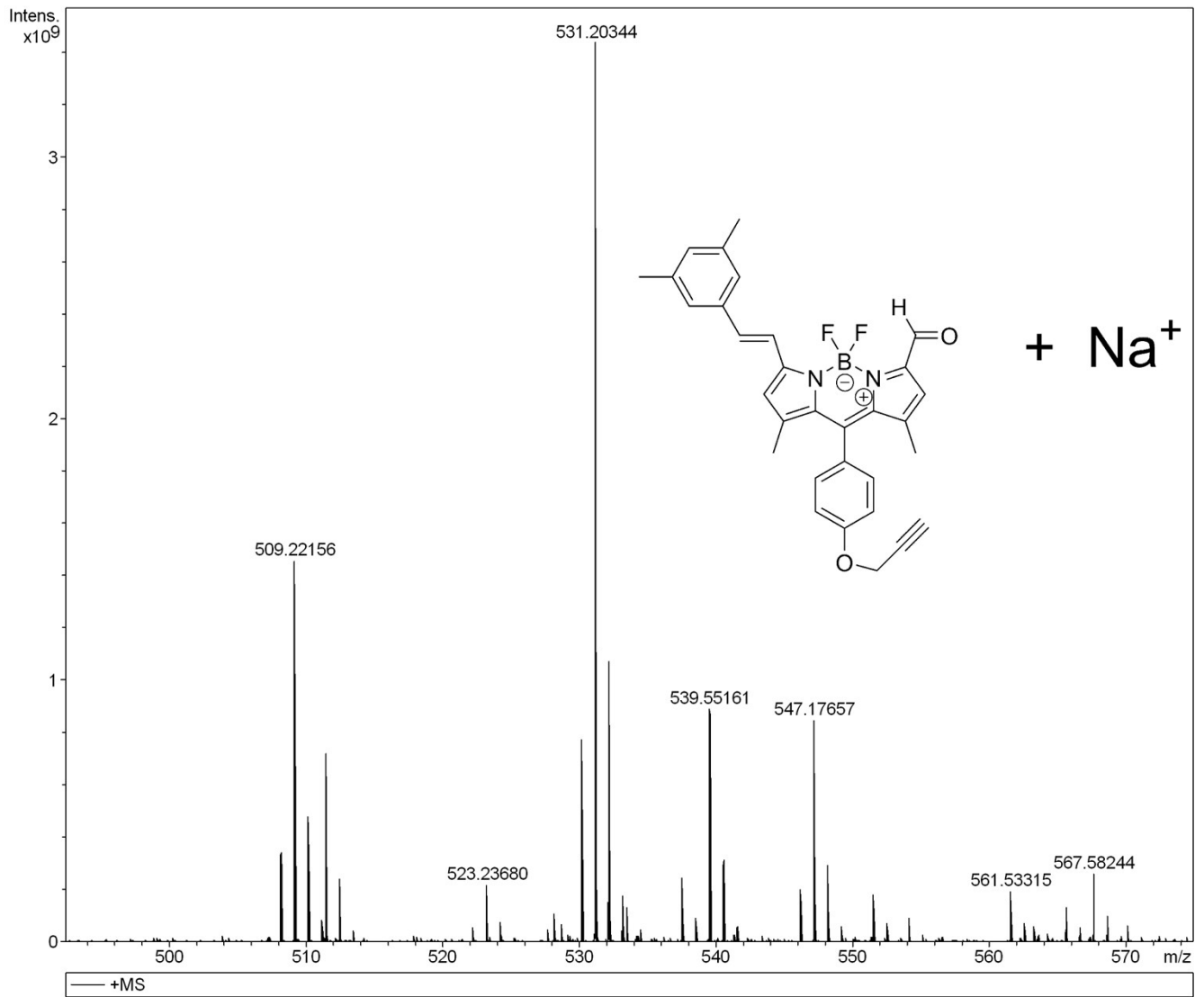


Fig. S21 HRMS spectrum of BOD-QQ.

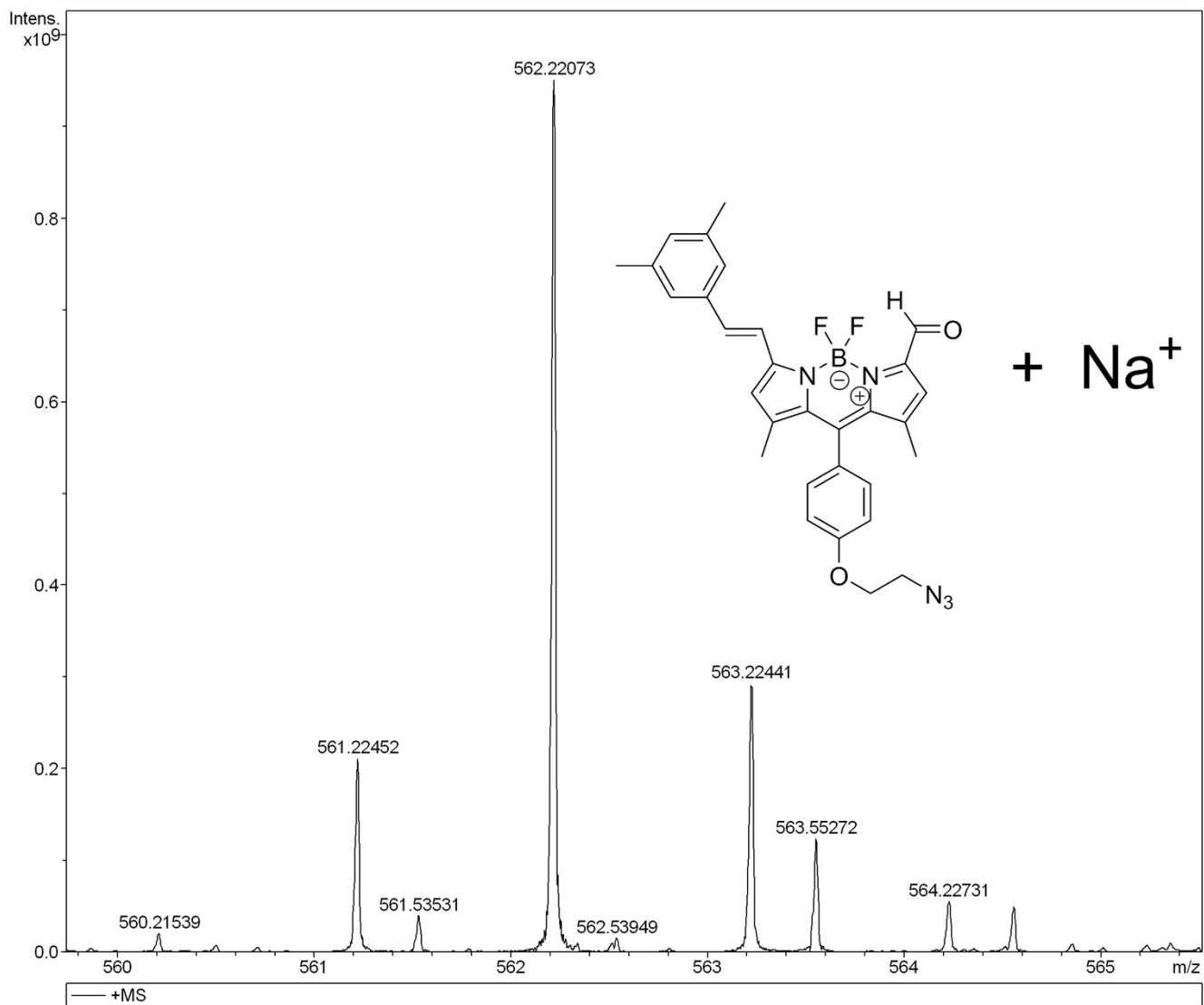


Fig. S22 HRMS spectrum of BOD-DQ.

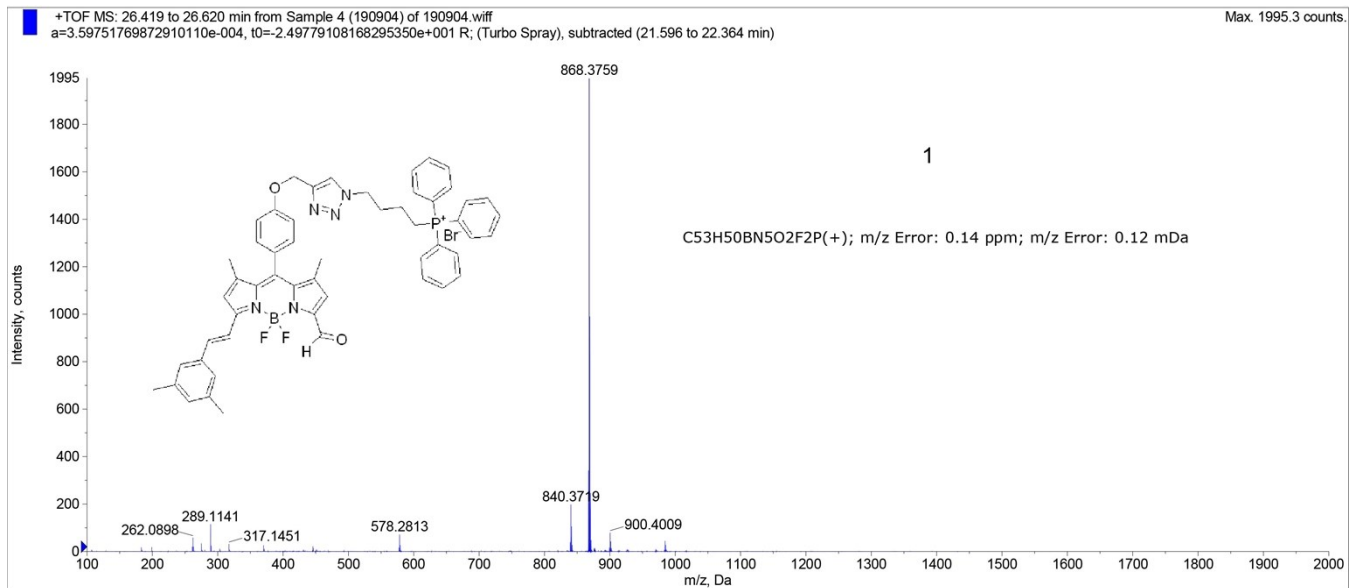


Fig. S23 HRMS spectrum of BOD-PPh₃.

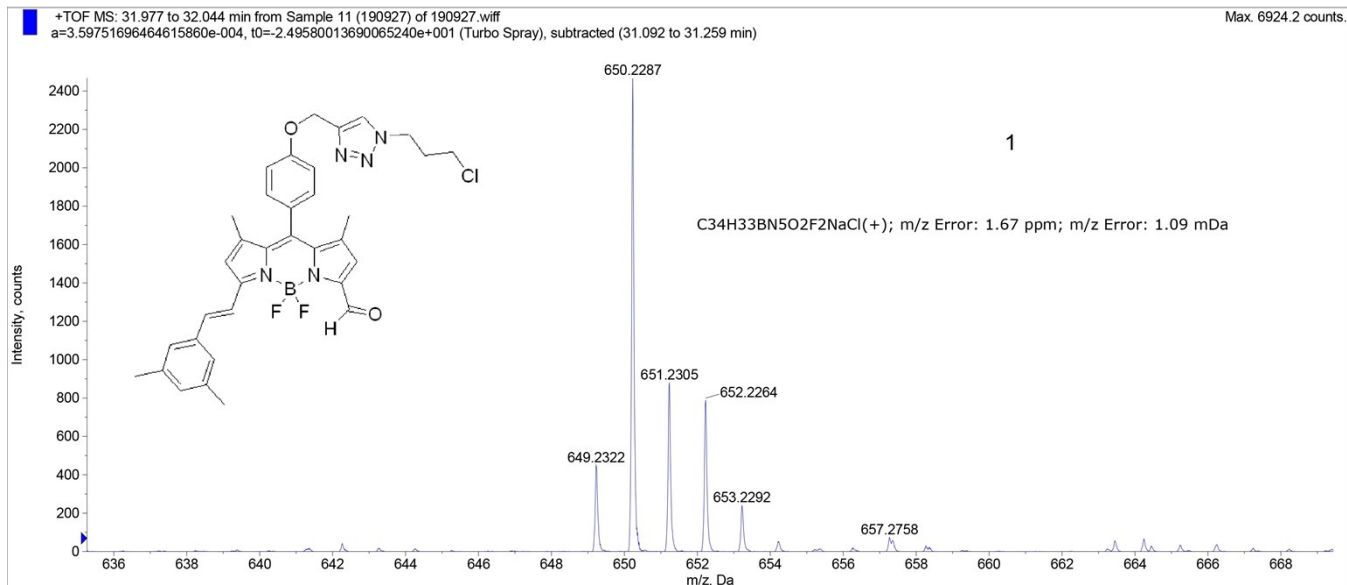


Fig. S24 HRMS spectrum of BOD-Cl.

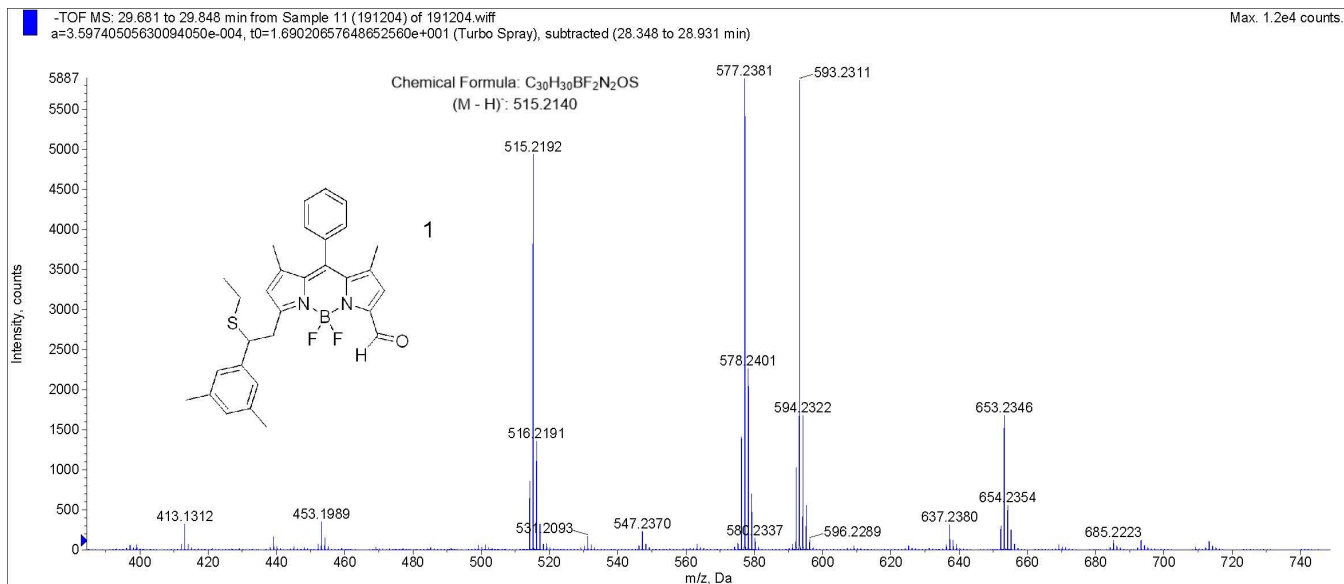


Fig. S25 HRMS spectrum of BOD-JQ-ESH.

BOD-Cys #12 RT: 0.11 AV: 1 NL: 4.19E6
T: FTMS - p ESI Full lock ms [100.0000-1000.0000]

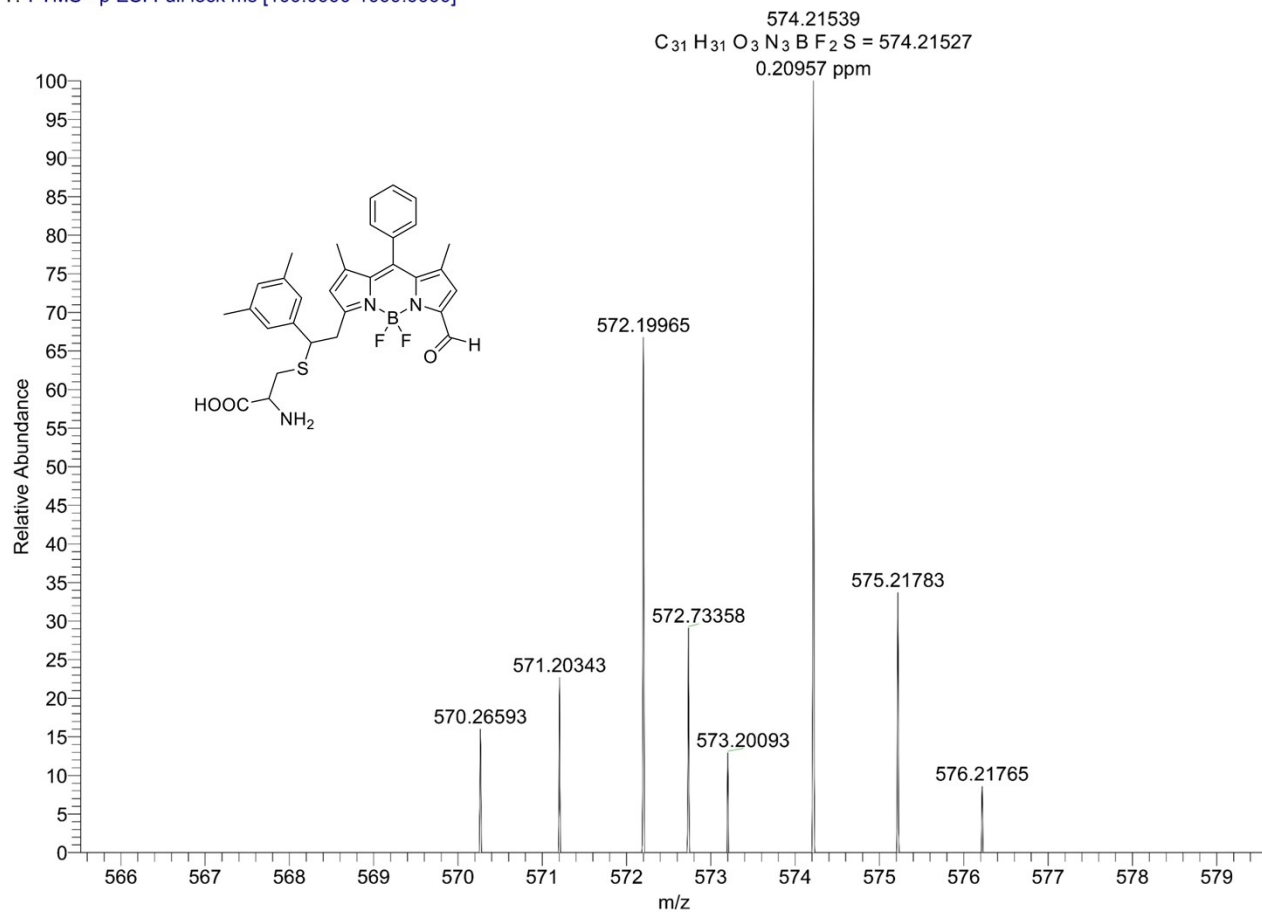


Fig. S26 HRMS spectrum of BOD-JQ-Cys.

3. UV absorbance emission spectra of BOD-JQ upon the addition of GSH, Cys and Hcy

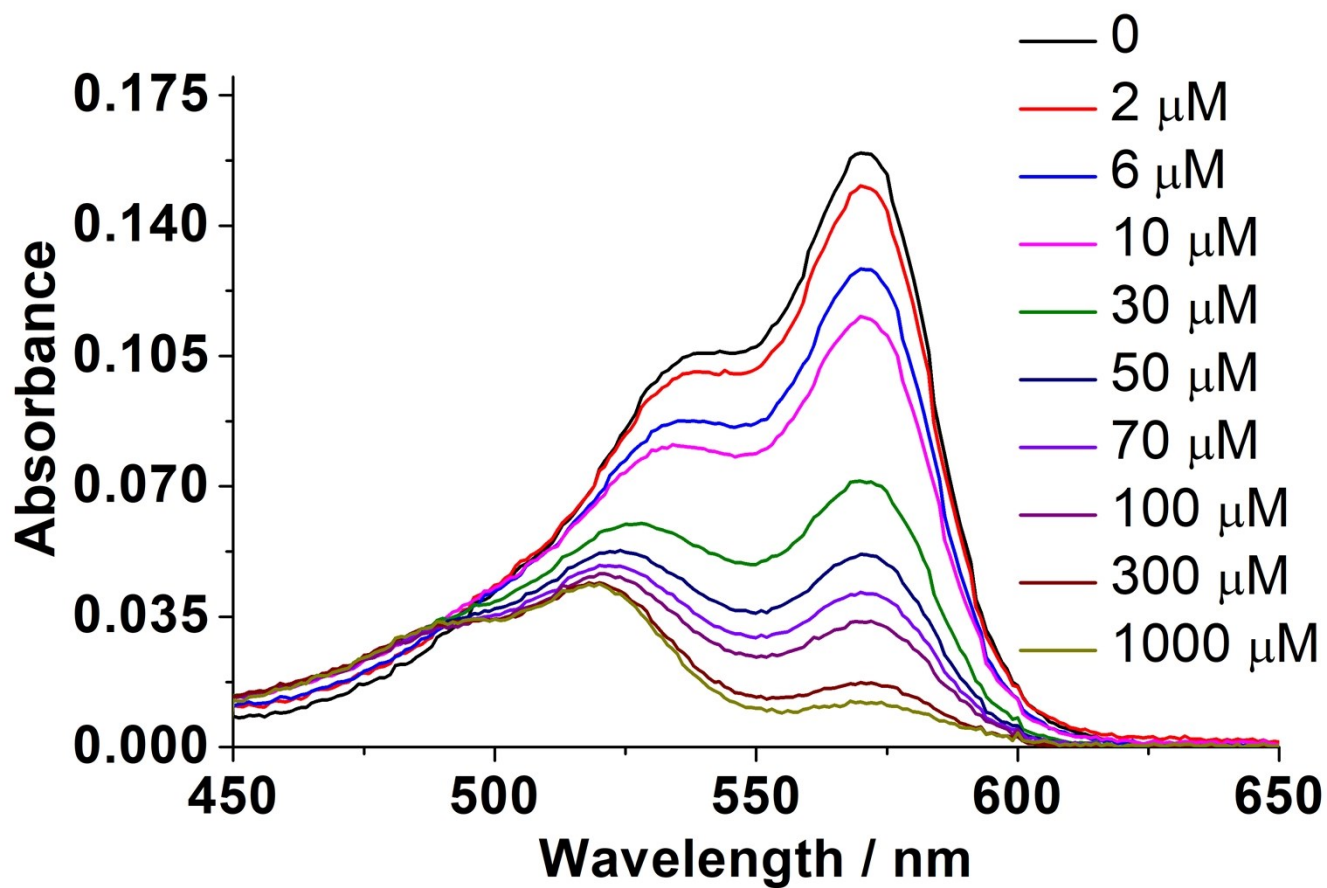


Fig. S27 UV absorbance and of BOD-JQ (5 μM) upon the addition of GSH (0, 2, 6, 10, 30, 50, 70, 100, 300, 1000 μM).

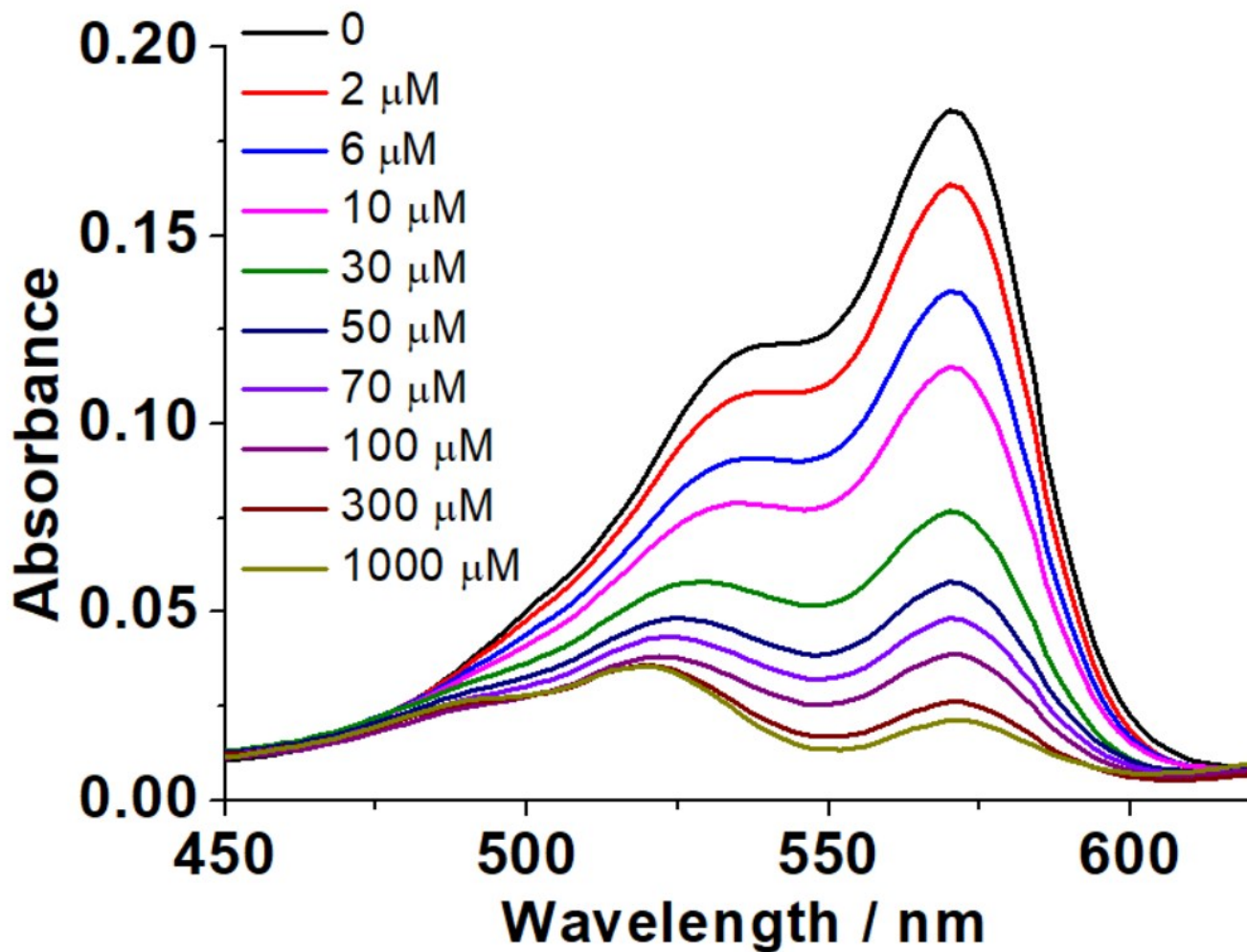


Fig. S28 UV absorbance and of BOD-JQ (5 μM) upon the addition of Cys (0, 2, 6, 10, 30, 50, 70, 100, 300, 1000 μM).

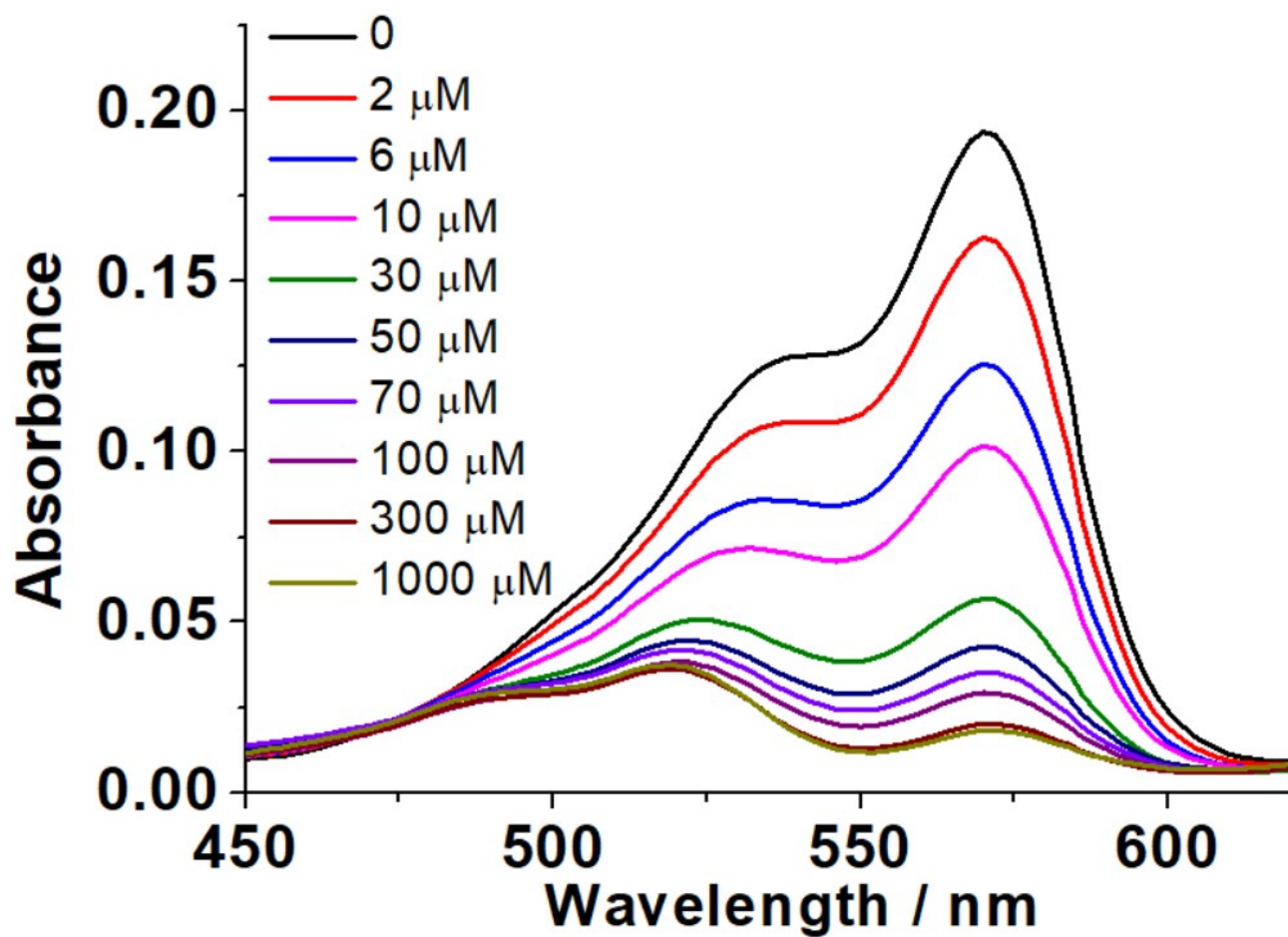


Fig. S29 UV absorbance and of BOD-JQ (5 μM) upon the addition of Hcy (0, 2, 6, 10, 30, 50, 70, 100, 300, 1000 μM).

4. The trend between fluorescence intensity ratio and the concentrations of GSH, Cys and Hcy

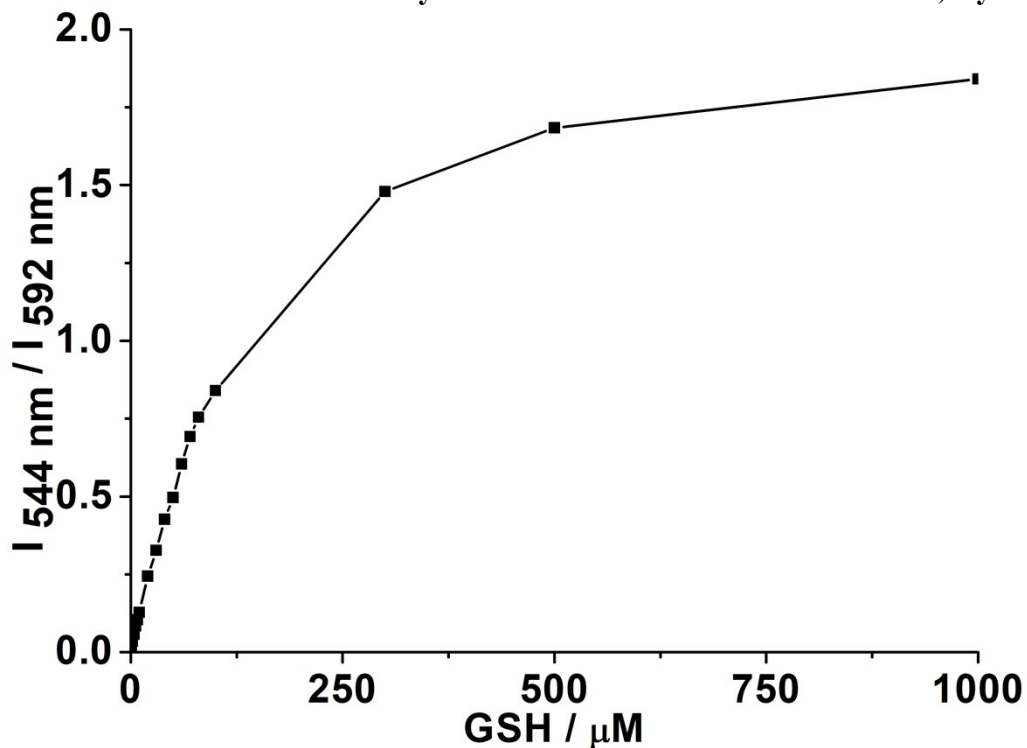


Fig. S30 Fluorescence intensity ratio ($I_{544 \text{ nm}} / I_{592 \text{ nm}}$) of BOD-JQ ($5 \mu\text{M}$) Vs the concentrations of GSH (0 -1 mM).

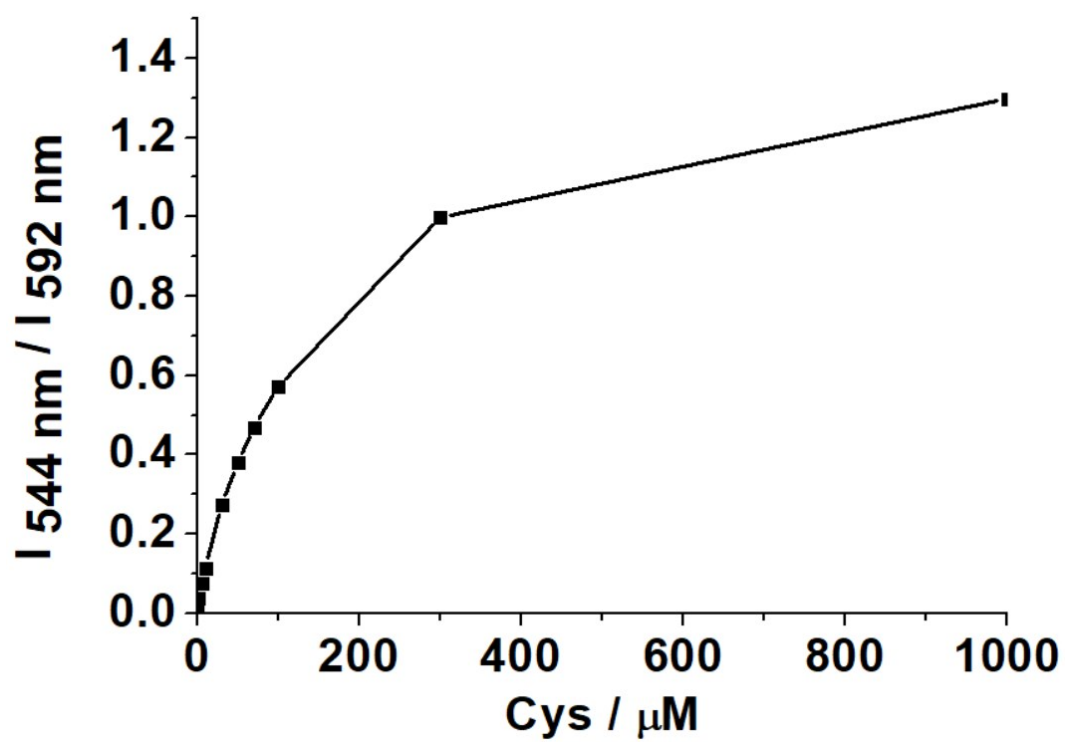


Fig. S31 Fluorescence intensity ratio ($I_{544 \text{ nm}} / I_{592 \text{ nm}}$) of BOD-JQ (5 μM) Vs the concentrations of Cys (0 -1 mM).

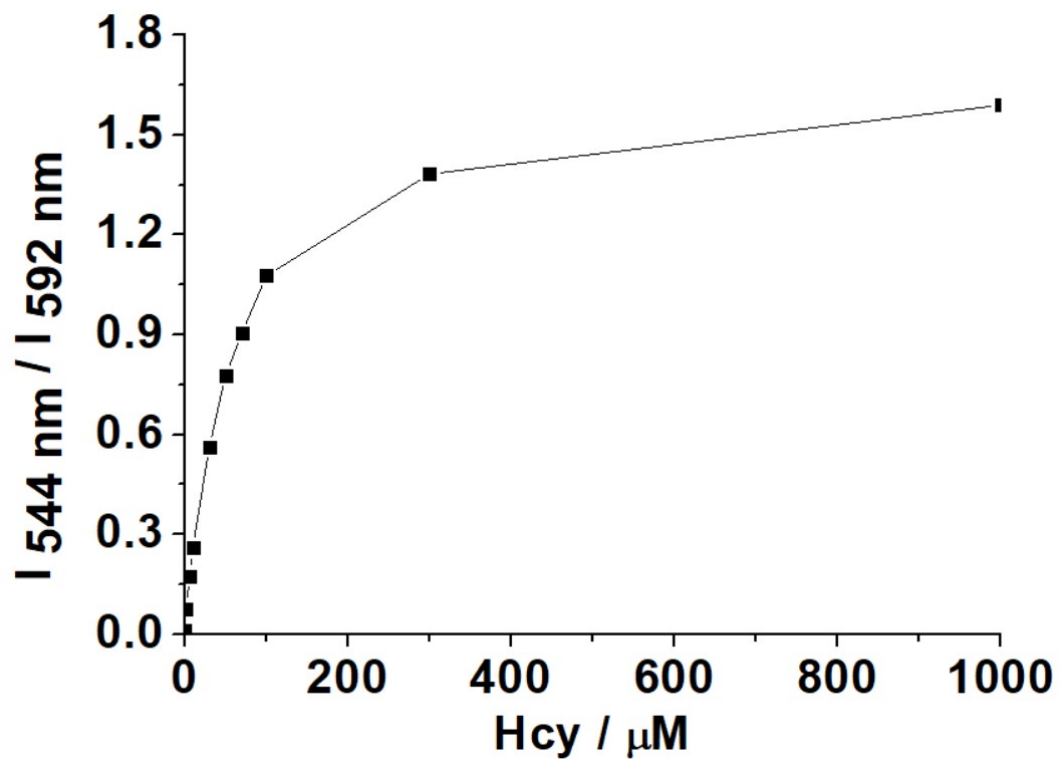


Fig. S32 Fluorescence intensity ratio ($I_{544 \text{ nm}} / I_{592 \text{ nm}}$) of BOD-JQ (5 μM) Vs the concentrations of Hcy (0 -1 mM).

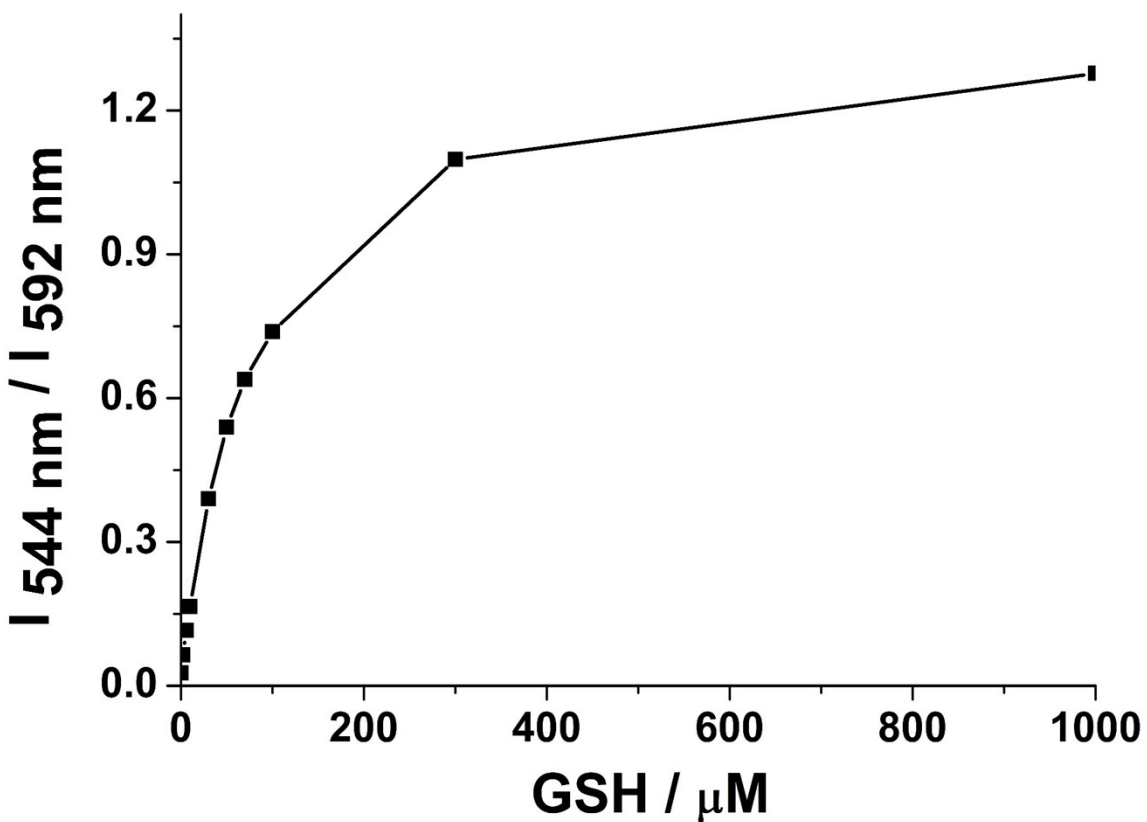


Fig. S33 Fluorescence intensity ratio ($I_{544 \text{ nm}} / I_{592 \text{ nm}}$) of BOD-PPh3 (5 μM) Vs the concentrations of GSH (0 -1 mM).

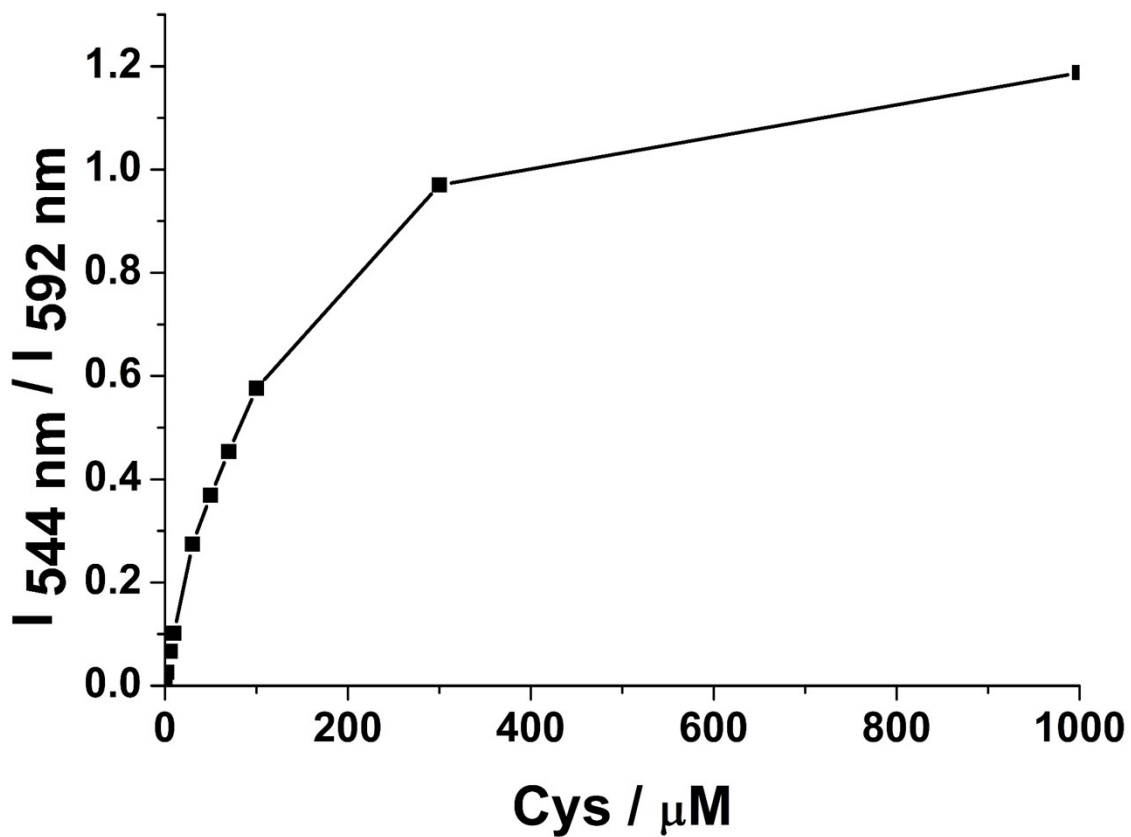


Fig. S34 Fluorescence intensity ratio ($I_{544 \text{ nm}} / I_{592 \text{ nm}}$) of BOD-PPh3 (5 μM) Vs the concentrations of Cys (0 -1 mM).

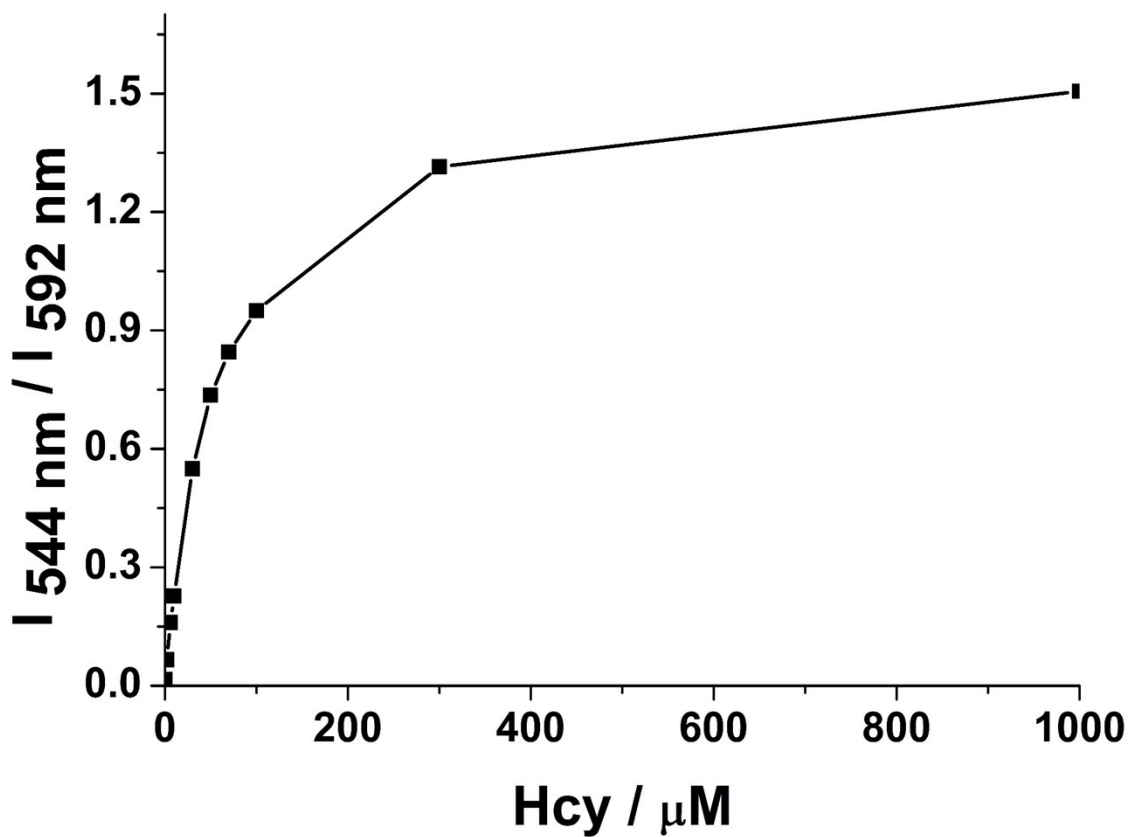


Fig. S35 Fluorescence intensity ratio ($I_{544 \text{ nm}} / I_{592 \text{ nm}}$) of BOD-PPh3 (5 μM) Vs the concentrations of Hcy (0 -1 mM).

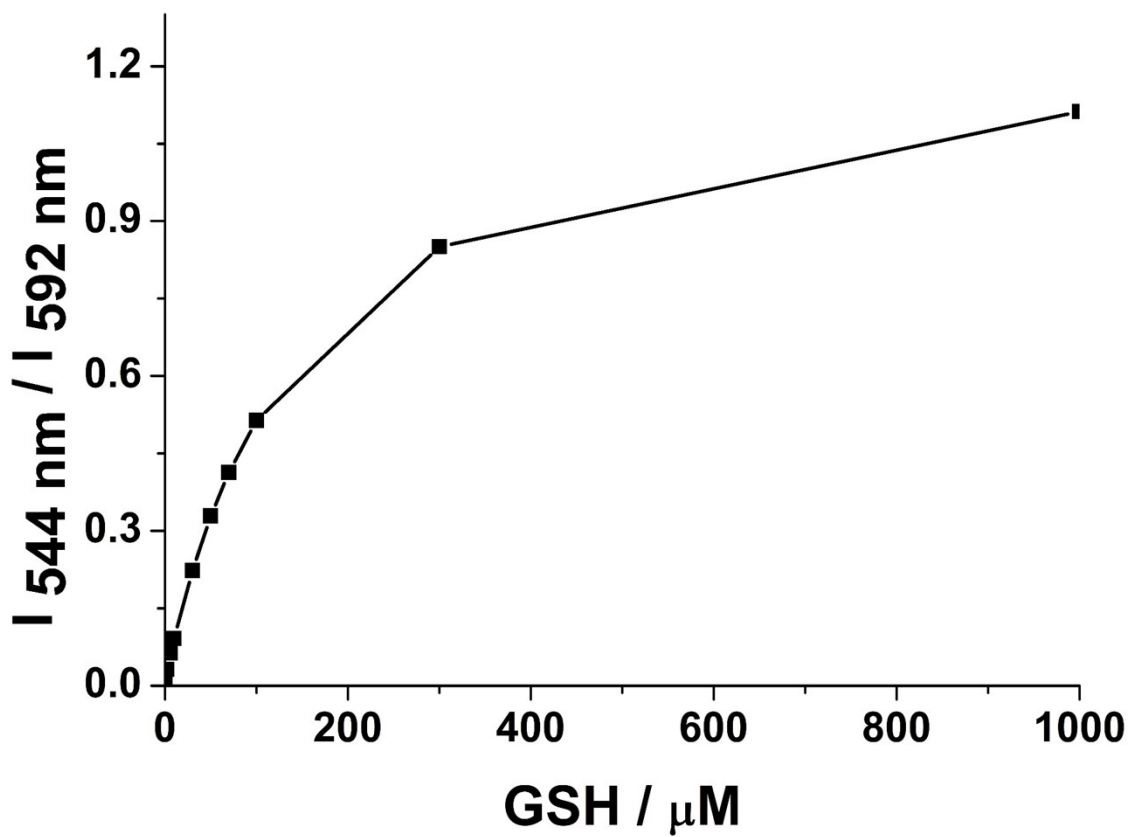


Fig. S36 Fluorescence intensity ratio ($I_{544 \text{ nm}} / I_{592 \text{ nm}}$) of BOD-Cl ($5 \mu\text{M}$) Vs the concentrations of GSH (0 -1 mM).

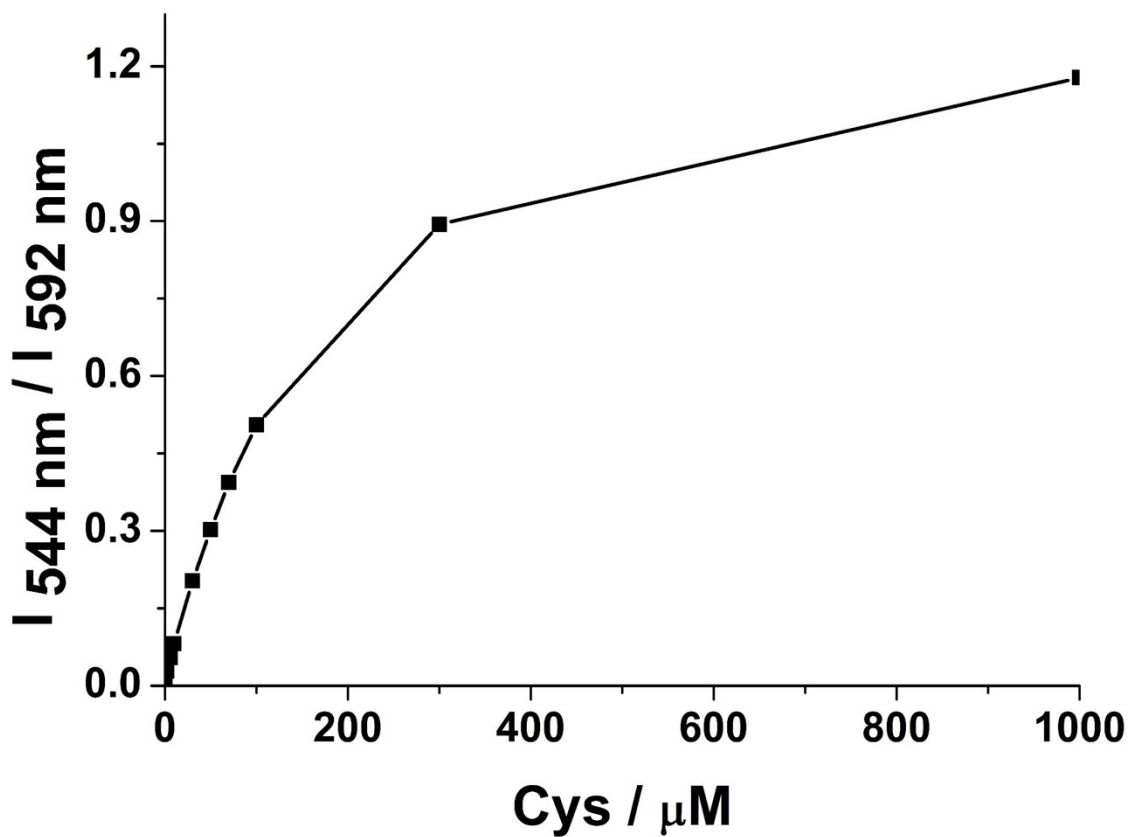


Fig S37 Fluorescence intensity ratio ($I_{544 \text{ nm}} / I_{592 \text{ nm}}$) of BOD-Cl (5 μM) Vs the concentrations of Cys (0 -1 mM).

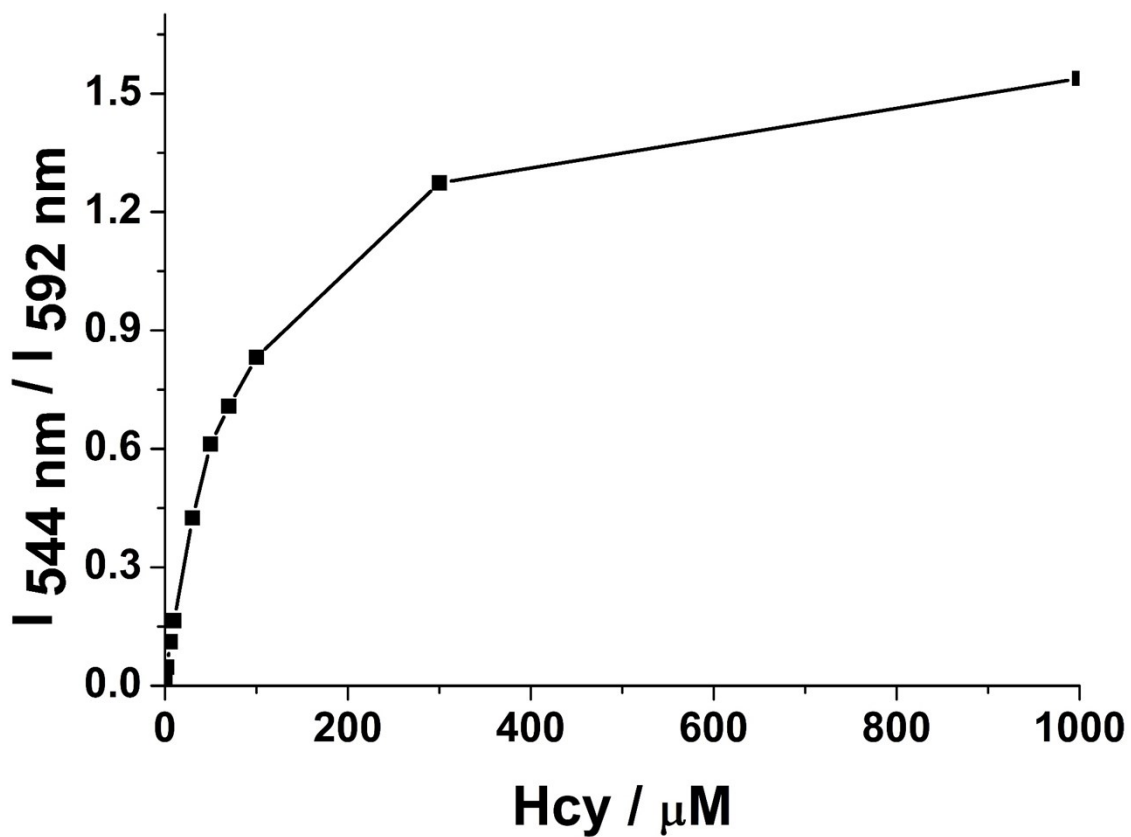


Fig. S38 Fluorescence intensity ratio ($I_{544 \text{ nm}} / I_{592 \text{ nm}}$) of BOD-Cl ($5 \mu\text{M}$) Vs the concentrations of Hcy (0 -1 mM).

5. Fluorescence emission spectra in the presence of biothiols

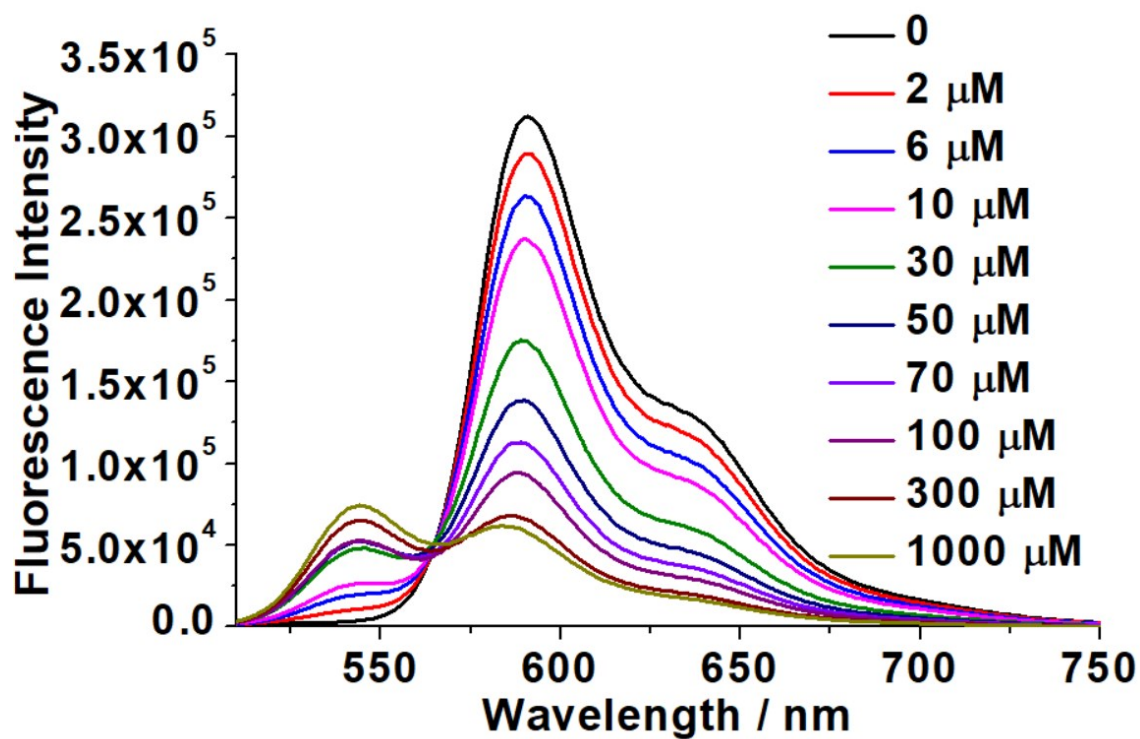


Fig. S39 Fluorescence emission spectra ($\lambda_{\text{ex}} = 510$ nm) of BOD-JQ (5 μM) upon the addition of Cys (0, 2, 6, 10, 30, 50, 70, 100, 300, 1000 μM).

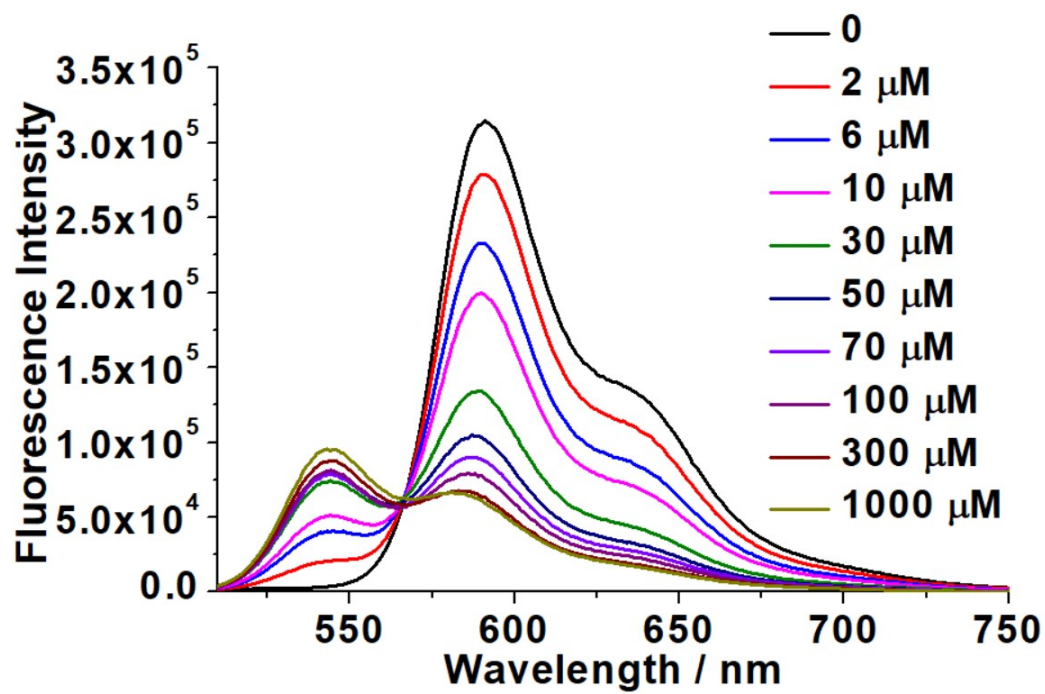


Fig. S40 Fluorescence emission spectra ($\lambda_{\text{ex}} = 510 \text{ nm}$) of BOD-JQ ($5 \mu\text{M}$) upon the addition of Hcy (0, 2, 6, 10, 30, 50, 70, 100, 300, 1000 μM).

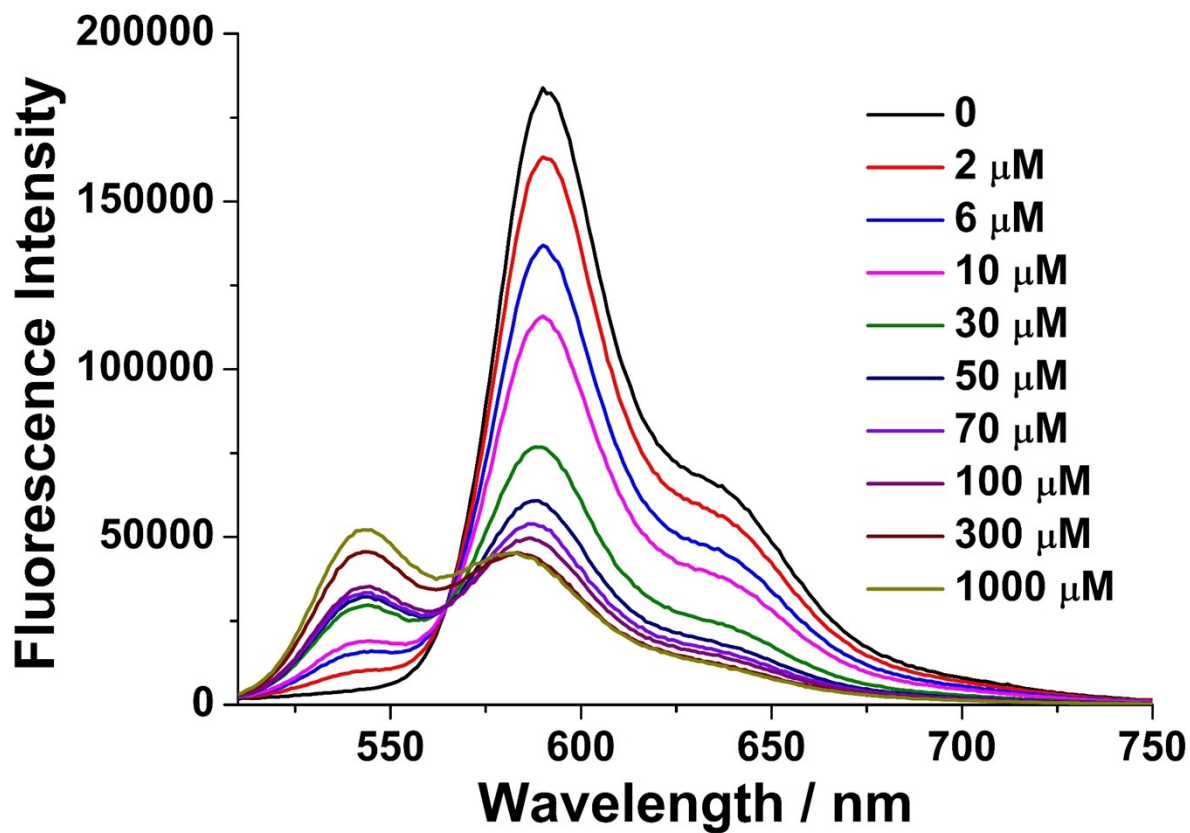


Fig. S41 Fluorescence emission spectra ($\lambda_{\text{ex}} = 510 \text{ nm}$) of BOD-PPh3 (5 μM) upon the addition of GSH (0, 2, 6, 10, 30, 50, 70, 100, 300, 1000 μM).

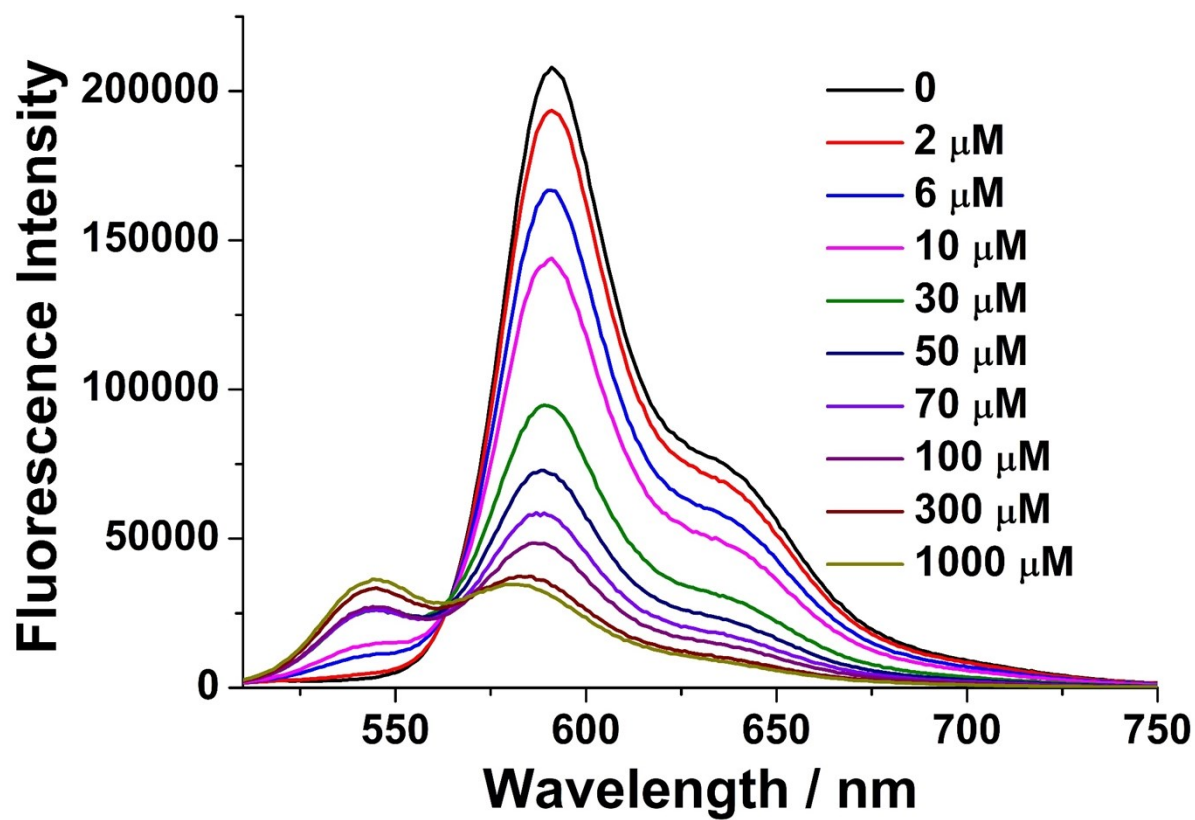


Fig. S42 Fluorescence emission spectra ($\lambda_{\text{ex}} = 510 \text{ nm}$) of BOD-PPh3 (5 μM) upon the addition of Cys (0, 2, 6, 10, 30, 50, 70, 100, 300, 1000 μM).

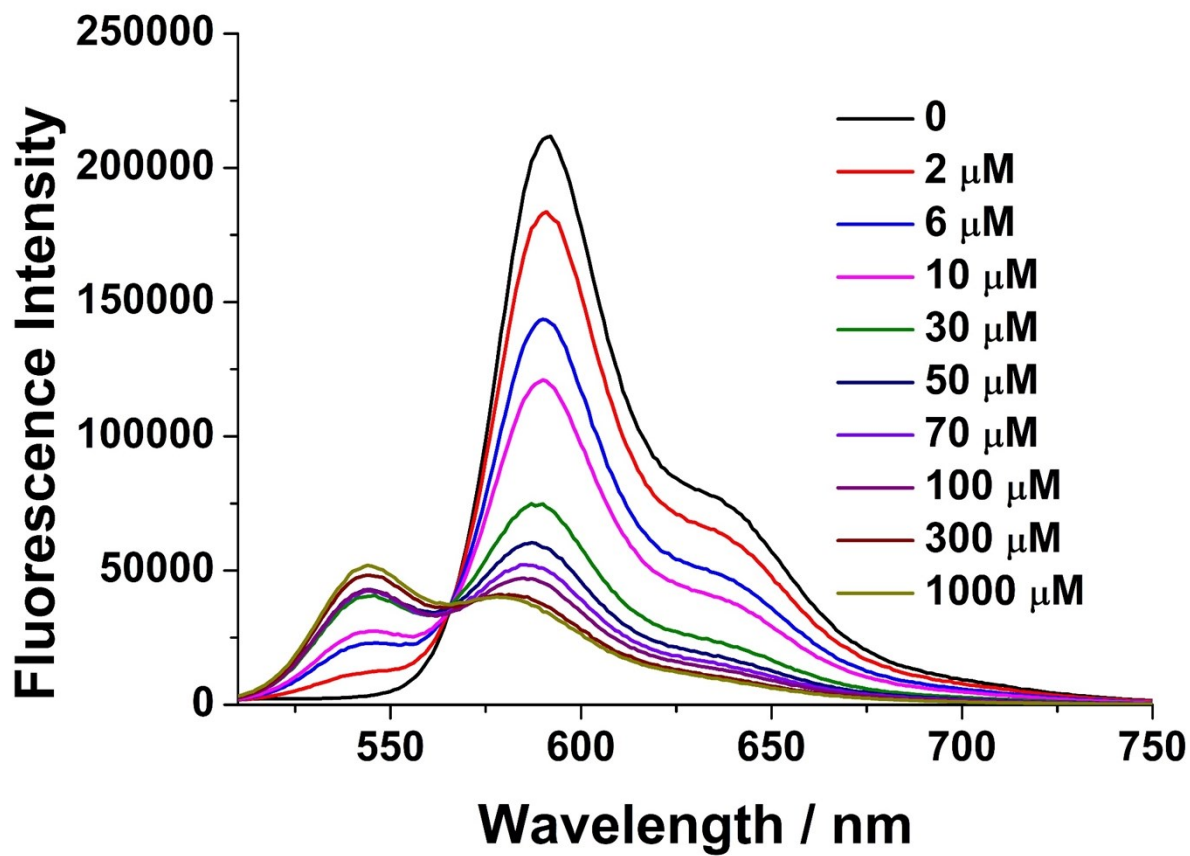


Fig. S43 Fluorescence emission spectra ($\lambda_{\text{ex}} = 510 \text{ nm}$) of BOD-PPh3 (5 μM) upon the addition of Hcy (0, 2, 6, 10, 30, 50, 70, 100, 300, 1000 μM).

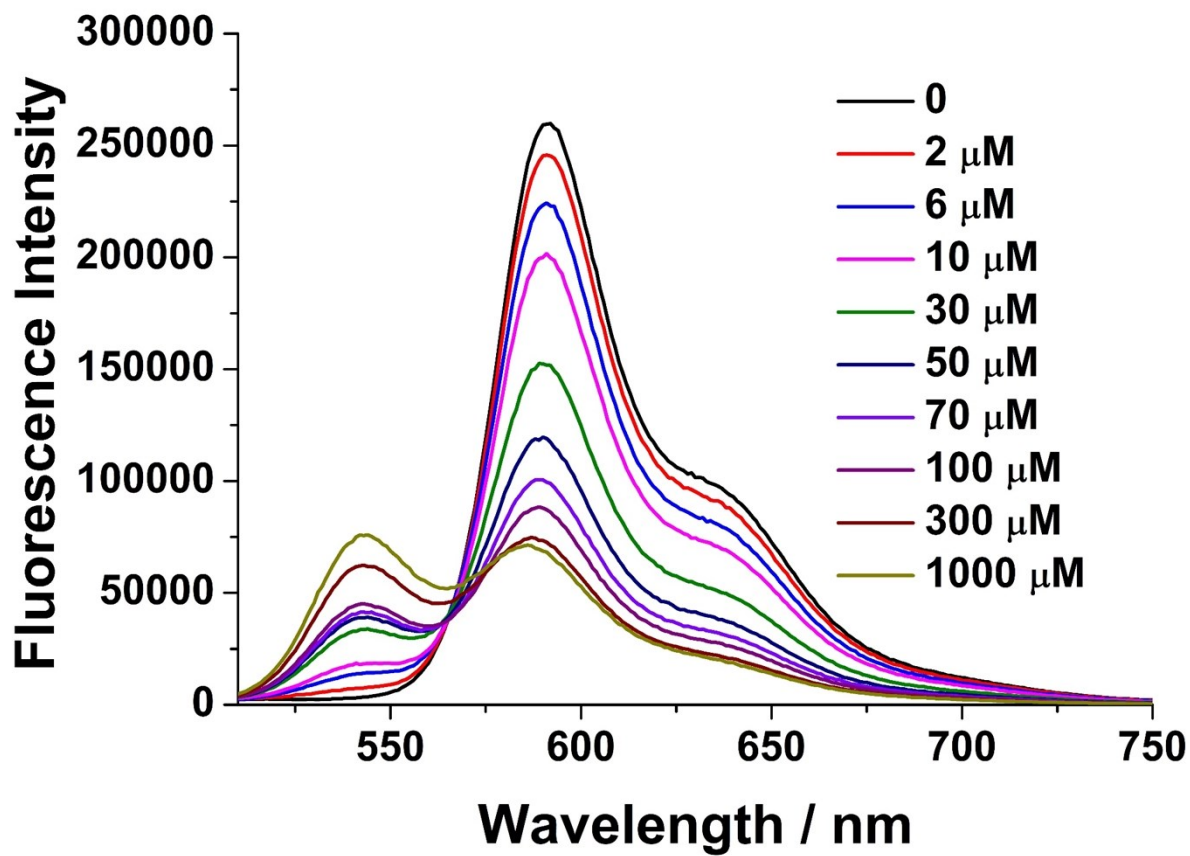


Fig. S44 Fluorescence emission spectra ($\lambda_{\text{ex}} = 510 \text{ nm}$) of BOD-Cl ($5 \mu\text{M}$) upon the addition of GSH (0, 2, 6, 10, 30, 50, 70, 100, 300, 1000 μM).

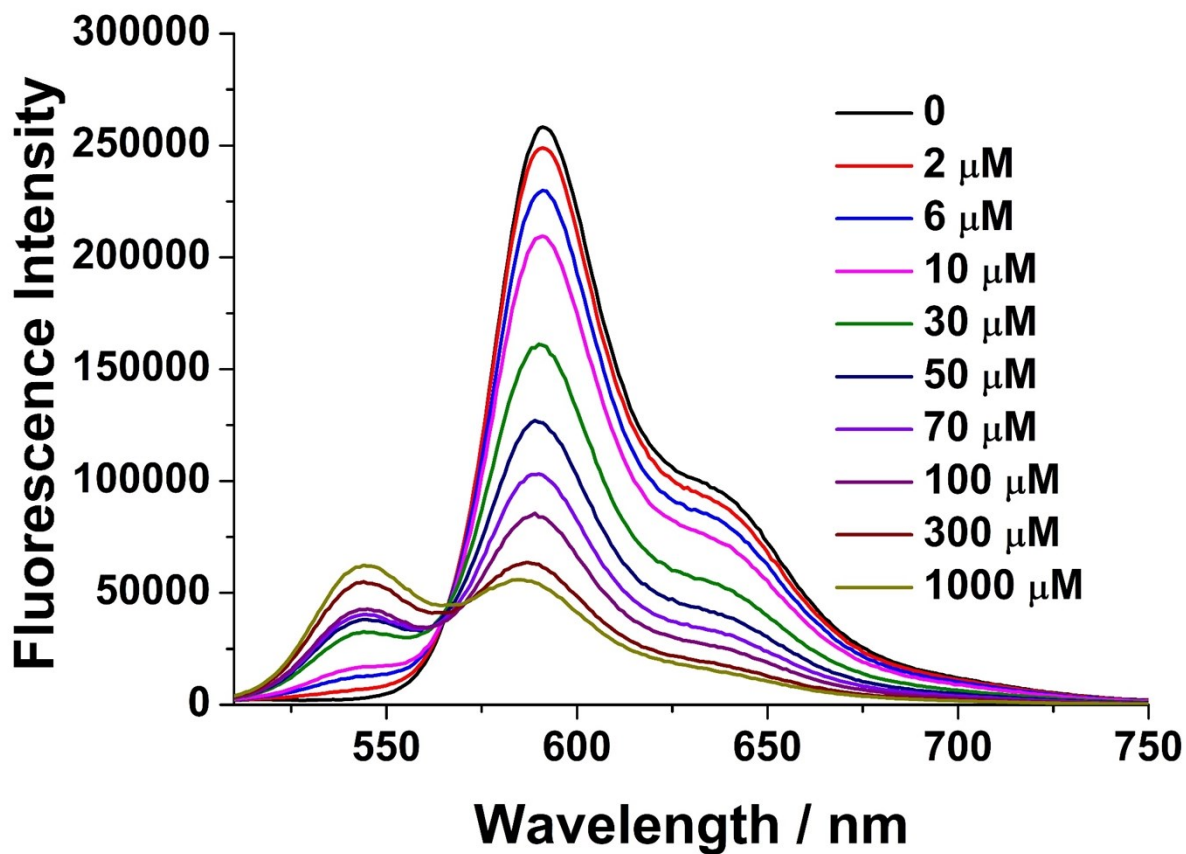


Fig. S45 Fluorescence emission spectra ($\lambda_{\text{ex}} = 510 \text{ nm}$) of BOD-Cl ($5 \mu\text{M}$) upon the addition of Cys (0, 2, 6, 10, 30, 50, 70, 100, 300, 1000 μM).

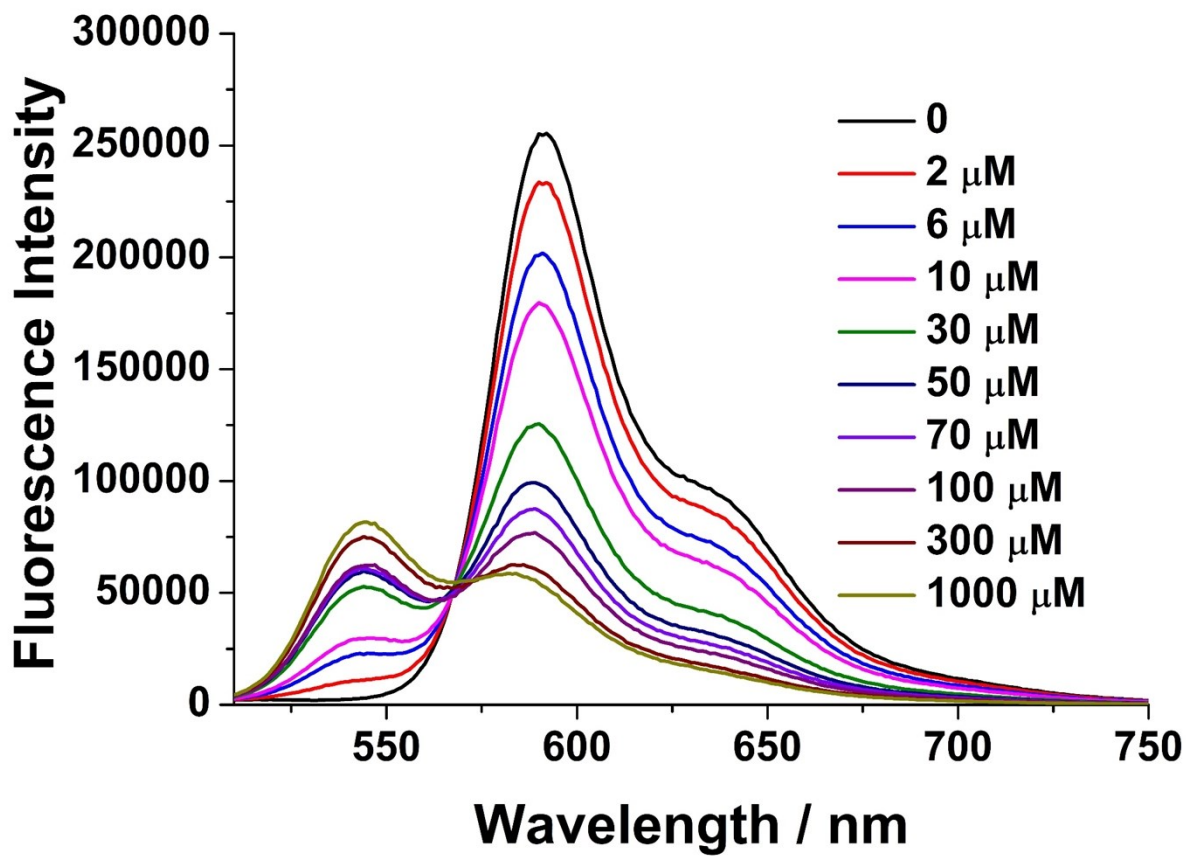


Fig. S46 Fluorescence emission spectra ($\lambda_{\text{ex}} = 510 \text{ nm}$) of BOD-Cl ($5 \mu\text{M}$) upon the addition of Hcy (0, 2, 6, 10, 30, 50, 70, 100, 300, 1000 μM).

6.The linear trend between fluorescence intensity ratio and the concentration of GSH, Cys and Hcy

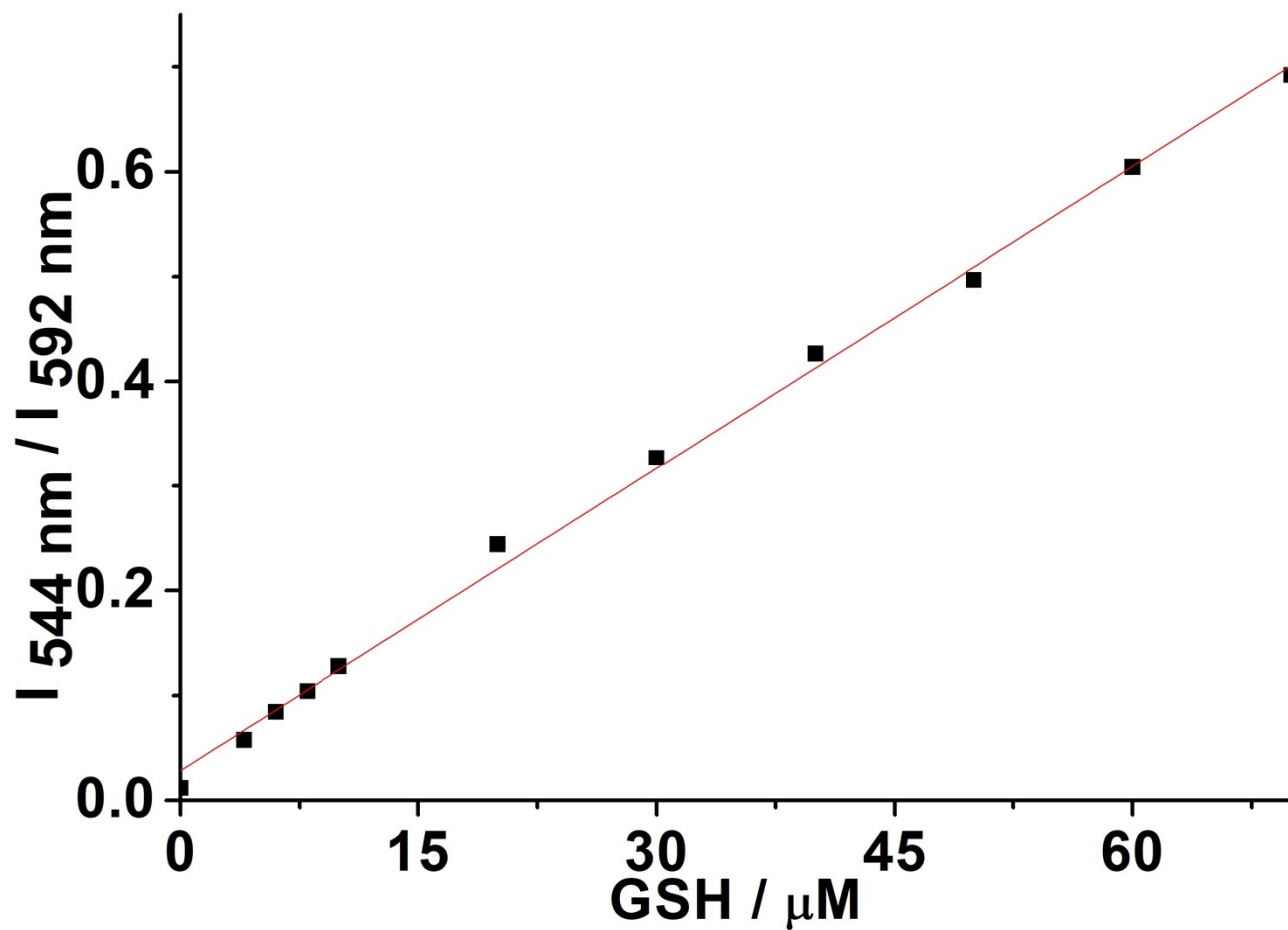


Fig. S47 The linear trend between fluorescence intensity ratio ($I_{544 \text{ nm}} / I_{596 \text{ nm}}$) and the concentration of GSH (4 – 70 μM).

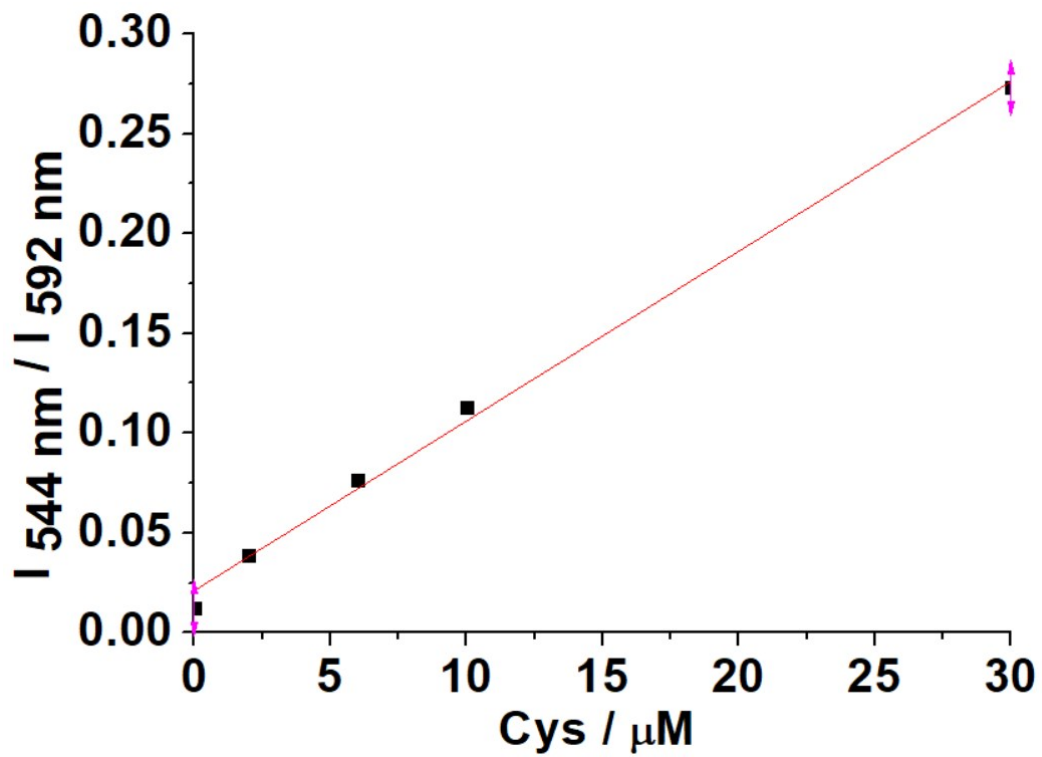


Fig. S48 The linear trend between fluorescence intensity ratio ($I_{544 \text{ nm}} / I_{596 \text{ nm}}$) and the concentration of Cys (2 – 30 μM).

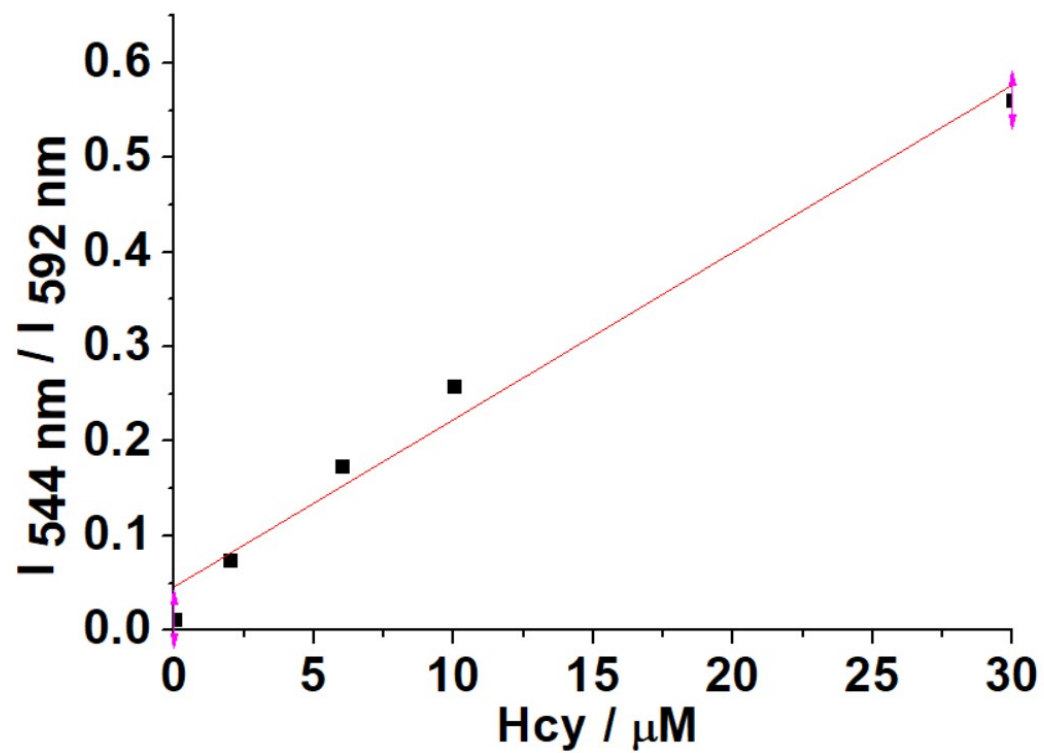


Fig. S49 The linear trend between fluorescence intensity ratio ($I_{544 \text{ nm}} / I_{596 \text{ nm}}$) and the concentration of Hcy (2 – 30 μM).

7. Competition graph

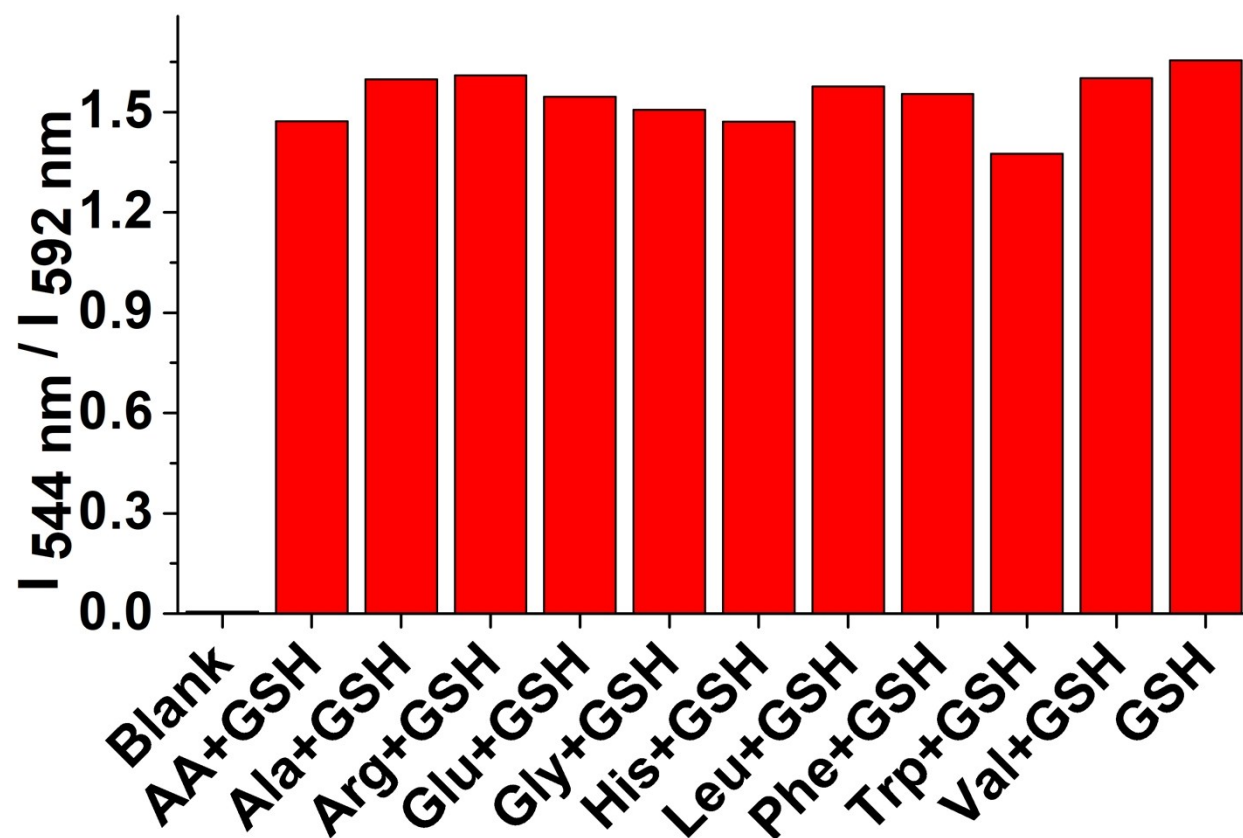


Fig. S50 Fluorescence intensity ratio ($I_{544 \text{ nm}} / I_{592 \text{ nm}}$) of BOD-JQ ($5 \mu\text{M}$) toward various substance ($500 \mu\text{M}$) competition graph with $500 \mu\text{M}$ GSH ($\lambda_{\text{ex}} = 510 \text{ nm}$)

8. Reversibility experiment

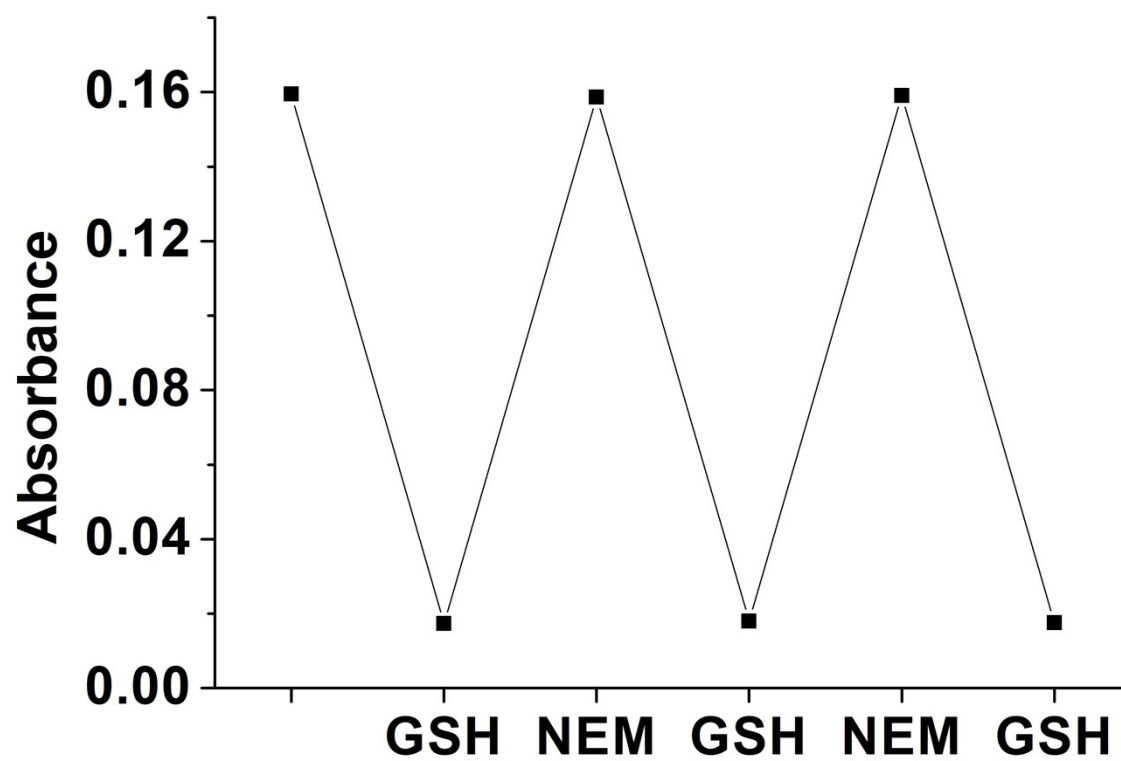


Fig. S51 Recorded absorbance ($\lambda = 570$ nm) of BOD-JQ (5 μ M) upon the addition of GSH and N-ethylmaleimide (NEM) (each 1 mM final concentration).

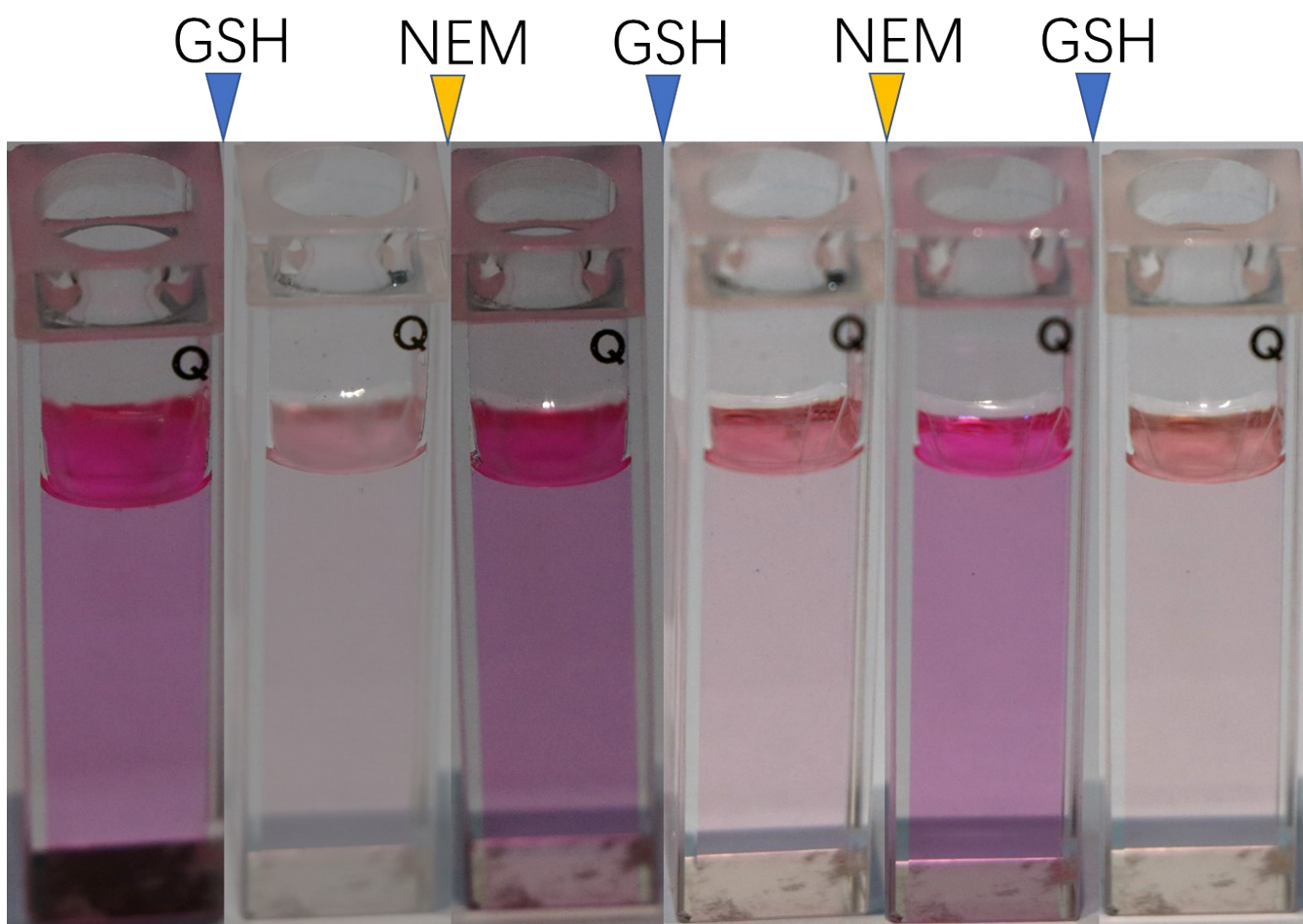


Fig. S52 Images of the solution of BOD-JQ ($5 \mu\text{M}$) after the addition of GSH (blue arrowhead) and NEM (orange arrowhead) (each 1 mM final concentration) were added alternately at 10-second intervals.

9. Dilution experiment spectra

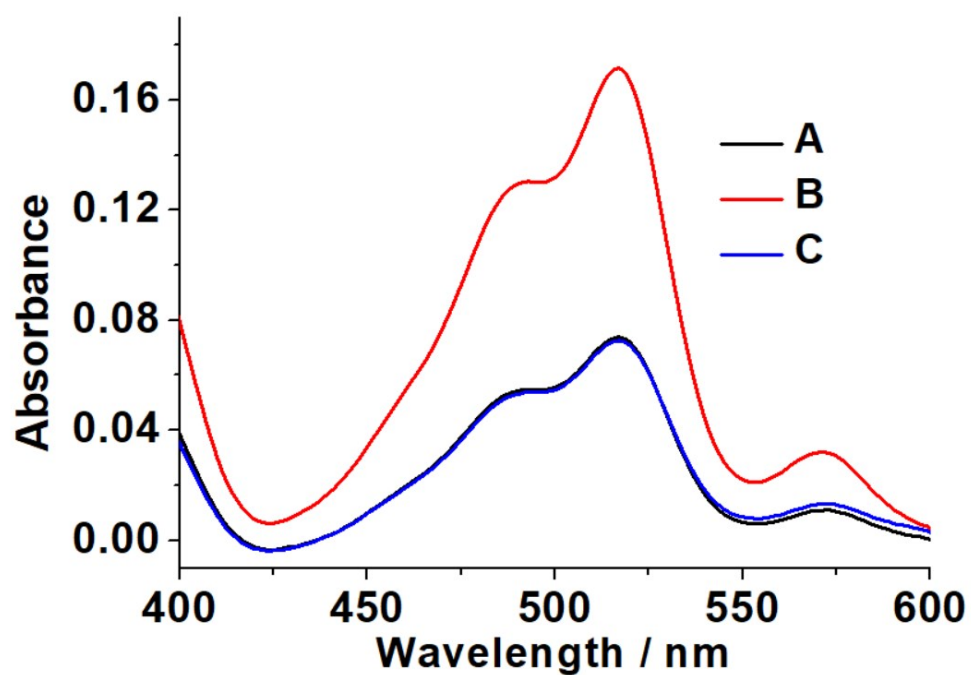


Fig. S53 Absorption spectra of BOD-JQ / GSH mixture in mixture solution. A: [Dye] = 5 μ M, [GSH] = 1mM; B: [Dye] = 10 μ M, [GSH] = 2 mM; C: 2-fold dilution of solution B.

10. Cells viability results

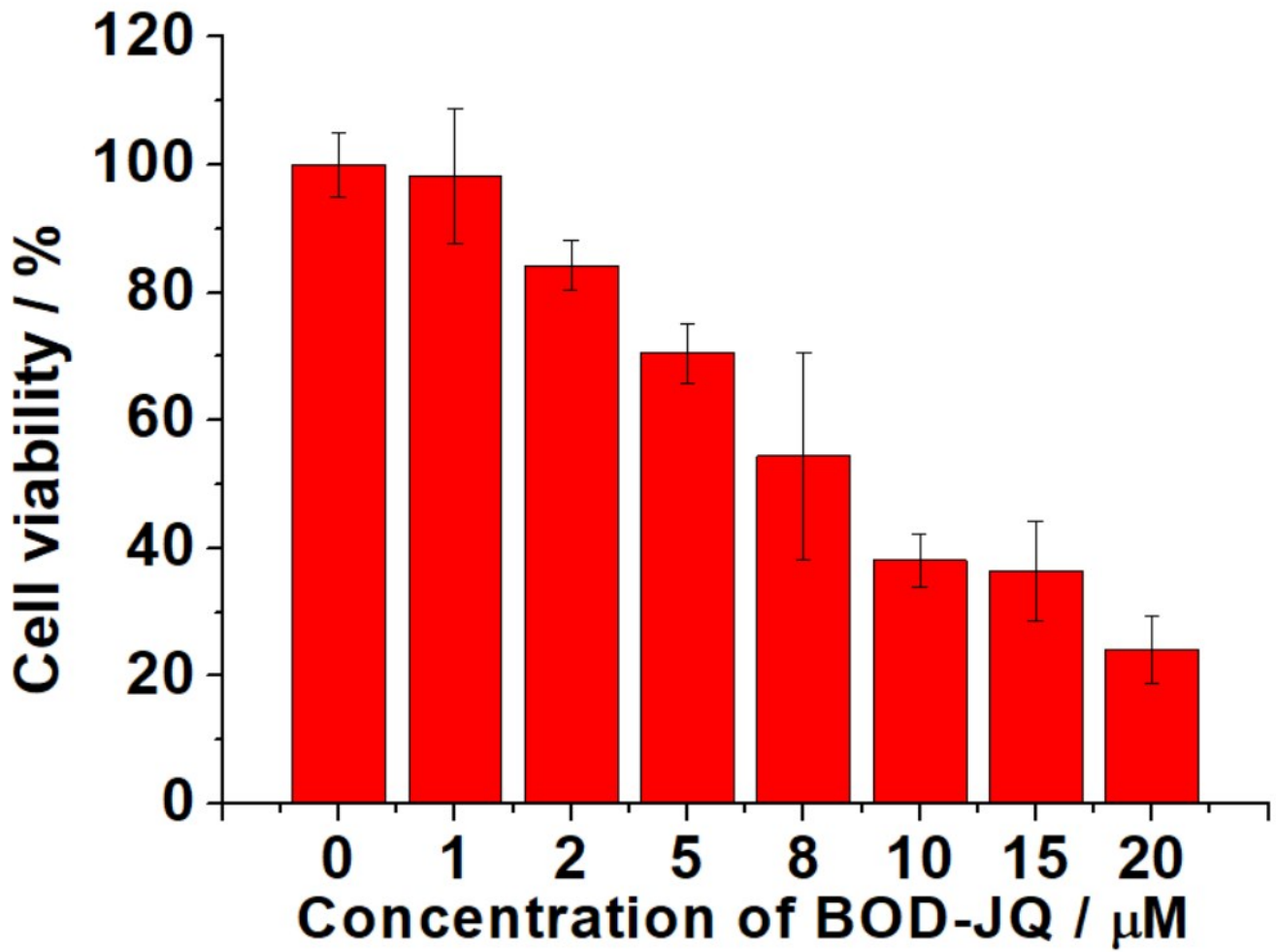


Fig. S54 Cells viability of B16F10 cells against BOD-JQ (24 hours). Error bars represent standard deviation (n = 4).

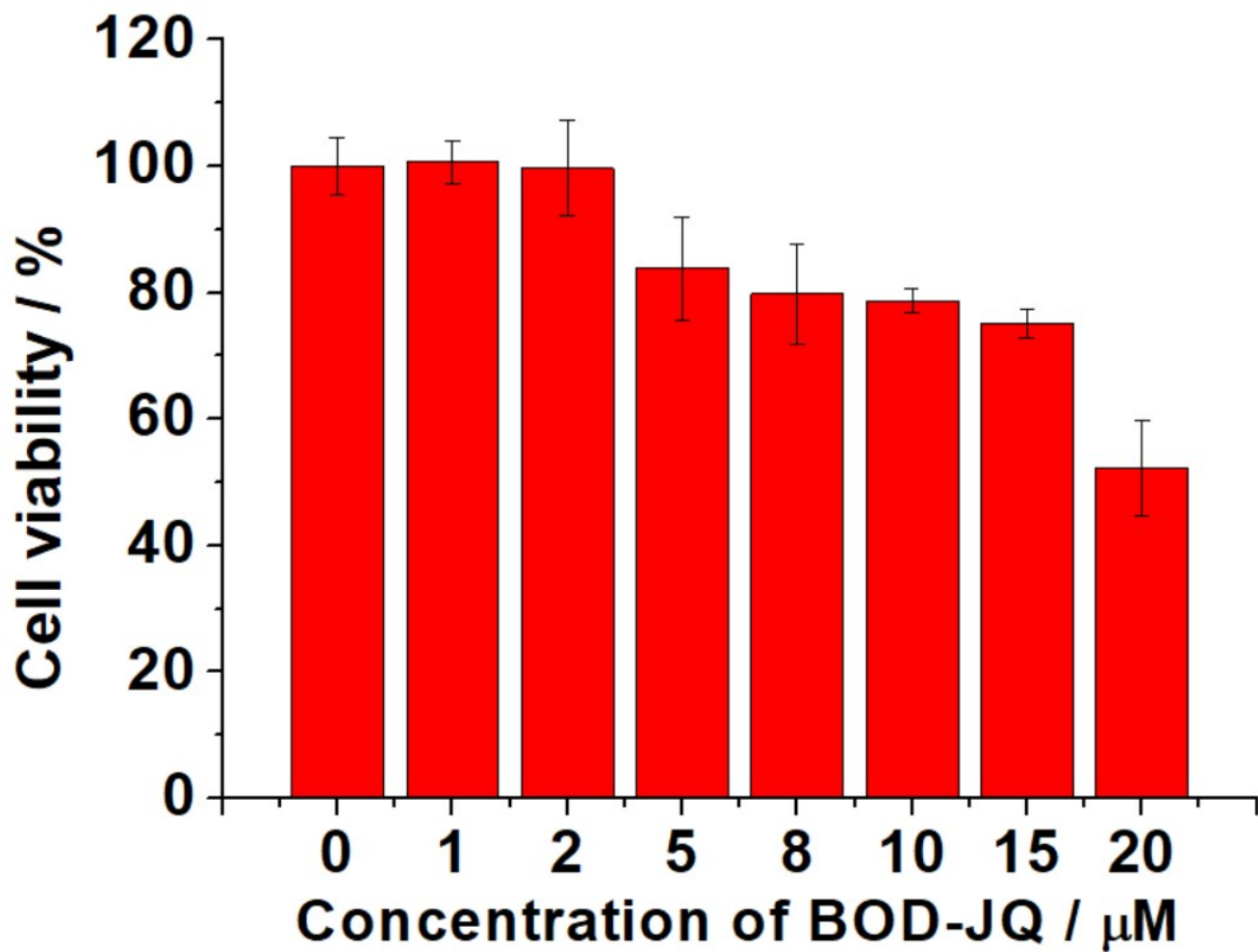


Fig. S55 Cells viability of HEK-A cells against BOD-JQ (24 hours). Error bars represent standard deviation (n = 4).

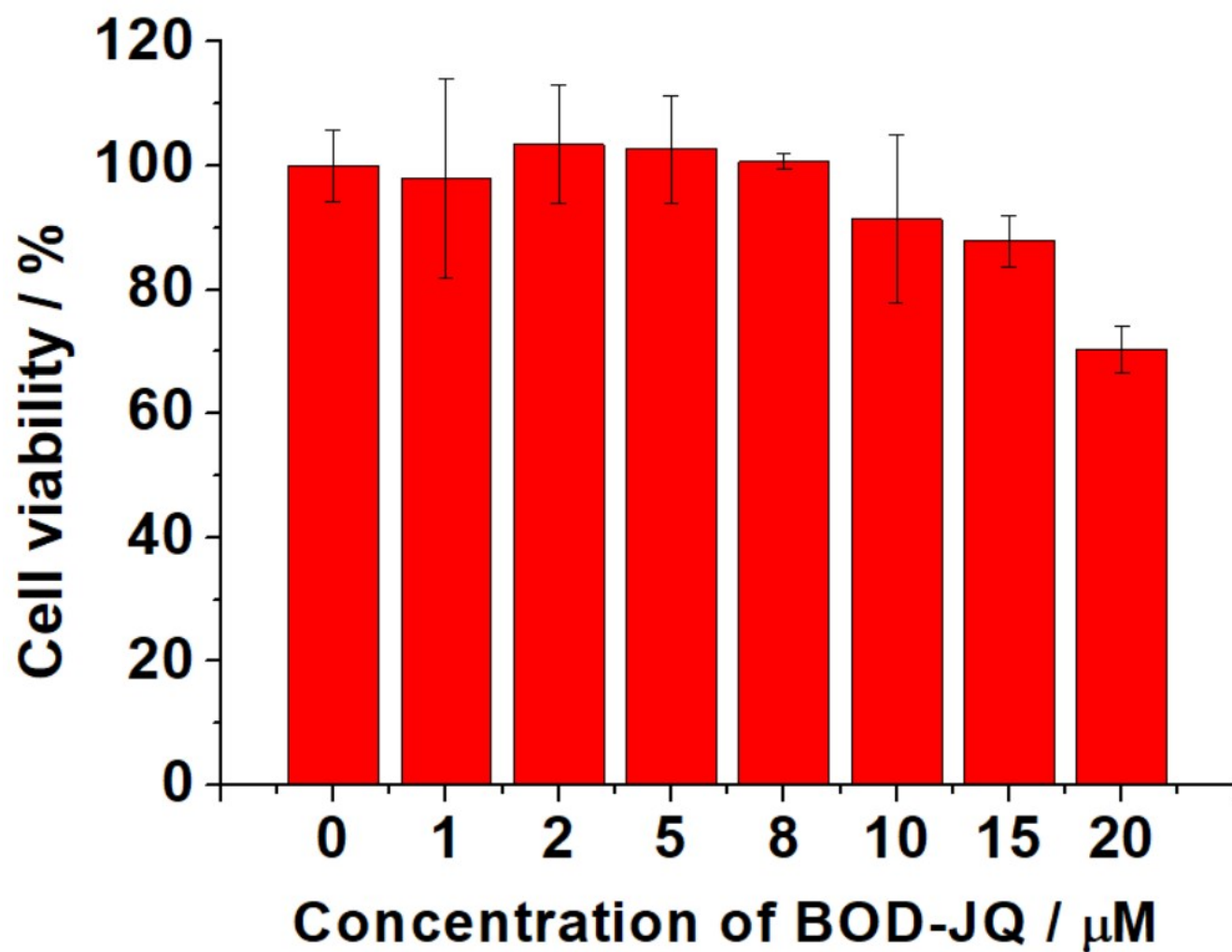


Fig. S56 Cells viability of A375 cells against BOD-JQ (24 hours). Error bars represent standard deviation (n = 4).

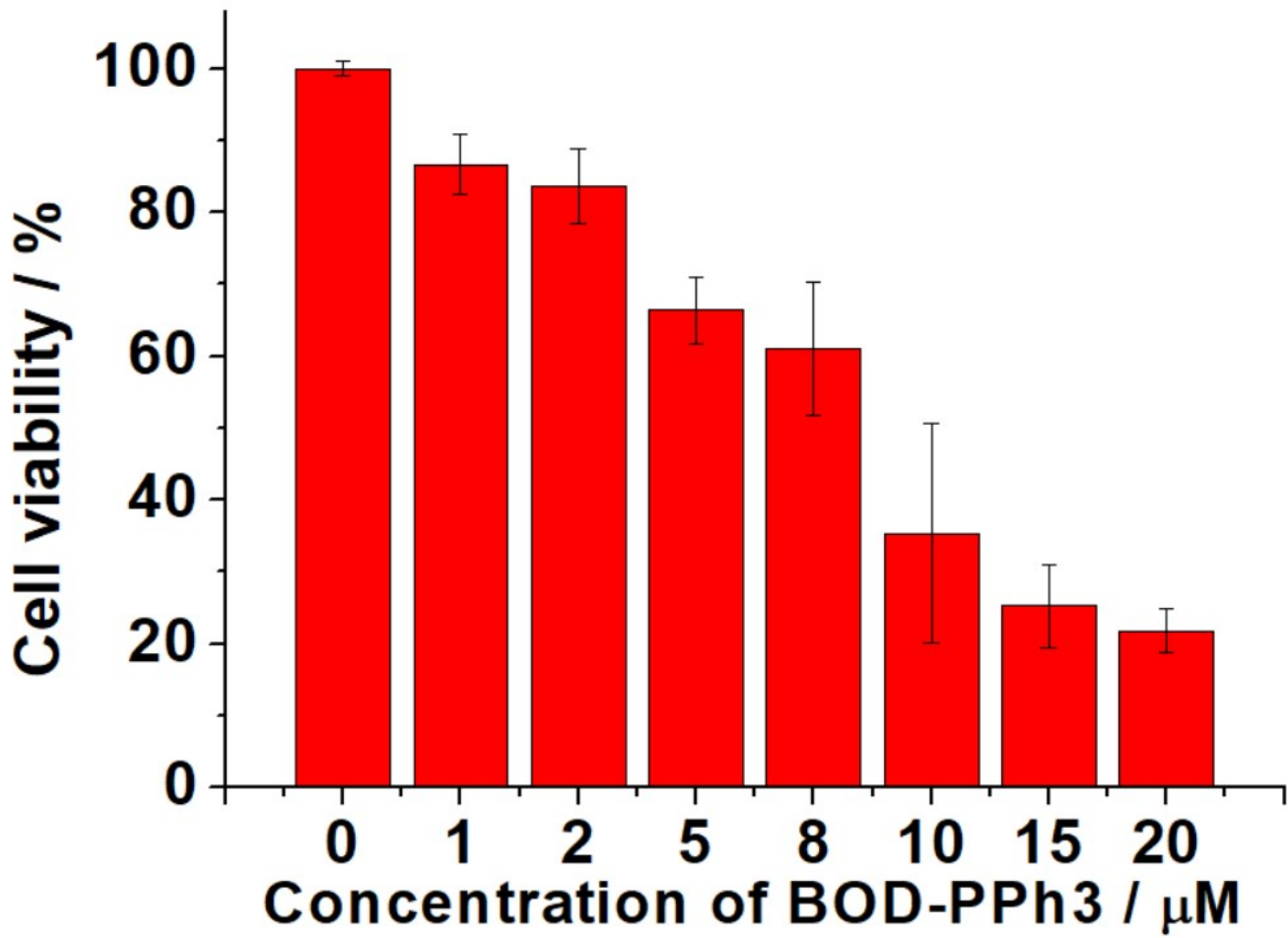


Fig. S57 Cells viability of B16F10 cells against BOD-PPh3 (24 hours). Error bars represent standard deviation (n = 4).

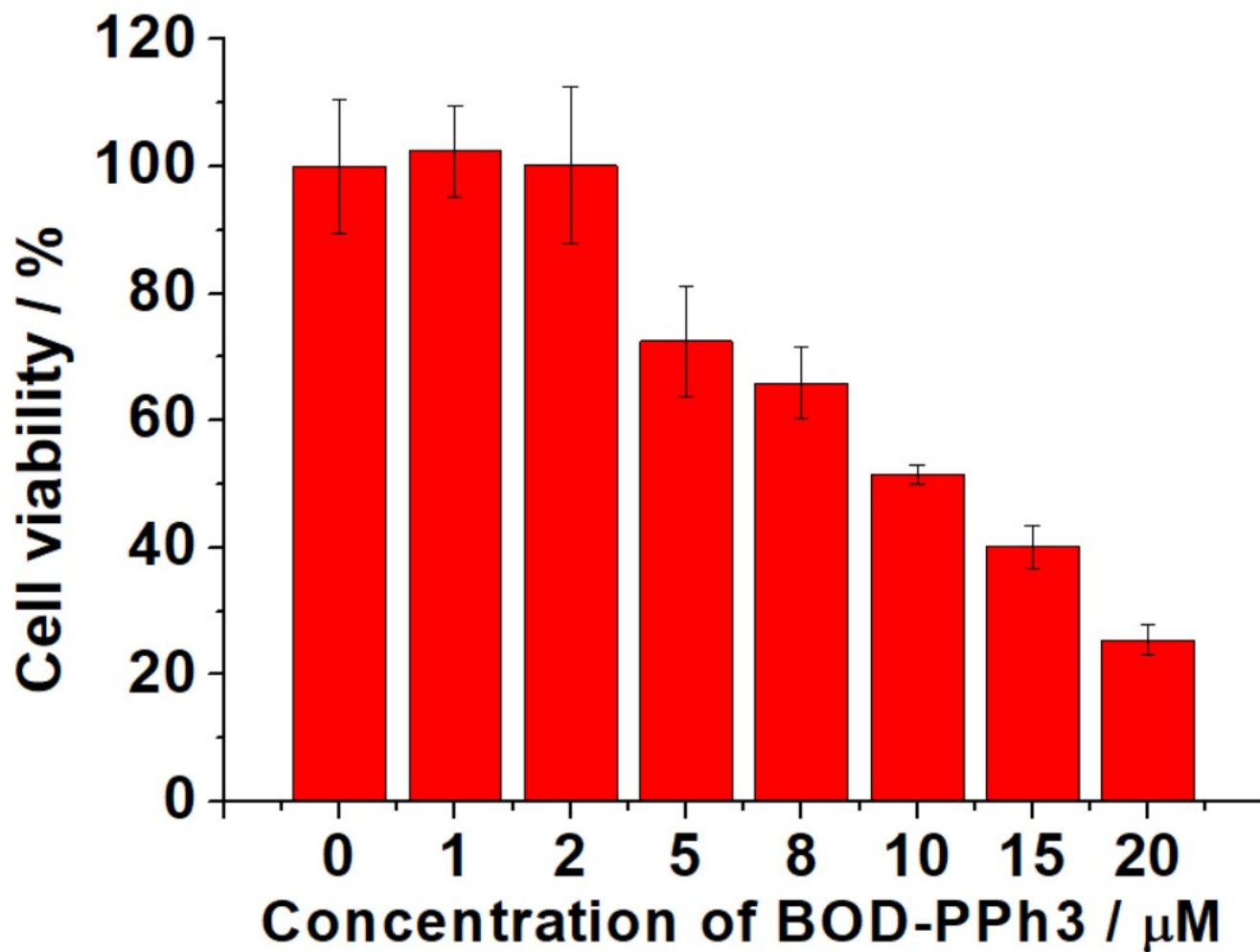


Fig. S58 Cells viability of HEK-A cells against BOD-PPh3 (24 hours). Error bars represent standard deviation (n = 4).

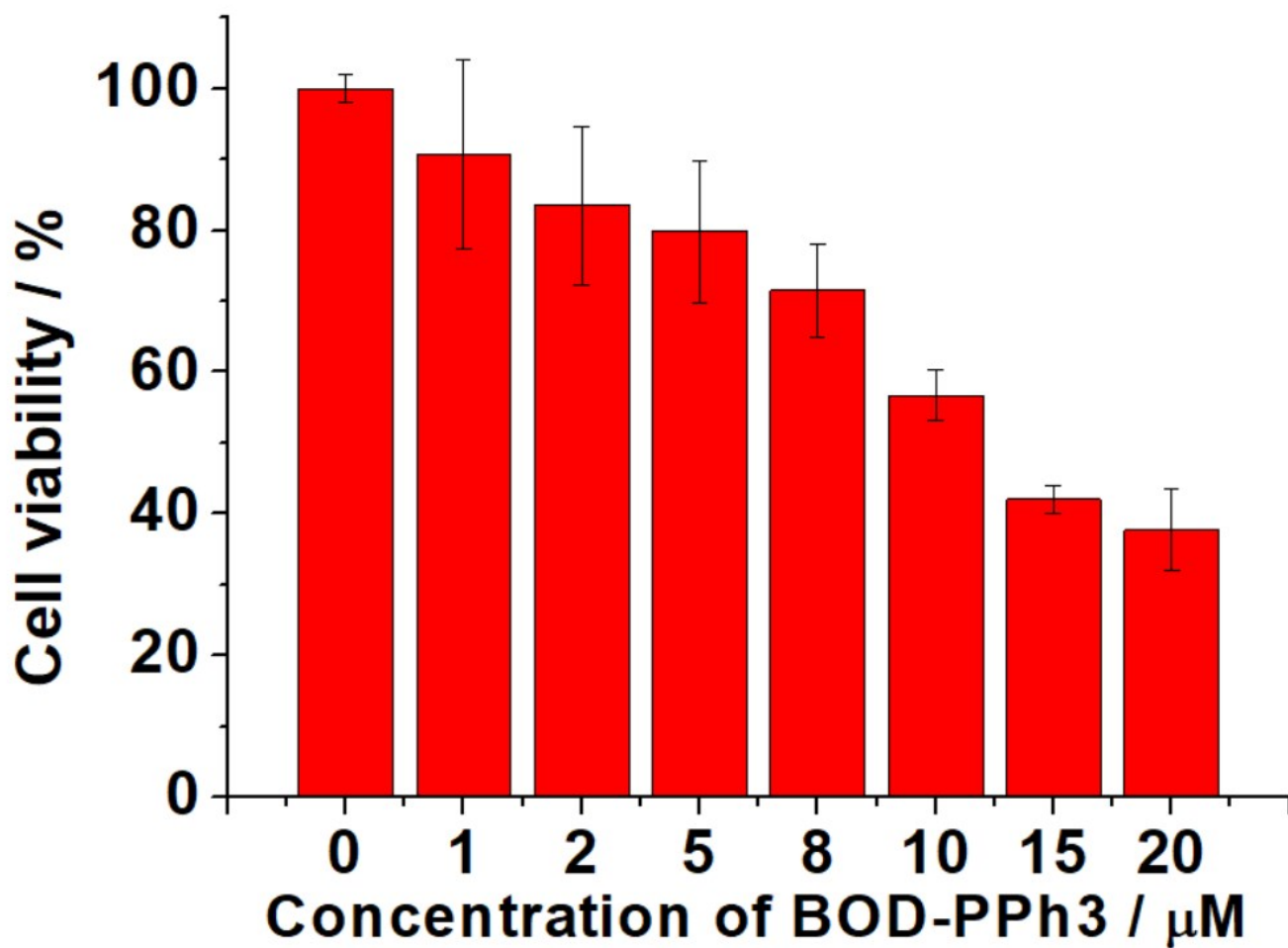


Fig. S59 Cells viability of A375 cells against BOD-PPh3 (24 hours). Error bars represent standard deviation (n = 4).

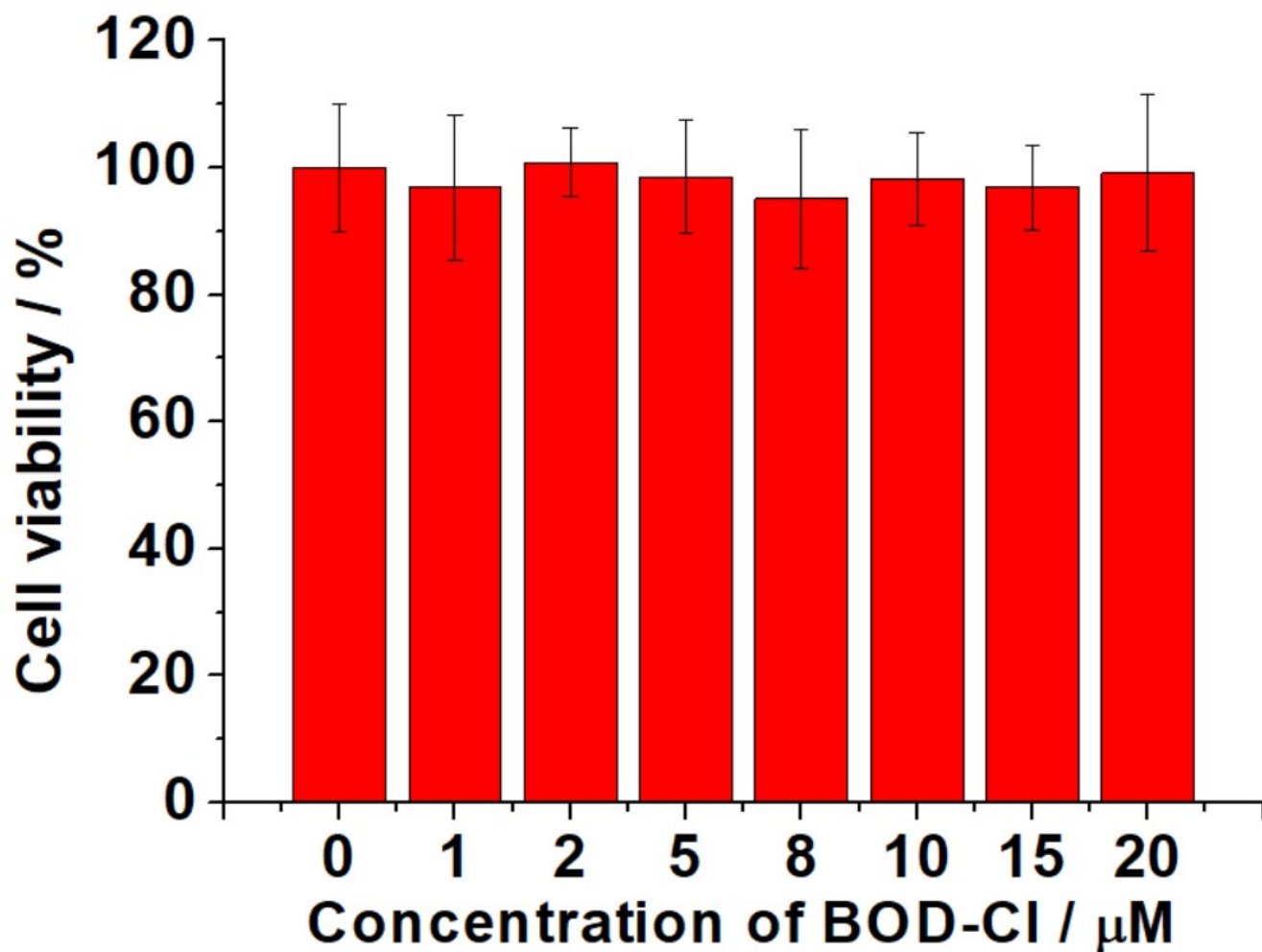


Fig. S60 Cells viability of B16F10 cells against BOD-Cl (24 hours). Error bars represent standard deviation ($n = 4$).

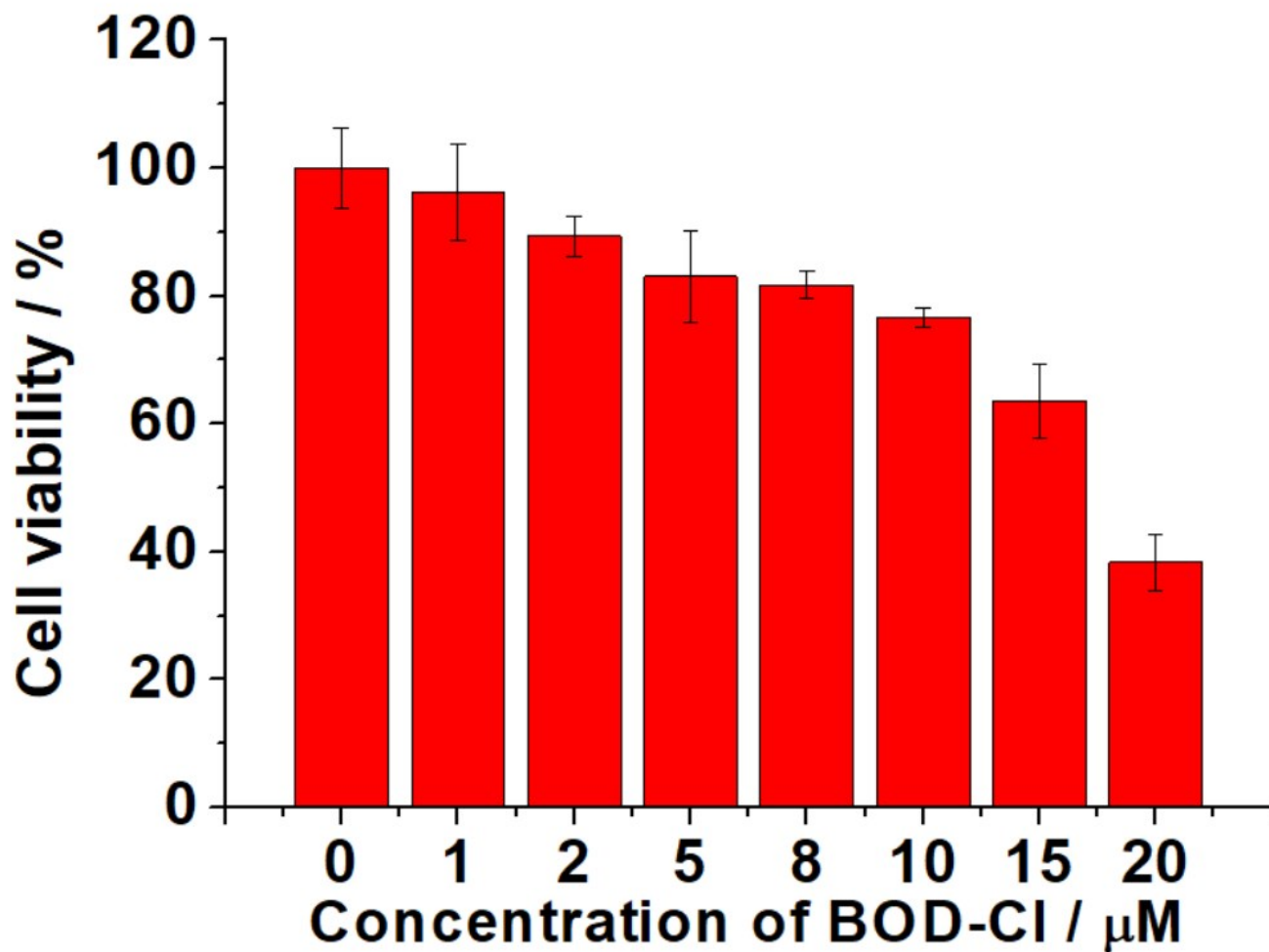


Fig. S61 Cells viability of HEK-A cells against BOD-Cl (24 hours). Error bars represent standard deviation (n = 4).

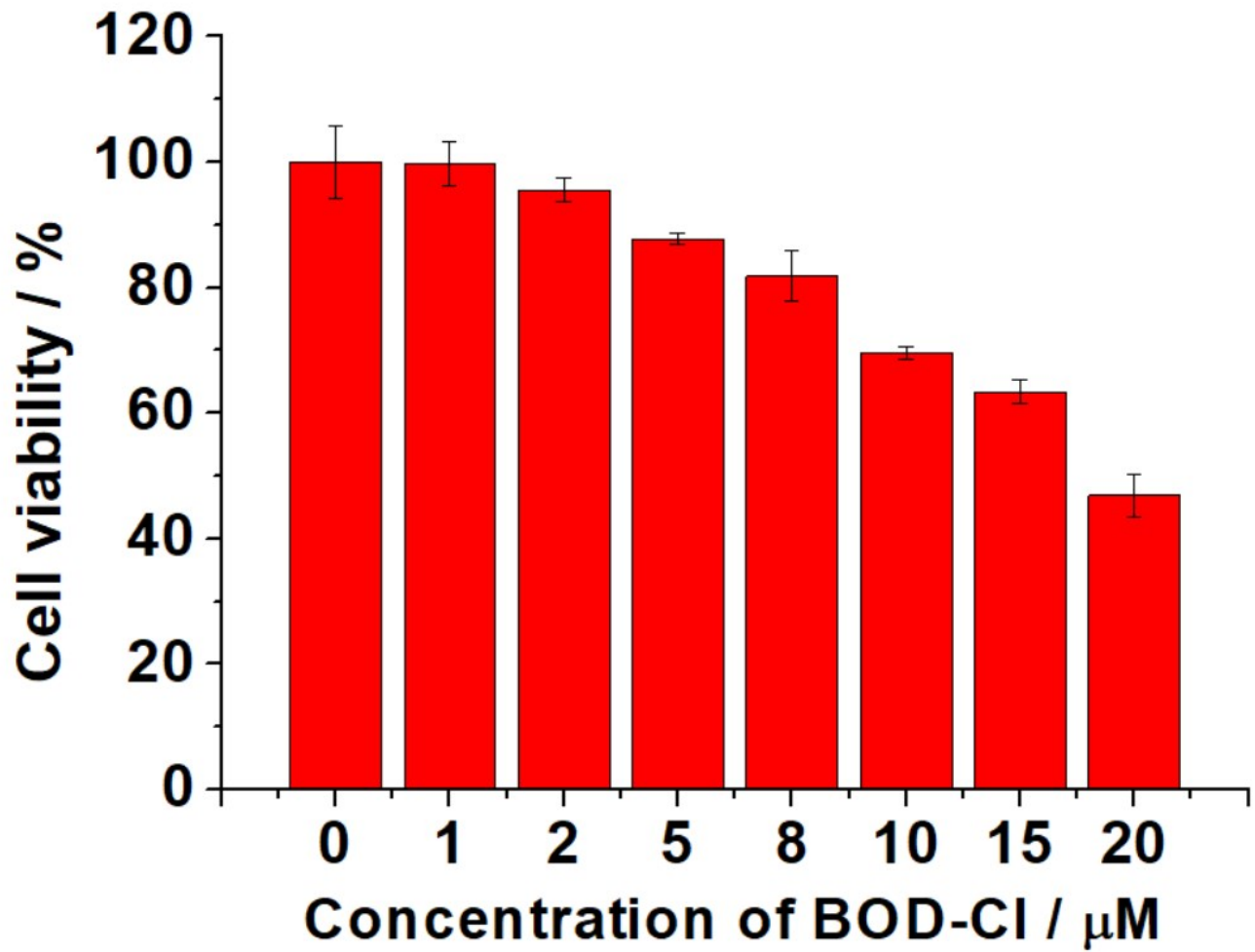


Fig. S62 Cells viability of A375 cells against BOD-Cl (24 hours). Error bars represent standard deviation (n = 4).

11. Targeting confocal fluorescence images of BOD-JQ.

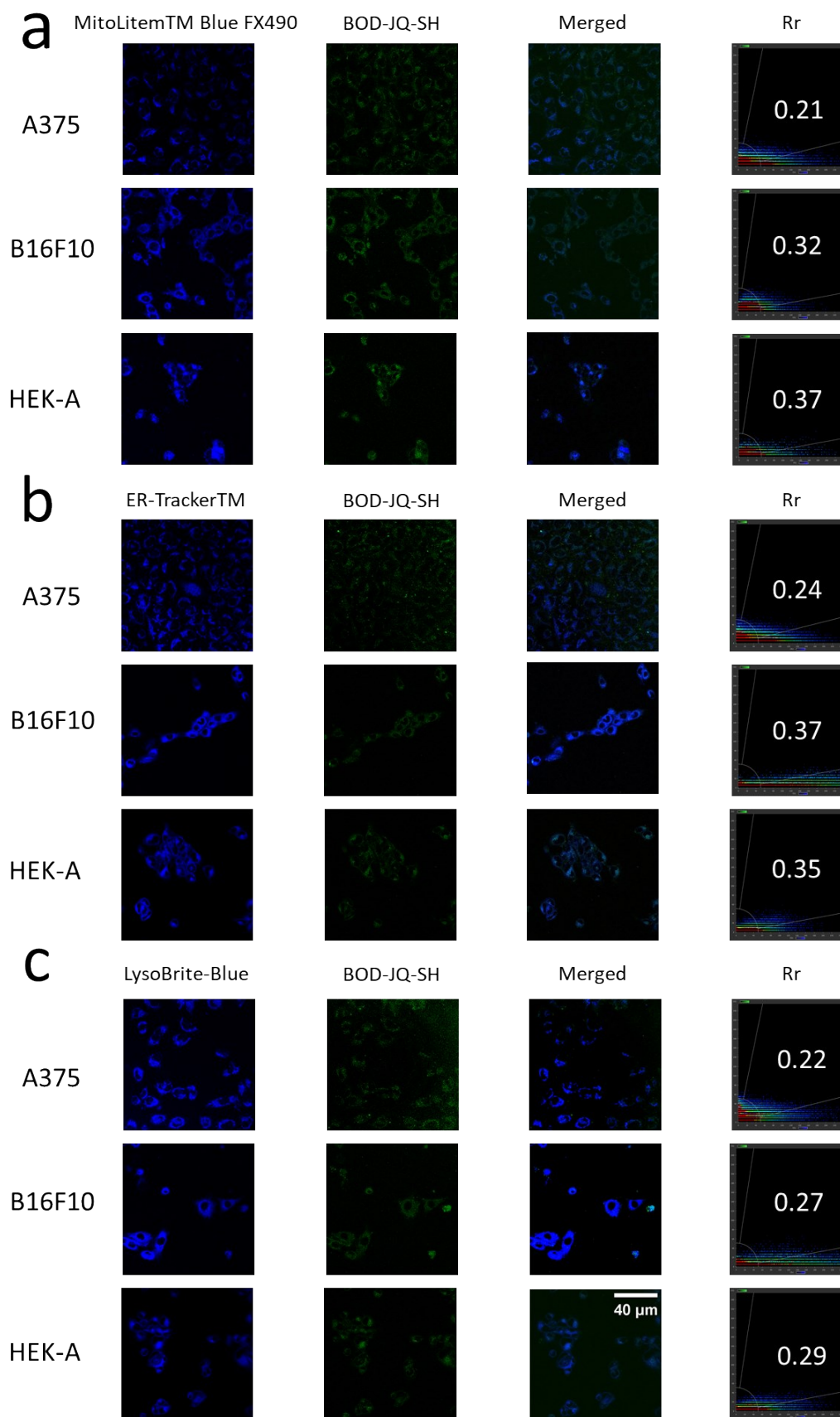


Fig. S63 Targeting confocal fluorescence images of BOD-JQ. (a) Confocal fluorescence images of

B16F10, A375 and HEK-A cells incubated with BOD-JQ(2 μ M) for 30 min. followed by containing with mitochondria tracker (MBF) for 5 min, from left to right: blue 430 – 470 nm, λ_{ex} = 405 nm (MBF); green 500 – 550 nm, λ_{ex} = 488 nm (BOD-JQ-SH); merged images of blue and green channels; intensity scatter plot of the blue and green channels (insert value is the Pearson's correlation coefficients (Rr)). (b) Confocal fluorescence images of B16F10, A375 and HEK-A Cells incubated with probe BOD-JQ(2 μ M) for 30 min followed by containing with endoplasmic reticulum tracker (ERT) for 5 min, from left to right: blue channel at 430 – 470 nm, λ_{ex} = 405 nm (ERT); green channel at 500 – 550 nm, λ_{ex} = 488 nm (BOD-JQ-SH); merged images of blue and green channels; intensity scatter plot of the blue and green channels (insert number is Rr). (c) Confocal fluorescence images of B16F10, A375 and HEK-A Cells incubated with probe BOD-JQ(2 μ M) for 30 min followed by containing with lysosome tracker (LBB) for 5 min, from left to right: blue channel at 430 – 470 nm, λ_{ex} = 405 nm (ERT); green channel at 500 – 550 nm, λ_{ex} = 488 nm (BOD-JQ-SH); merged images of blue and green channels; intensity scatter plot of the blue and green channels (insert number is Rr).

12. Real-time biothiols imaging with BOD-JQ.

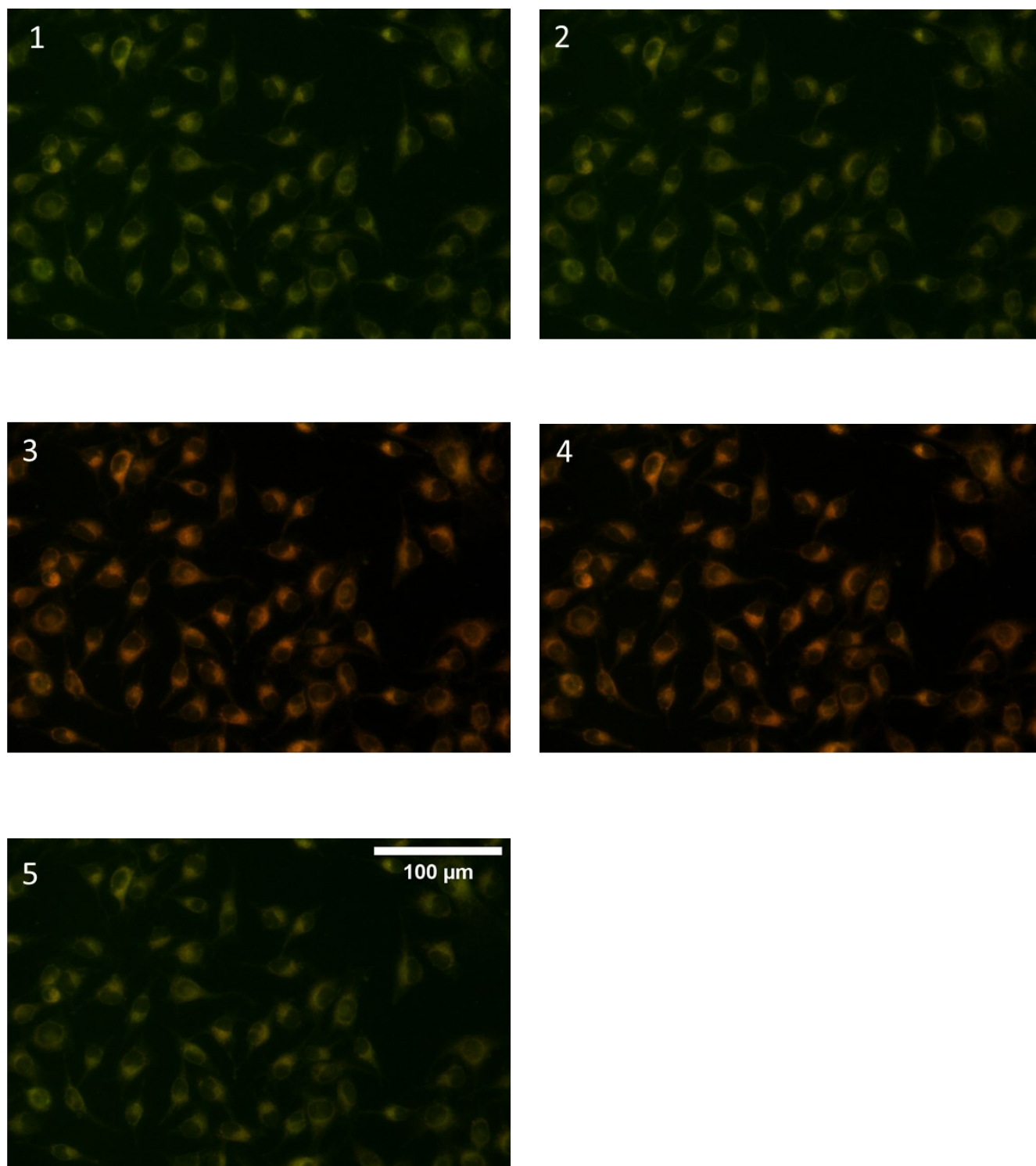


Fig. S64 Real-time biothiols imaging with BOD-JQ. (a) Ratio images for B16F10 cells upon the incubation with BOD-JQ (2 μM) and followed by the addition of NEM (500 μM) and GSH ethyl ester (5 mM). Scale bar = 100 μm .

Reference

- [1] L. Yi, H. Li, L. Sun, L. Liu, C. Zhang, Z. Xi, *Angew. Chem. Int. Ed.* **2009**, *48*, 4034-4037.
- [2] K. Umezawa, M. Yoshida, M. Kamiya, T. Yamasoba, Y. Urano, *Nat. Chem.* **2017**, *9*, 279-286.
- [3] T. Matsumoto, Y. Urano, T. Shoda, H. Kojima, T. Nagano, *Org. Lett.* **2007**, *9*, 3375-3377.
- [4] D. Zhai, S.-C. Lee, S.-W. Yun, Y.-T. Chang, *Chemical Commun.* **2013**, *49*, 7207-7209.
- [5] J. Kang, F. Huo, J. Chao, C. Yin, *Spectrochim. Acta. A Mol. Biomol. Spectrosc.* **2018**, *195*, 16-20.
- [6] X. Jiang, J. Chen, A. Bajić, C. Zhang, X. Song, S. L. Carroll, Z.-L. Cai, M. Tang, M. Xue, N. Cheng, C. P. Schaaf, F. Li, K. R. MacKenzie, A. C. M. Ferreon, F. Xia, M. C. Wang, M. Maletić-Savatić, J. Wang, *Nat. Commun.* **2017**, *8*, 16087.
- [7] Y. Yue, C. Yin, F. Huo, J. Chao, Y. Zhang, *Sens. Actuators B Chem.* **2016**, *223*, 496-500.
- [8] Wu, W.; Guo, H.; Wu, W.; Ji, S.; Zhao, J. *J. Org. Chem.* **2011**, *76*, 7056-7064.
- [9] Baruah, M.; Qin, W.; Flors, C.; Hofkens, J.; Vallée, R. A. L.; Beljonne, D.; Van der Auweraer, M.; De Borggraeve, W. M.; Boens, N. *J. Phys. Chem. A.* **2006**, *110*, 5998-6009.
- [10] Huang, L.; Zhao, J.; Guo, S.; Zhang, C.; Ma, J. *J. Org. Chem.* **2013**, *78*, 5627-5637.
- [11] Wang, Z.; Xie, Y.; Xu, K.; Zhao, J.; Glusac, K. D. *J. Phys. Chem. A.* **2015**, *119*, 6791-6806.
- [12] Ma, J.; Yuan, X.; Kucukoz, B.; Li, S.; Zhang, C.; Majumdar, P.; Karatay, A.; Li, X.; Gulyaglioglu, H.; Elmali, A. *J. Mater. Chem. C.* **2014**, *2*, 3900-3913.
- [13] Zhang, C.; Zhao, J.; Wu, S.; Wang, Z.; Wu, W.; Ma, J.; Guo, S.; Huang, L. *J. Am. Chem. Soc.* **2013**, *135*, 10566-10578.